

Final Report

NASA CR-111774

July 15, 1970

**AN ANALYTICAL STUDY OF SOLID PROPELLANT
COMBUSTION DURING RAPID DEPRESSURIZATION**

By: CHARLES E. WOOLDRIDGE

Prepared for:

NATIONAL AERONAUTICS AND SPACE ADMINISTRATION
LANGLEY RESEARCH CENTER
LANGLEY STATION
HAMPTON, VIRGINIA 23365

Attention: RAYMOND T. MOORE
CONTRACTING OFFICER

CONTRACT NAS1-9396

SRI Project PHU-8131

Approved:

E. M. KINDERMAN, *Director*
Physical Sciences (Applied Physics Laboratory)

C. J. COOK, *Executive Director*
Physical Sciences Division

Copy No.

Page intentionally left blank

ABSTRACT

This paper discusses a modification of the solid propellant combustion model previously developed at Stanford Research Institute. The model was modified to contain two heat release zones in the gas phase, one adjacent to the wall governed by the wall temperature and a second primary flame governed by the final flame temperature. Comparisons are shown between predictions of the model and data obtained at both Stanford Research Institute and United Technology Center. It is demonstrated that the calculated behavior of six ammonium perchlorate propellants utilizing different binder systems agreed with the measured trends when only the burning rate, flame temperature, and total heat release were varied in the model from one propellant to another. Similar results were obtained when aluminum was added to one of the propellants.

Page intentionally left blank

PREFACE

This study of solid propellant transient combustion was performed principally by the author. Thanks are due to Dr. G. A. Marxman for many stimulating discussions during the program and to Dr. D. C. Wooten who made valuable comments concerning the mathematical analysis. Finally, the author is deeply indebted to Miss Margery Brothers who was responsible for the long and tedious computer calculations.

The project was under the overall management of the Chief, Solid Propulsion Technology, Code RPS, OART, NASA, Washington, D.C. (R. W. Ziem), with technical management by Propulsion Branch, Langley Research Center, Hampton, Virginia (G. Burton Northam).

Page intentionally left blank

CONTENTS

| | |
|---|-----|
| ABSTRACT | iii |
| PREFACE | v |
| ILLUSTRATIONS | ix |
| TABLES | x |
| NOMENCLATURE | xi |
| I INTRODUCTION | 1 |
| II MATHEMATICAL FORMULATION OF THE COMBUSTION MODEL | 5 |
| III PARAMETRIC STUDY OF THE MODEL | 15 |
| IV COMPARISONS WITH EXPERIMENTAL DATA | 29 |
| V CONCLUDING REMARKS | 45 |
| APPENDIXES | |
| A PERTURBATION ANALYSIS OF THE MODEL | A-1 |
| B COMPUTER CODE AND REPRESENTATIVE OUTPUT FORMATS | B-1 |
| C TRANSIENT COMBUSTION BEHAVIOR WITH A DECREASE IN BURNING RATE | C-1 |
| REFERENCES | R-1 |

Page intentionally left blank

ILLUSTRATIONS

| | | |
|------------|--|----|
| Fig. 1 | Strand Burning Rate Versus Pressure | 10 |
| Fig. 2 | Flame Temperature Versus Burning Rate | 16 |
| Fig. 3a,b | Effect of Variable Q_s/Q_t at High Pressure (PU-269) . . | 17 |
| Fig. 4 | Effect of Variable Q_s/Q_t at Low Pressure (PU-269) . . . | 19 |
| Fig. 5 | Linear Burning Rate Response as a Function of Pressure (PU-269) | 20 |
| Fig. 6a,b | Effect of Variable Q_t at High Pressure (PU-269) | 21 |
| Fig. 7a,b | Effect of Variable n_1 at High Pressure (PU-269) | 23 |
| Fig. 8a,b | Effect of Variable n_2 at High Pressure (PU-269) | 24 |
| Fig. 9a,b | Effect of Variable E_w at High Pressure (PU-269) | 25 |
| Fig. 10a,b | Effect of Variable T'_w at High Pressure (PU-269) | 26 |
| Fig. 11a,b | Effect of Variable κ at High Pressure (PU-269) | 27 |
| Fig. 12 | Comparison of Theory with Observed Pressurization Response (PU-269) | 30 |
| Fig. 13 | Calculated Extinction Behavior (PU-269) | 32 |
| Fig. 14 | Comparison of Calculated and Observed Extinction Behavior (UTX-10645) | 35 |
| Fig. 15 | Calculated Extinction Behavior in the Slab Motor (UTX-10645) | 36 |
| Fig. 16 | Comparison of Calculated and Observed Extinction Behavior (UTX-10661) | 37 |
| Fig. 17 | Calculated Extinction Behavior in the Slab Motor (UTX-10661) | 38 |
| Fig. 18 | Extinguishment Characteristics of UTX-10645 and UTX-10691 in the Swing-Nozzle Motor | 39 |

| | | |
|---------|---|----|
| Fig. 19 | Calculated Extinction Behavior in the Swing-Nozzle Motor (UTX-10645) | 41 |
| Fig. 20 | Extinguishment Characteristics of UTX-11327 in the Window Motor | 42 |
| Fig. 21 | Extinguishment Characteristics of UTX-11325 in the Window Motor | 43 |

TABLES

| | | |
|----|--|----|
| I. | Propellant Formulations Considered During This Program | 33 |
|----|--|----|

NOMENCLATURE

| | |
|-----------|--|
| A | kinetics parameter |
| A_b | burning surface area |
| A_t | nozzle throat area |
| c_p | specific heat capacity of gas at constant pressure |
| c_s | specific heat capacity of solid |
| E_w | activation energy for pyrolysis at interface |
| E_D | activation energy for pressure-insensitive surface-coupled reactions in Eq. 2. |
| E_f | activation energy in the outer reaction zone |
| E_h | activation energy in the inner reaction zone |
| E_H | activation energy for pressure-sensitive surface-coupled reactions in Eq. 1 |
| H_D | preexponential factor in Eq. 2 |
| H_H | preexponential factor in Eq. 1 |
| k_g | thermal conductivity of gas phase |
| k_s | thermal conductivity of solid |
| L | heat of vaporization per unit mass of propellant |
| m | exponent in Eq. 1 |
| m_1 | exponent in Eq. 22 |
| \dot{m} | rate of external mass addition |
| m^* | nondimensional rate of external mass addition by pulser = $\dot{m}/\rho_s r_i A_b$ |
| n_1 | order of gas-phase reaction in the inner zone |
| n_2 | order of gas-phase reaction in the outer zone |

| | |
|-------|---|
| p | chamber pressure |
| q_g | nondimensional heat of reaction in the outer flame zone |
| q_s | nondimensional heat of reaction in the inner flame zone |
| Q_D | pressure-insensitive surface-coupled heat release in Eq. 2 |
| Q_g | heat of combustion in the outer reaction zone |
| Q_H | pressure-sensitive surface-coupled heat release in Eq. 1 |
| Q_s | heat of combustion in the inner reaction zone |
| Q_t | total heat of combustion |
| R | gas constant |
| r | burning rate |
| T | temperature |
| t | time |
| V | chamber volume |
| w_1 | nondimensional rate of species production in the inner flame zone |
| w_2 | nondimensional rate of species production in the outer flame zone |
| W_1 | rate of species production in the inner flame zone |
| W_2 | rate of species production in the outer flame zone |
| x | distance away from propellant surface |
| x_f | flame standoff distance (microns) |
| y^* | transformed distance |

Greek Letters

| | |
|----------|--------------------------------|
| α | kinetics parameter |
| β | W_1/W_2 |
| γ | specific heat ratio, c_p/c_v |
| δ | Dirac delta function |

ζ nondimensional location of the outer flame zone
 κ thermal diffusivity of solid = $k/\rho_s c_s$
 ρ_s density of propellant
 ν propellant burning rate index

Subscripts

c chamber conditions
 cr critical value
 f gas-phase flame
 g gas phase
 i initial value at $t = 0$
 l limiting value
 o conditions at $x \rightarrow \infty$
 w conditions at wall (gas-solid interface)
 * denotes nondimensional quantity normalized to steady-state value;
 e.g., $r^* = r/r_i$, $T_f^* = T_f/T_{f_i}$. Note one exception: $T_o^* = T_o/T_{w_i}$.
 Also, $t^* = r_i^2 t/\kappa$ and $x^* = r_i x/\kappa$.

I INTRODUCTION

The understanding of composite solid propellant combustion has gradually advanced over the year with major contributions coming from several other groups¹⁻⁶ in addition to the work at Stanford Research Institute (SRI).⁷ The theoretical models that have been advanced through the years have differed only in the treatment of the heat release in the gas phase and in the vicinity of the solid surface. The heat release process has usually been assumed to be quasi-steady in nature; i.e., time lags associated with the chemical reaction processes are assumed to be small in comparison with the thermal response time of the solid phase. The heat release acts as a boundary condition on the solid phase that in turn, has been treated in a one-dimensional way in spite of the heterogeneous nature of the propellant.

Thus, the main question is how to treat the heat release process in a quasi-steady way and still retain the important aspects of the transient combustion process. In general, the combustion process of a solid propellant is extremely complex. Chemical reactions may occur both in the solid phase near the regressing surface and throughout the gas-phase boundary layer up to the point where the final flame temperature T_f is reached. The approach at SRI, both in earlier work⁷ and in the current model to be discussed in detail below, has been to consider the heat release as occurring in two thin zones, one associated with the surface temperature and one with the final flame temperature. This representation avoids the necessity of specifying the heat release distribution across the entire gas-phase thermal layer and replaces it by the simpler choice of the ratio of heat release in the two zones.

Early theoretical studies^{7, 11} showed that the presence of surface-coupled heat release would tend to make propellants more unstable and more

difficult to extinguish by rapid depressurization. Experimental studies confirmed these initial qualitative predictions. It was shown that axial-mode traveling wave instability could be induced with AP (ammonium perchlorate) propellants, but not KP (potassium perchlorate) propellants.⁹ It was also demonstrated that AP propellants were more difficult to extinguish than KP propellants.^{5, 8, 11}

The qualitative predictational success of the initial analytical concept of surface-coupled heat release led to an attempt to develop a quantitative transient combustion model that would predict the actual behavior of any given propellant formulation with a minimum of input information. Such a model was developed, based upon the stability limit line in the burning rate/pressure coordinate system which was derived in Ref. 12.

The initial analysis was patterned after the original burning rate behavior in terms of two parameters, the parameter A that described the pyrolysis behavior of the propellant surface and the parameter α that described the kinetics of the gas-phase heat release process. The SRI formulation extended the definition of α to include the kinetics of the surface-coupled heat release process as well. It was assumed that α has a constant value along the stability limit line, which will be discussed in more detail later. Knowing the transient response of any propellant at the pressure where its burning rate curve crosses the stability limit line allows the calculation of the response at any other pressure.

Reasonable agreement was obtained between the model and available experimental stability data.^{9, 10, 12} However, Culick² later pointed out that the linearized versions of all theories could be shown to be inherently of the same mathematical form; i.e., only comparison with nonlinear experiments in which the pressure and burning rate changes were not perturbations could be expected to delineate important aspects of the theoretical model.

One nonlinear experiment of practical importance is that of combustion extinction by rapid depressurization. The development of a combustion model that could describe this phenomenon would be of great value in the correlation of data from different motor sizes and, therefore, in the

prediction of the critical depressurization rate for one motor using data from another or for one propellant using data from another. Up to the present time, depressurization data have generally been correlated by plotting the critical initial depressurization rate required for extinction $(dp/dt)_{cr}$ versus the initial pressure p_i . Such a correlation is very useful for a given configuration in an engineering sense because of its simplicity, but it cannot be expected to be successful when either the propellant type or the motor size is changed because it actually represents an attempted linearization of a nonlinear problem. Evidence to support this conclusion is shown by the data of United Technology Center (UTC),^{5 6} in which it is shown that the exhaust pressure, the motor size, and the propellant type all have a strong influence on the $(dp/dt)_{cr}$ vs p_i results.

Similar depressurization data have been obtained at SRI, as well as pressurization data from an experiment that was devised to emphasize the role of the burning rate variation in the measured pressure variation.^{8, 11} Reference 9 compared these SRI experimental results to predictions of the initial SRI model that was based upon a modification of the Denison-Baum model¹³ to account for heat release that is tied to the surface conditions. It was found that an unexpected nonlinear damping behavior was present in the SRI model, leading to an unsatisfactory nonlinear predictive ability including the observation that the required $(dp/dt)_{cr}$ calculated at a given value of p_i was always considerably less than the experimental value.¹¹ Because of this behavior the current program has been devoted to a reformulation of the SRI combustion model in a more self-consistent way and to a more comprehensive comparison of the predictions of the revised model with extinction data obtained at both SRI and UTC.

Page intentionally left blank

II MATHEMATICAL FORMULATION OF THE COMBUSTION MODEL

To emphasize the importance of the surface-coupled portion of the heat release and, at the same time, to make the mathematical analysis tractable, it was assumed in the original SRI model⁷ that the heat release zone of a solid propellant can be divided into two regions: one thin zone adjacent to the propellant surface in which the rate of chemical reaction is governed by the wall temperature T_w , and a second thin zone further out in the gas phase in which the rate of chemical reaction is governed by the final flame temperature T_f . It was assumed that the surface heat release acts as a boundary condition on the solid phase.

The new model developed here is based on the same assumptions. The difference from the original model comes in the mathematical representation of the surface-coupled heat release. The original formulation supposed the surface-coupled heat release to be composed of two parts, a pressure-sensitive part

$$Q_H = H_H \left(\frac{p}{T_w} \right)^m e^{-E_H/RT_w} \quad (1)$$

and a pressure-insensitive part

$$Q_D = H_D e^{-E_D/RT_w} \quad (2)$$

Qualitative comparison with traveling-wave instability data indicated that Q_H was, in general, an order of magnitude larger than Q_D .¹¹ This is an indication that gas-phase reactions near the surface that are coupled to the wall temperature T_w are more important than solid-phase reactions just below the surface.

In the original model it was also necessary to assume a function for the transient behavior of the gas-phase heat release during transition from one steady state to another in order to satisfy the steady-state

conditions at both ends of the calculation. In the new model this is not necessary because the steady-state conditions are met by variations in the reaction rates, but not the heat release, in the two flame zones.

The original formulation went on to use the flame speed equation, which related the instantaneous flow of reactant into the gaseous reaction zone to the instantaneous gas-phase reaction rate, originally proposed by Denison and Baum.¹³ Two recent review papers by Culick^{1,2}, have emphasized the fact that the original gas-phase flame speed treatment by Denison and Baum,¹³ which was utilized in the SRI model, is a valid analysis for the flame speed of a deflagration wave proceeding through a gas-filled container such as a tube, but does not account for heat transfer to a solid wall near the flame. In the solid propellant formulation, of course, the calculated flame speed in the gas phase is equated to the burning rate of the surface so that the surface and the flame travel along with a fixed distance between them (in the steady state).

Culick's analyses apply to steady-state conditions, but because the gas-phase portion of the transient propellant combustion problem can be considered quasi-steady, his results can be applied to that problem when the boundary conditions are modified appropriately to account for the transient behavior of the solid.

In view of the observation that most of the surface-coupled heat release appears to be pressure-sensitive ($Q_H \gg Q_D$), the starting point for the new model is the assumption that the total heat release takes place in two infinitesimally thick gas-phase zones. One zone is located at the surface and governed by the wall temperature T_w and one is located further out in the gas phase and governed by the final flame temperature T_f .

The flame speed equation relates the instantaneous mass leaving the wall to the instantaneous mass being consumed in the two flame zones, based upon the assumption that the thermal relaxation time in the gas phase is very small compared to the thermal relaxation time of the solid. In this case

$$\rho_s r = \int \left[w_1 \delta(x-0) + w_2 \delta(x-x_f) \right] dx = W_1 + W_2 \quad (3)$$

where W_1 is the rate of species production at the surface ($x=0$), W_2 is the rate of production in the outer flame zone ($x=x_f$), and δ represents the Dirac delta function. Equation (3) states that all of the material leaving the surface has been converted into combustion products at the end of the outer flame zone.

The thermal equation for the gas phase is

$$\rho_s r c_p \frac{dT}{dx} - \frac{d}{dx} \left(k_g \frac{dT}{dx} \right) = \begin{cases} Q_s W_1 & \text{in inner zone} \\ 0 & \text{between zones} \\ Q_g W_2 & \text{in outer zone} \end{cases} \quad (4)$$

Integration of this equation across the gas phase from the outer edge of the inner flame zone to the outer edge of the outer flame zone gives

$$\rho_s r c_p (T_f - T_w) + \left(k_g \frac{\partial T}{\partial x} \right)_{w+} = Q_g W_2 \quad (5)$$

where the x coordinate is measured outward from the surface. Across the inner flame zone, taking account of the changes in specific heat and thermal conductivity,

$$\rho_s r (c_p - c_s) T_w - \left(k_g \frac{\partial T}{\partial x} \right)_{w+} + \left(k_s \frac{\partial T}{\partial x} \right)_{w-} = Q_s W_1 \quad (6)$$

Combining Eqs. (5) and (6) gives

$$\left(k_s \frac{\partial T}{\partial x} \right)_{w-} = Q_s W_1 + Q_g W_2 - \rho_s r (c_p - c_s) T_w - \rho_s r c_p (T_f - T_w) \quad (7)$$

where the superscript has now been dropped from w and it is understood that this is the boundary condition on the solid-phase temperature profile. It is convenient to add and subtract $c_s T_0$, rearrange terms, and use Eq. (3) to get

$$\left(k_s \frac{\partial T}{\partial x} \right)_{w-} = \rho_s r \left[-c_p (T_f - T_0) - (c_p - c_s) T_0 + c_s (T_w - T_0) + Q_s \frac{W_1}{W_1 + W_2} + Q_g \frac{W_2}{W_1 + W_2} \right] \quad (8)$$

Using the steady-state relation for the derivative of Eq. (8),

$$\left(k_s \frac{\partial T}{\partial x} \right)_{w-} = \rho_s r c_s (T_w - T_0) \quad (9)$$

it can be seen that in the steady state it must also be true that

$$c_p (T_f - T_0) + (c_p - c_s) T_0 = Q_s \frac{W_1}{W_1 + W_2} + \frac{W_2}{W_1 + W_2} \quad (10)$$

The steady-state variation of T_f is predicted from thermochemical calculations. Thus, either Q_s and Q_g or W_1 or W_2 must be made to vary through a transient calculation in such a way that the proper steady-state conditions are approached after transition through the transient. In the present model, Q_s and Q_g are considered constant, and W_1 and W_2 are forced to vary in the proper way to satisfy the known steady-state variation of T_f .

The next step is to choose specific relationships for W_1 and W_2 . Following the work of Denison and Baum,¹³ in view of the fact that all reactions are now associated with the gas phase, let

$$W_1 = K_1 p^{n_1} T_w^{n_1+2} \exp(-E_h/RT_w) \quad (11)$$

and

$$W_2 = K_2 p^{n_2} T_f^{n_2+2} \exp(-E_f/RT_f) \quad (12)$$

In Eqs. (11) and (12), n_1 and n_2 are considered to be constants while E_h and E_f are assumed to be functions of pressure alone since the temperature occurs explicitly in the argument of the exponential. Since E_h and E_f are assumed to be functions of pressure alone, their instantaneous behavior can be calculated from the steady-state equations corresponding to the instantaneous pressure; this technique of solution automatically assures that the thermochemical prediction will be satisfied in the steady state.

Culick¹ discusses the fact it is an approximation to consider a delta function flame zone with a finite reaction rate such as that given by Eq. (11) or Eq. (12). Delta function representation is an approximation that will be valid if the standoff distance x_f is much larger than the thickness of the heat release zone, which is true under most circumstances of interest.

An expression for the outer flame zone location can be conveniently

obtained by use of the transformation of Culick² for the gas-phase thermal equation:

$$\zeta = \exp(\rho_s r_c x / k_g) \quad (13)$$

If it is assumed that k_g is constant, the thermal equation between the two flame zones becomes

$$\frac{d^2T}{d\zeta^2} = 0 \quad (14)$$

i.e., the temperature profile is linear between the two heat release zones in the ζ -coordinate system. Using the heat transfer rate at the outer edge of the inner heat release zone and the known flame temperature as the two boundary conditions, one can solve Eq. (14) to obtain

$$\zeta_f = \frac{Q_g}{Q_g - c_p (T_f - T_w) (1 + \beta)} \quad (15)$$

where $\beta = W_1/W_2$. Equation (15) reduces to Culick's result² when there is no heat release associated with the inner boundary; i.e., when Q_s and W_1 (and therefore β) are taken as zero. The physical location of the outer heat release zone x_f is then given by

$$x_f = \frac{k_g}{\rho_s r_c p} \ln \zeta_f \quad (16)$$

The remaining point to be considered is the calculation of reference values for the activation energies E_h and E_f . According to the present analysis, reference values are calculated by choosing a value for the magnitude of the linear response at the point on the burning rate curve where an intersection with the "stability limit line" occurs. This is illustrated in Fig. 1 where the burning rate curves of the one SRI propellant (PU-269) and the five UTC propellants studied under this program are shown with the stability limit line from Ref. 10. (See also Refs. 9 and 12 for more details.) The limit line shown in Fig. 1 can be approximated for computational purposes by the equation

$$r_\ell = 0.00239 p_\ell^{0.726} \quad (17)$$

where r_ℓ is given in in./sec and p_ℓ in psia.

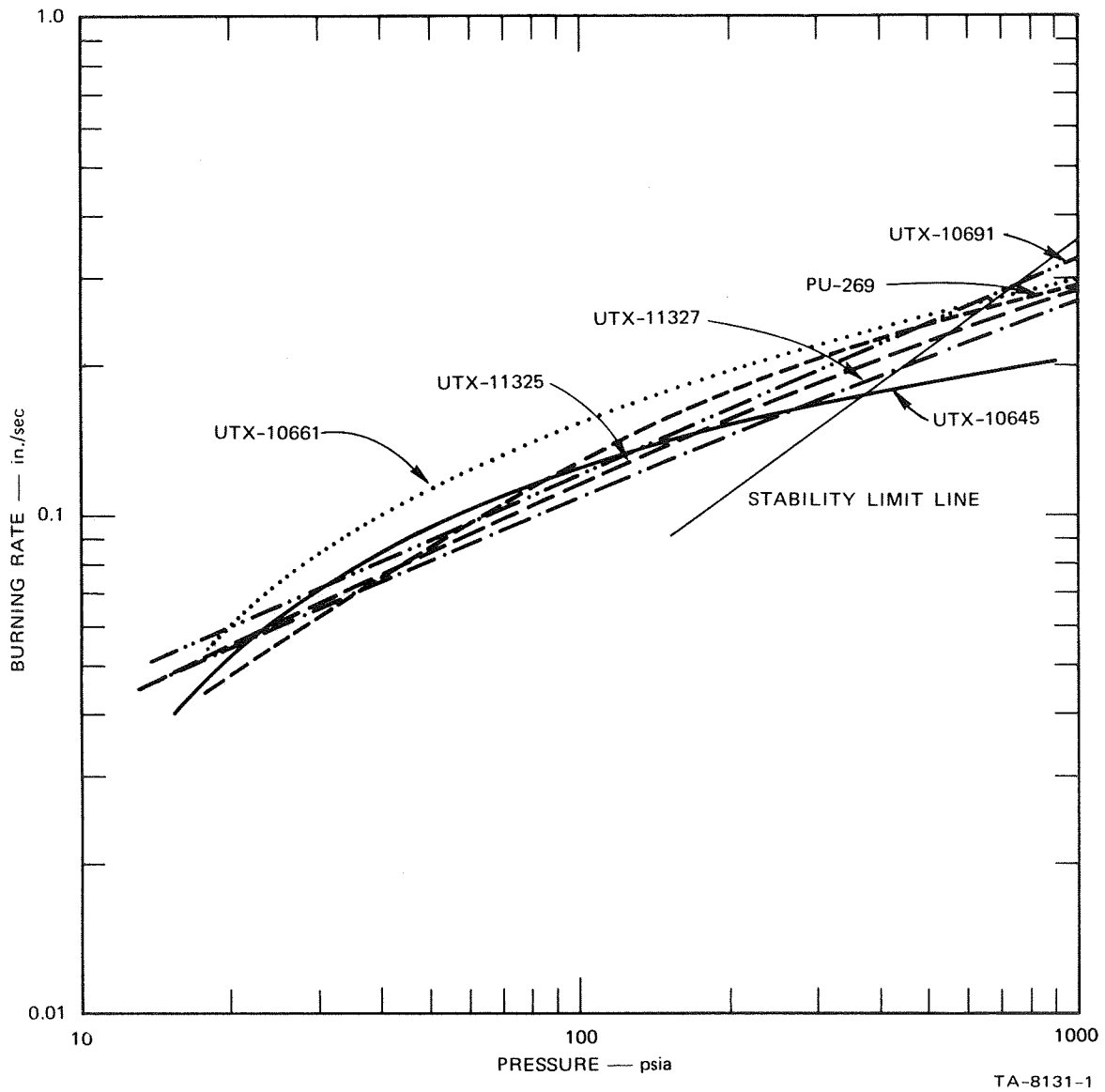


FIGURE 1 STRAND BURNING RATE VERSUS PRESSURE

Equation (17) is a least-squares fit of all the traveling wave instability data obtained at SRI.⁹

Two parameters govern the linear response, A and α . The parameter A is a pyrolysis kinetics parameter given by

$$A = \frac{E_w}{RT_w} \left(1 - \frac{T_0}{T_w} \right). \quad (18)$$

The parameter α , first introduced by Denison and Baum,¹³ is a kinetics parameter related to the chemistry of the two reaction zones. It is obtained from a perturbation of the boundary condition at the wall, Eq. (8), where the perturbation is written in the form^{7, 13}

$$\frac{k_s}{\rho_s c_s \bar{r}} \left(\frac{\partial \tilde{T}_w}{\partial x} \right)_w = \left[1 + A (1 - \alpha) \right] \tilde{T}_w + \nu \alpha \left(1 - \frac{T_0}{T_w} \right) \tilde{\rho} \quad (19)$$

For a chosen constant level of linear response, the relationship between the two governing linear parameters A and α can be approximated by an expression of the form

$$\alpha = a_1 \ln A + a_2 \quad (20)$$

An expansion of Eq. (8) cast into the form of Eq. (19) using Eq. (18) for A, results in two expressions for α which can be solved simultaneously to obtain expressions for E_f and E_h , the variable activation energies, at the stability limit. Once values^l of E_f and E_h are established, values of E_f and E_h through any transient process^l can be established by steady-state equations since they are functions of pressure only. The value of α can also be calculated at any other pressure; the equation used for this in the numerical analysis is

$$\alpha = \frac{\bar{T}_w}{\bar{T}_w - T_0} \left\{ q_s w_1 + q_g w_2 - \frac{RT_w}{E_w} q_s w_1 N_1 + \left[\frac{c_p \bar{T}_f}{c_s \bar{T}_w} - q_g w_2 N_2 \right] \left[\frac{1 - \frac{RT_w}{E_w} w_1 N_1}{w_2 N_2} \right] \right\} \quad (21)$$

where

$$q_s = \frac{Q_s}{c_s \bar{T}_w} \quad q_g = \frac{Q_g}{c_s \bar{T}_w}$$

$$w_1 = \frac{\bar{W}_1}{\bar{W}_1 + \bar{W}_2} \quad w_2 = \frac{\bar{W}_2}{\bar{W}_1 + \bar{W}_2} = 1 - w_1$$

$$N_1 = n_1 + 2 + \frac{\bar{E}_h}{RT_w} \quad N_2 = n_2 + 2 + \frac{\bar{E}_f}{RT_f}$$

A complete derivation of the technique for obtaining E_{h_ℓ} and E_{f_ℓ} and the expression shown in Eq. (21) is given in Appendix A.

The calculation of the transient behavior of any propellant requires starting calculations at both the limiting pressure and the initial pressure to establish initial values of the governing propellant parameters. The following steps are involved:

1. Choose reference values of T_w at a burning rate of 0.1 in./sec and of T_f at 100 psia. Any reference points could be chosen as long as they are used in a consistent manner.
2. Choose values for the propellant parameters μ , ρ_s , c_s , c_p , k_g , and γ .
3. Choose values for the kinetic parameters E_w , n_1 , n_2 , and m_1 . The parameter m_1 relates the measured propellant burning rate at a given pressure to the calculated thermochemical flame temperature at the same pressure through the simple equation

$$T_f^* = r^{*m_1} \quad (22)$$

for the steady state.

4. Assign values to the heat releases Q_s and Q_g that are considered to be constant.
5. Assign values to the constants a_1 and a_2 , corresponding to the chosen response; i.e., the chosen value of α at the threshold

Pressure. For the current calculations, $a_1 = 0.226$ and $a_2 = 0.170$ have been used, corresponding to a linear response level of

$$\left| \frac{1}{v} \frac{\tilde{r}}{\tilde{p}} \right| \approx 7,$$

a reasonable value for most composite AP propellants.⁷

6. At the threshold pressure point:
 - a. Calculate the threshold pressure p_ℓ by satisfying both the known burning rate/pressure dependence and Eq. (17).
 - b. Using the procedure outlined in Appendix A, calculate the activation energies E_{h_ℓ} and E_{f_ℓ} .
7. At the chosen initial pressure:
 - a. Calculate W_{1i} and W_{2i} from the two simultaneous equations

$$\left[c_p (T_{f_i} - T_0) + (c_p - c_s) T_0 - Q_s \right] W_{1i} = \left[Q_g - c_p (T_{f_i} - T_0) - (c_p - c_s) T_0 \right] W_{2i} \quad (23)$$

$$\frac{r_i}{r_\ell} = \frac{W_{1i} + W_{2i}}{W_{1\ell} + W_{2\ell}} \quad (24)$$

- b. Use the calculated values of W_{1i} and W_{2i} with Eqs. (11) and (12) to calculate E_{h_i} and E_{f_i} .

A listing of the numerical program and a sample printout for a typical calculation are given in Appendix B.

A short comment should be made concerning the use of the transformation

$$y^* = 1 - e^{-x^*} \quad (25)$$

where $x^* = r_i x / \kappa$. (The distance x is measured positive into the propellant away from its surface for the solid phase calculation.) This transformation changes the infinite spatial domain in the solid $0 \leq x^* \leq \infty$ into a

finite domain $0 \leq y^* \leq 1$ in the y^* coordinate system. It was first used by the author in Ref. 11. Recently Merkle et al.⁴ have pointed out that great care must be exercised in applying this transformation because the temperature derivative at the cold boundary ($y^* = 1$) is nonanalytic. This factor can easily be seen if we consider the temperature profile corresponding to the transformation of Eq. (25):

$$\frac{T^* - T_0^*}{T_w^* - T_0^*} = (1 - y^*)^{r^*} \quad (26)$$

Another advantage of the transformation is shown by Eq. (26); i.e., initially the temperature profile is linear in the transformed coordinate. The temperature derivative is now given by

$$\frac{\partial T^*}{\partial y^*} \sim r^* (1 - y^*)^{r^* - 1} \quad (27)$$

For $r^* < 1$ and $y^* = 1$, the derivative then becomes infinite and one must take care in the numerical analysis to be sure that this singularity must not be allowed to affect the computation of the temperature profile. This computation is accomplished as described in detail in Appendix B of Ref. 11 by making use of the fact that $T^* = T_0^*$ at $y^* = 1$; i.e., only the derivatives at the other mesh points are needed to obtain the total solution and no difficulty has ever been encountered in obtaining the correct steady-state temperature profile after a decrease in burning rate. An example of such a calculation is shown in detail in Appendix C. In addition to the advantages cited previously, use of the transformation given by Eq. (25) allows an important saving of numerical computation time by reducing substantially the number of mesh points required inside the solid.

III PARAMETRIC STUDY OF THE MODEL

Before proceeding to a comparison of predicted and observed extinction behavior it is instructive to carry out a parametric study of the model in both the linear and nonlinear regimes to determine which of the chosen input parameters have the largest effects on the observed output. In this case the effects of varying the parameters Q_s/Q_t , Q_t , n_1 , n_2 , E_w , T_w , and κ have been studied under conditions of a step pressure change of 1% and 20% (the 20% change was actually applied as a steep ramp over a time period of 0.2 msec) at 1000 psia chamber pressure using typical values for the SRI PU-269 AP propellant. The computed thermochemical flame temperature of this propellant is shown in Fig. 2 with the flame temperatures of the five UTC propellants that will be considered in the next section.

In addition to the parameters listed above, a few other inputs are needed to start the program. Values used for these inputs are:

$$c_s = c_p = 0.4$$

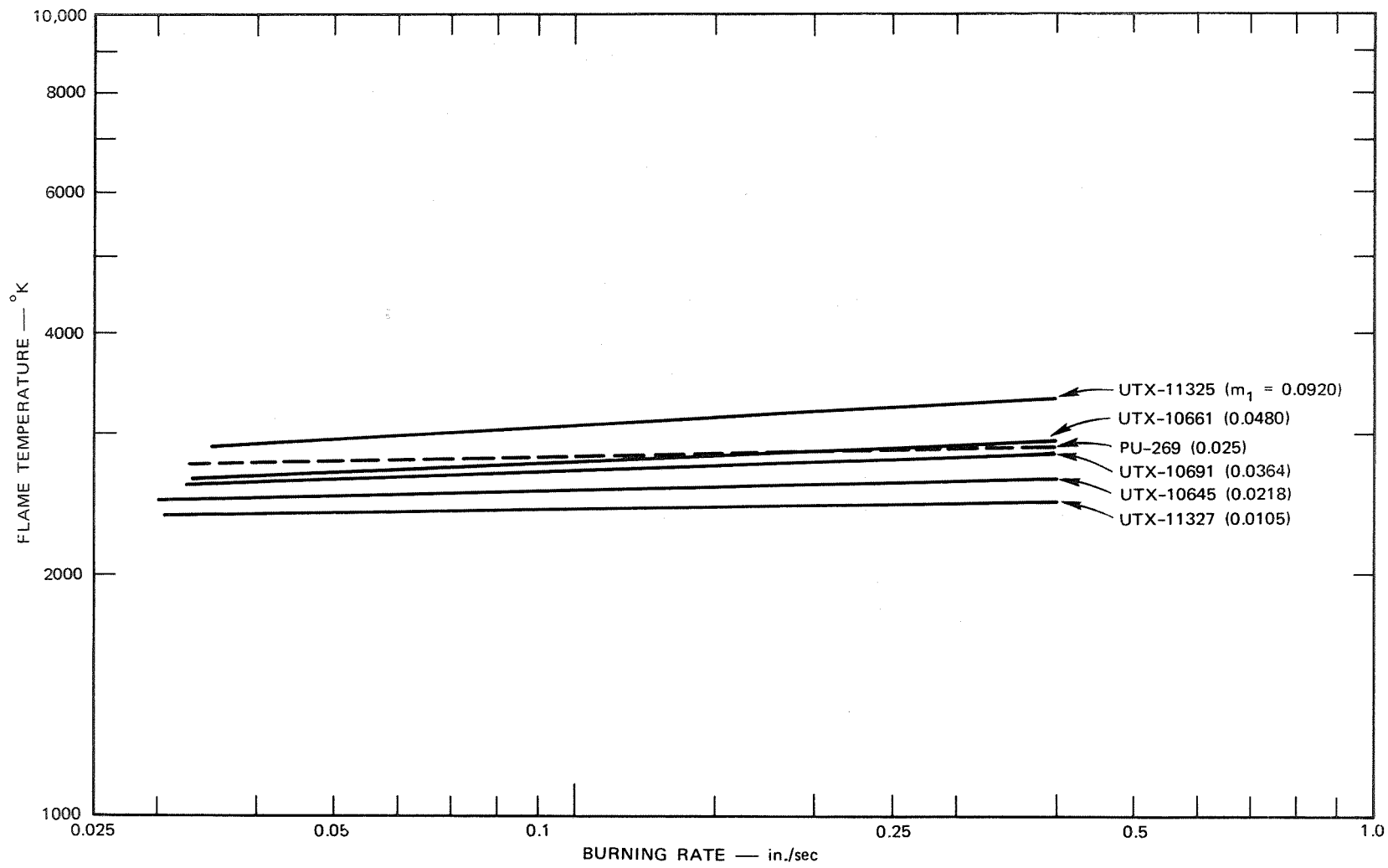
$$T_0 = 300^{\circ}\text{K}$$

$$\gamma = 1.2$$

$$k_g = 0.0004$$

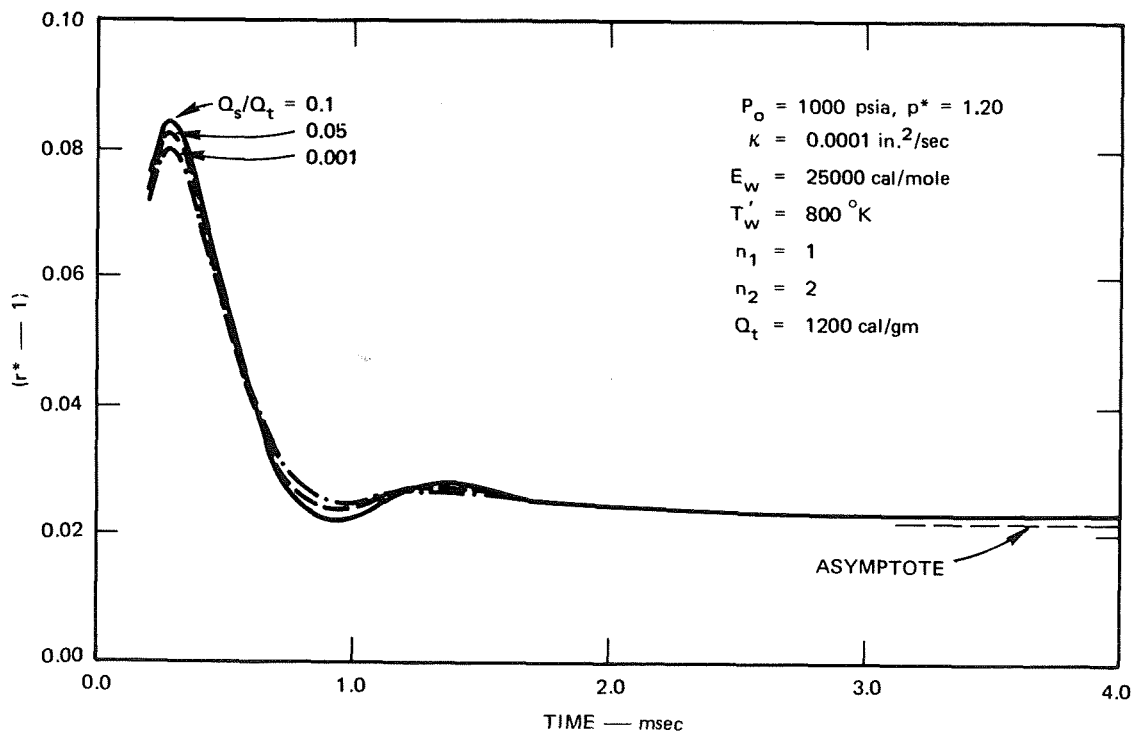
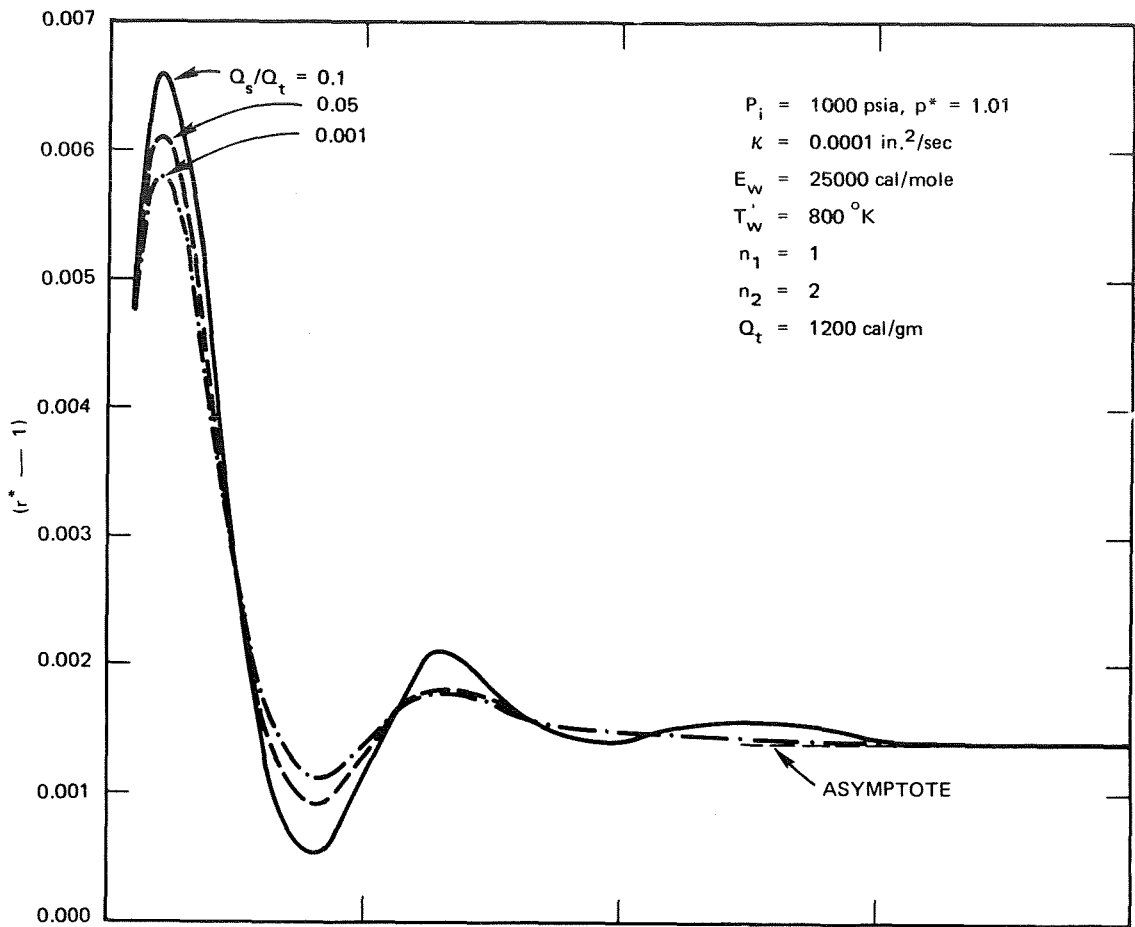
$$\rho_s = 0.06$$

It can be shown that variations in ρ_s , which may at first appear to be an important parameter, do not affect the response. Figure 3 shows the effect of varying Q_s/Q_t , the ratio of heat release associated with the surface reaction zone to the total heat release. At the chosen chamber pressure, which is higher than the pressure at which the burning rate curve crosses the stability limit line (see Fig. 1), the response increases as Q_s/Q_t increases. Thus, more surface heat release is destabilizing; the effect



TA-8131-2

FIGURE 2 FLAME TEMPERATURE VERSUS BURNING RATE



TA-8131-3

FIGURE 3 EFFECT OF VARIABLE Q_s/Q_t AT HIGH PRESSURE (PU-269)

is proportionately (but not absolutely) smaller for the larger pressure increase. Note that the asymptotic steady state is also shown.

An extremely interesting result is obtained when the effect of variable Q_s/Q_t at a pressure below the stability limit crossing is considered. In Fig. 4, where results are plotted for a chamber pressure of 400 psia, it can be seen that an increase in Q_s/Q_t reduces the response; in addition, the overall response level appears to be larger than that shown in Fig. 3a.

This behavior can be understood if we plot the burning rate response in its proper nondimensional form, shown in Fig. 5 for $Q_s/Q_t = 0.05$ and 0.1 . Note that the curves cross at the pressure (645 psia) where the burning rate curve crosses the stability limit line in Fig. 1; this is built into the numerical analysis through the specification of the parameter α at that point. The salient fact is the increase in slope as Q_s/Q_t increases; the absolute value of the slope is governed by the chosen value of Q_t . This increase in slope may explain why propellants with surface-coupled heat release tend toward instability: not only does their response reach a certain level at the stability limit, but it also tends to increase more rapidly as the pressure is increased beyond that limit point. This result may help to explain the small scatter that is observed experimentally about the stability limit line.^{9, 10, 12}

Figure 6 shows the effect of varying the total heat release on the observed burning rate response. It can be seen that increasing the heat release as the ratio Q_s/Q_t remains constant decreases the response somewhat. Numerical computations have shown that the allowable range of choice for Q_t is rather limited once values have been assigned to the other parameters. In the present case when Q_t is reduced below about 1100 cal/gm, the ratio W_1/W_2 becomes negative, implying that the main flame requires more species for consumption than are leaving the wall, a physically meaningless case. On the other hand, when Q_t is increased above about 1400 cal/gm, the slope of the curves shown in Fig. 5 becomes negative, which violates a basic assumption of the theory; namely, that the observed burning rate response should increase with increasing pressure. These results are in agreement with Eq. (10), which shows that for the values of c_p and T_f

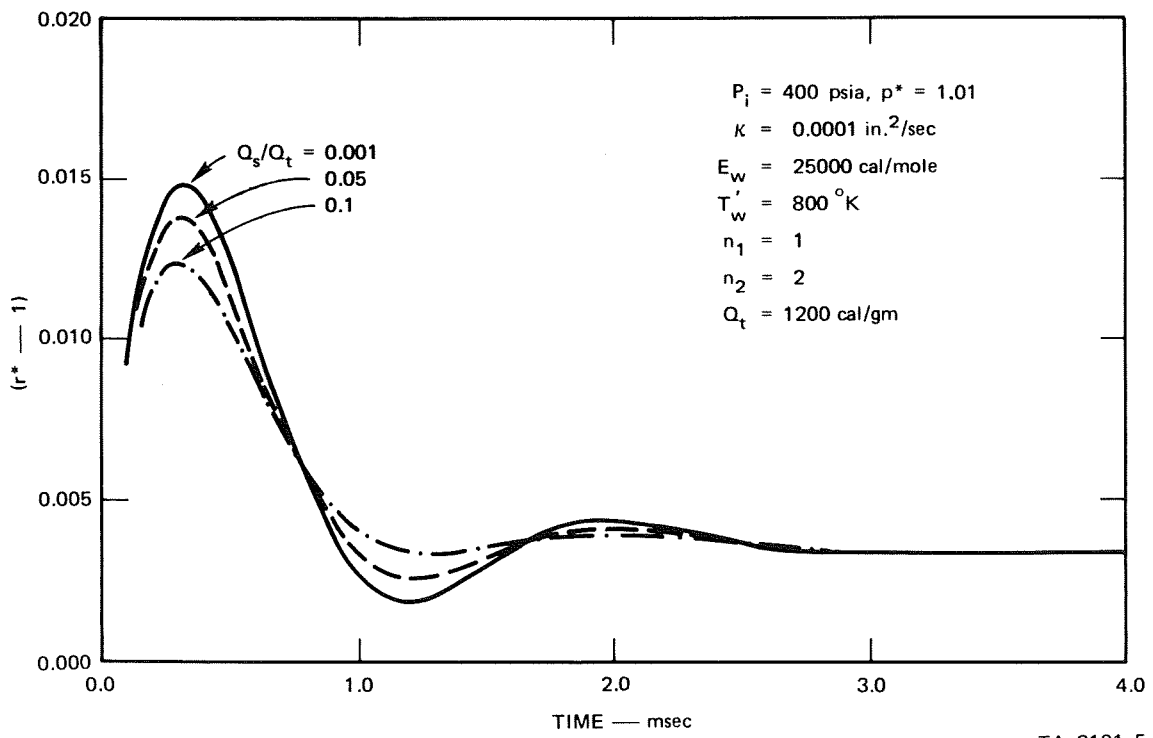


FIGURE 4 EFFECT OF VARIABLE Q_s/Q_t AT LOW PRESSURE (PU-269)

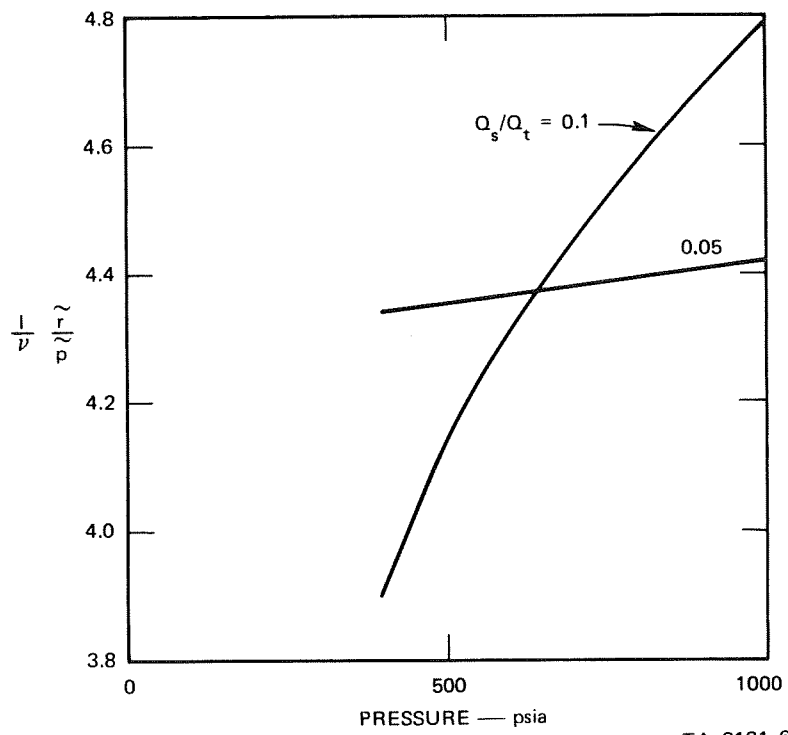
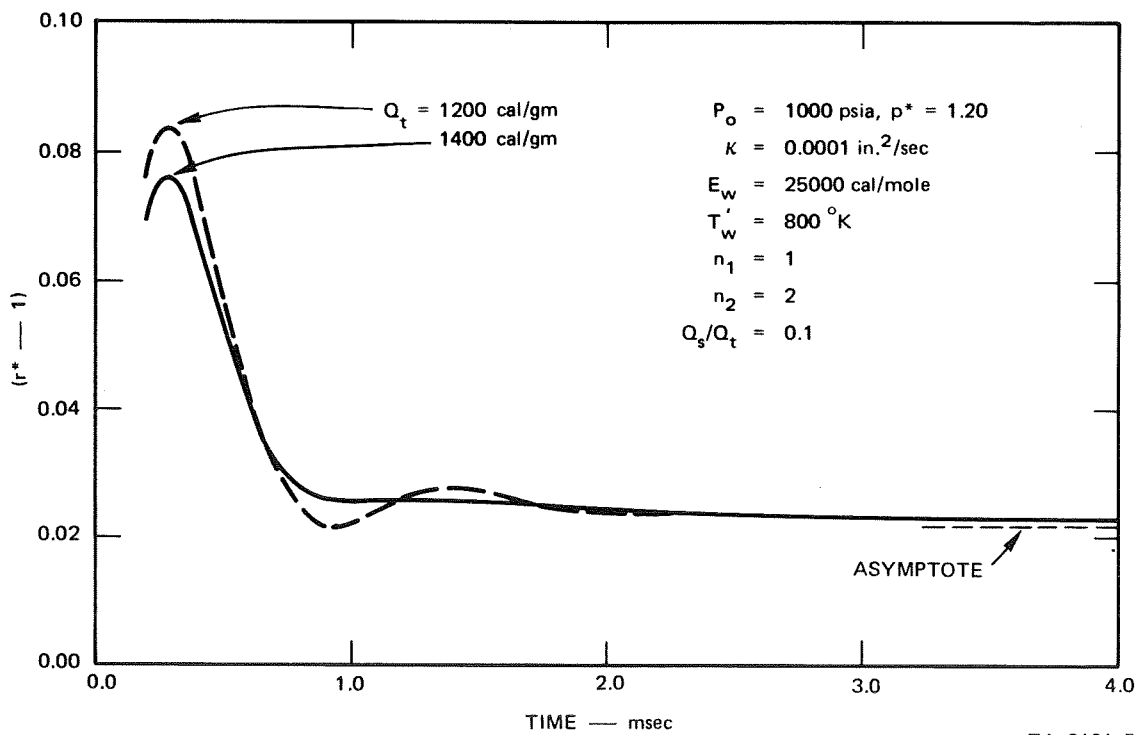
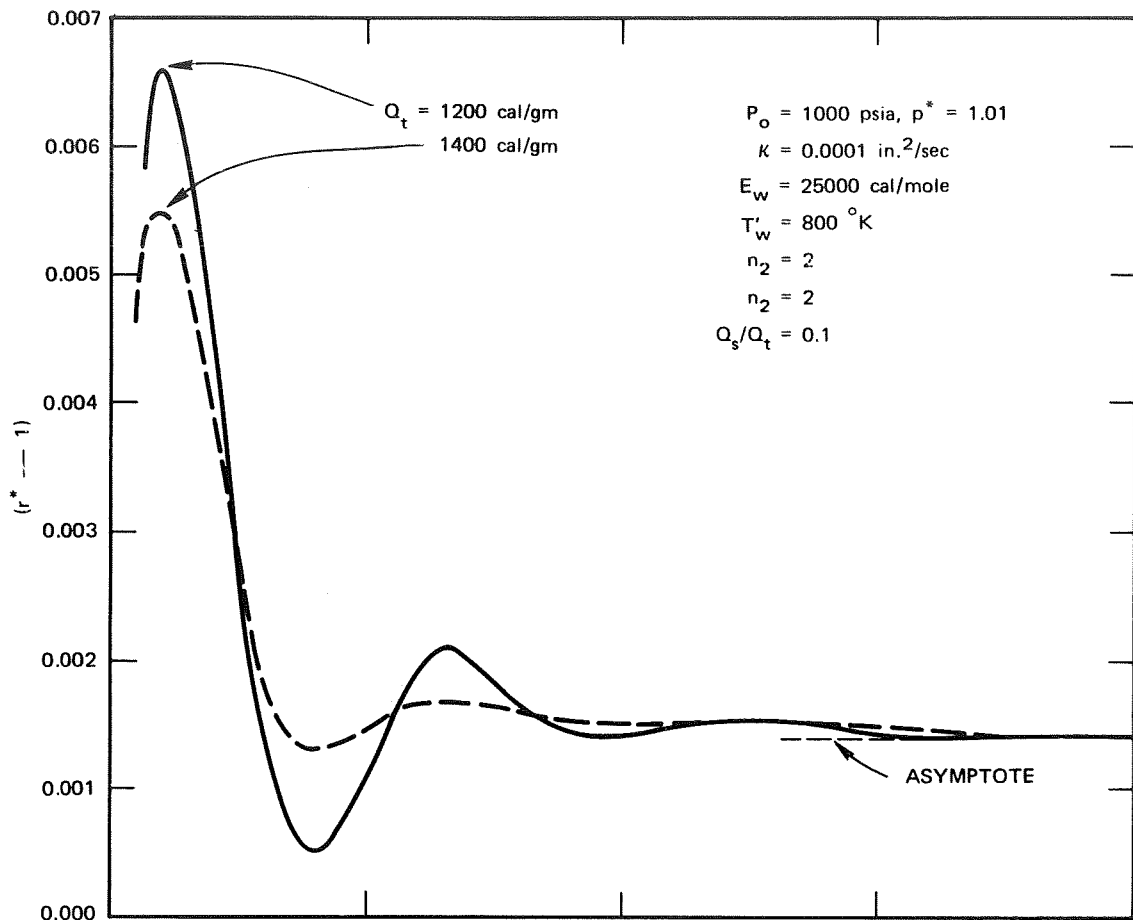


FIGURE 5 LINEAR BURNING RATE RESPONSE AS A FUNCTION OF PRESSURE (PU-269)

TA-8131-6



TA-8131-7

FIGURE 6 EFFECT OF VARIABLE Q_t AT HIGH PRESSURE (PU-269)

being used the total heat release should be in the neighborhood of 1200 cal/gm, lending further consistency to the calculations.

Figures 7 and 8 show the effects of varying the reaction rate pressure exponents n_1 and n_2 . It can be seen that a variation in n_1 affects the burning rate response slightly whereas a variation in n_2 has practically no effect. This apparently occurs because changes in n_1 or n_2 are offset by changes in the calculated behavior of E_h and E_f with pressure, leading to nearly the same burning rate response.

The effect of varying the pyrolysis activation energy at the surface is shown by Fig. 9. Increasing the activation energy in general acts to decrease the burning rate response time and therefore to damp the observed oscillation. Decreasing the chosen surface temperature, on the other hand, also acts to decrease the response time but does not destroy the oscillation so readily, as shown by Fig. 10.

Figure 11 shows the effect of varying the thermal diffusivity κ . As one would expect, the characteristic response time of the burning rate is proportional to κ ; i.e., the first peak for $\kappa = 0.0005 \text{ in}^2/\text{sec}$ occurs at a time that is approximately a multiple of five times the value of the time at which the curve for $\kappa = 0.0001 \text{ in}^2/\text{sec}$ exhibits its peak.

With the calculations just discussed as a background, it is now appropriate to turn to a discussion of experimental data.

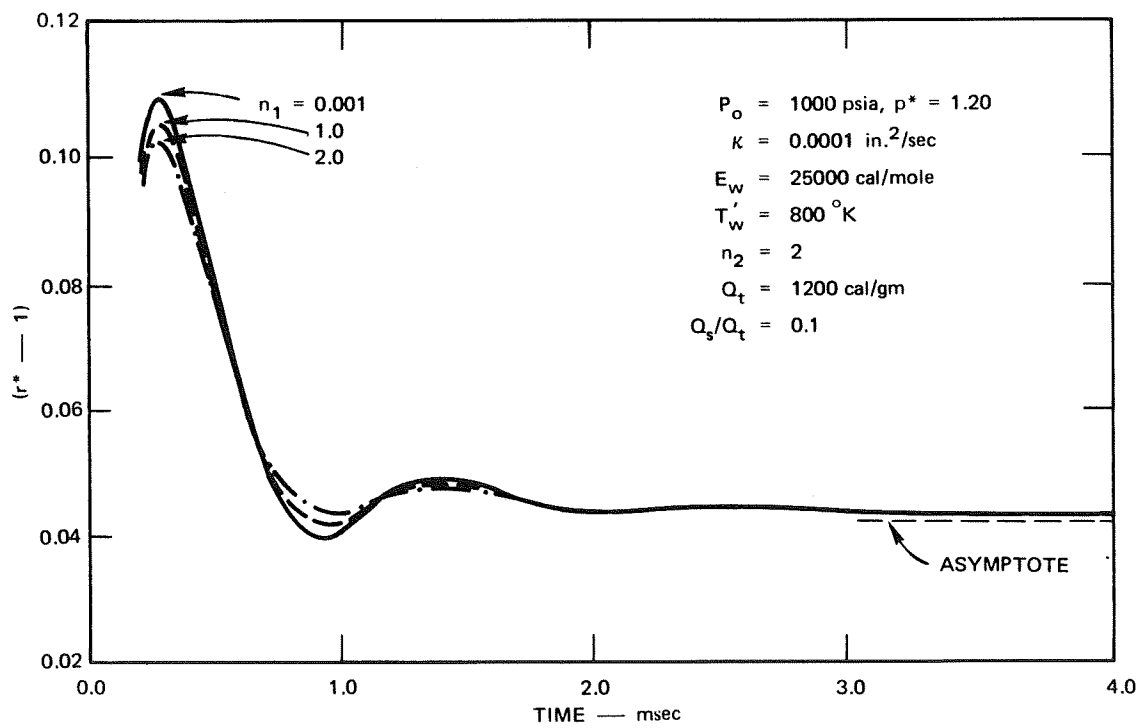
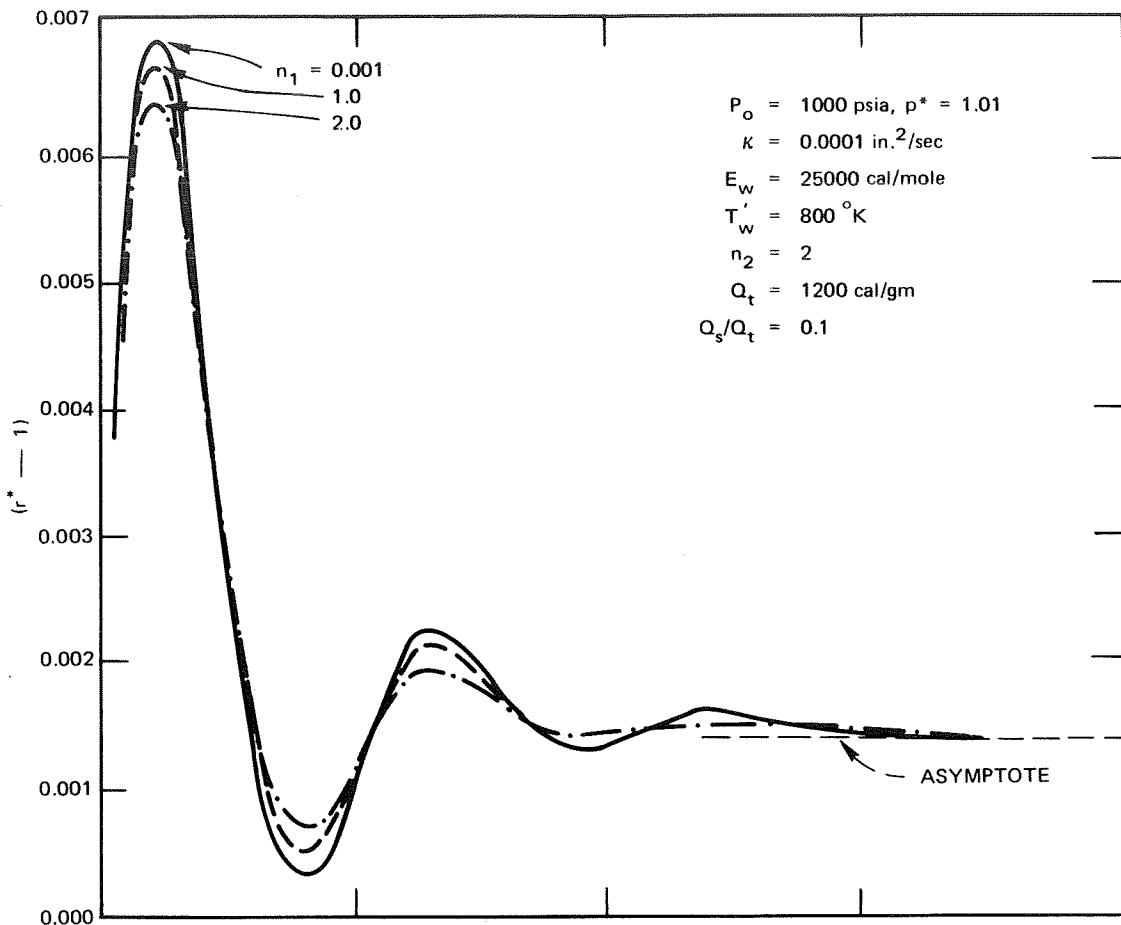
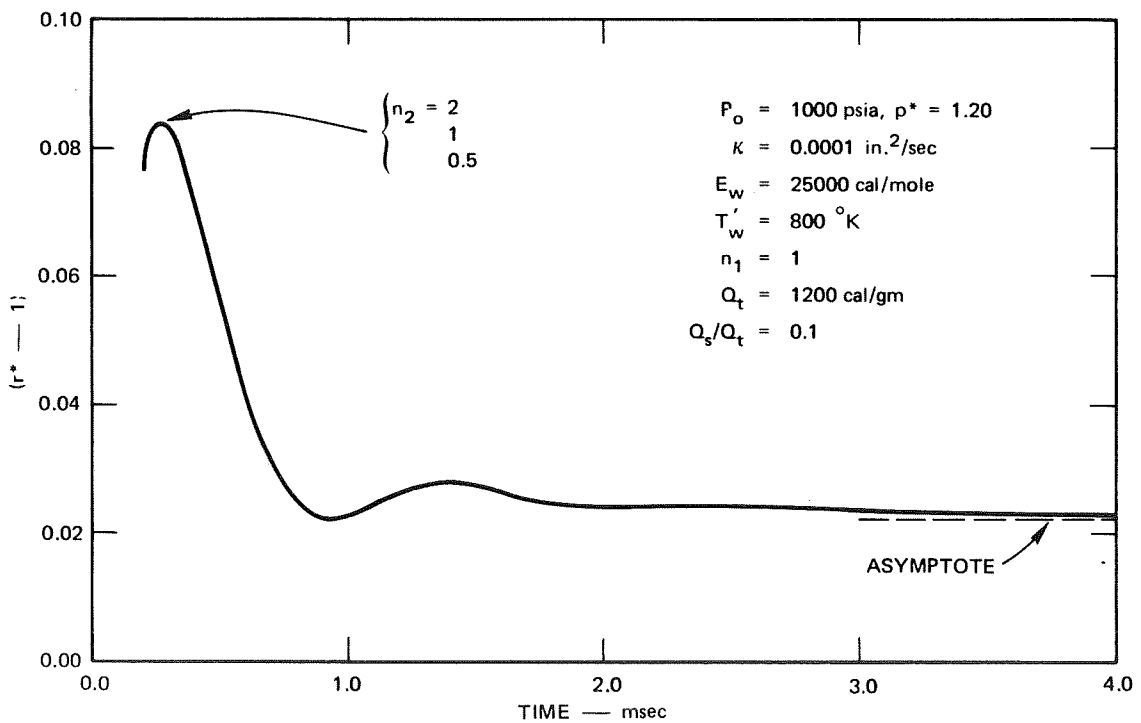
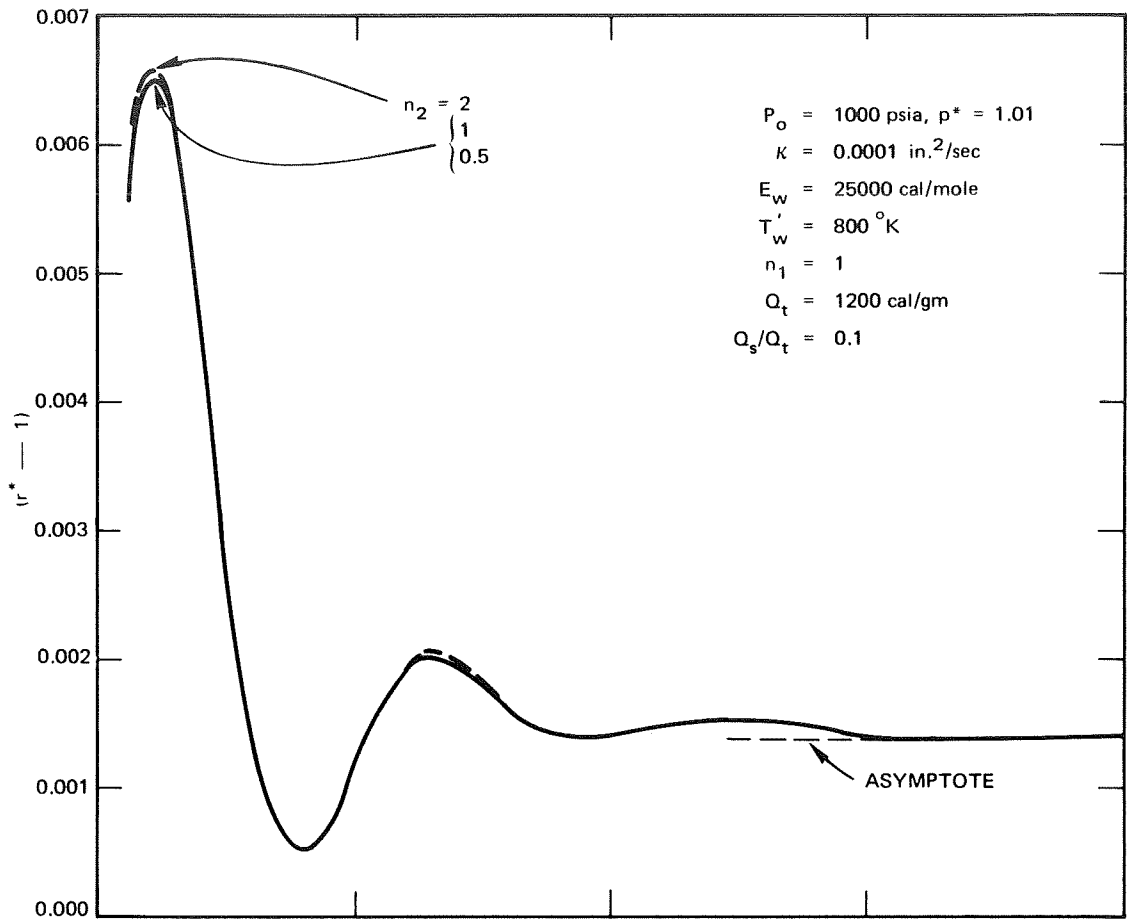
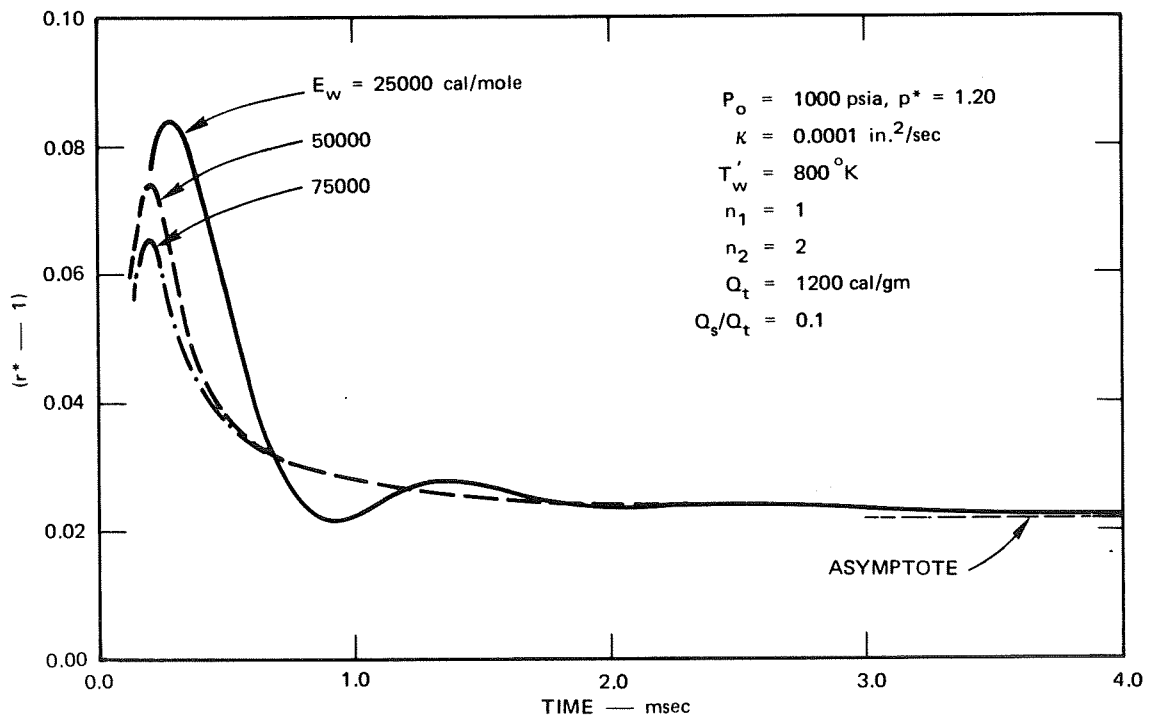
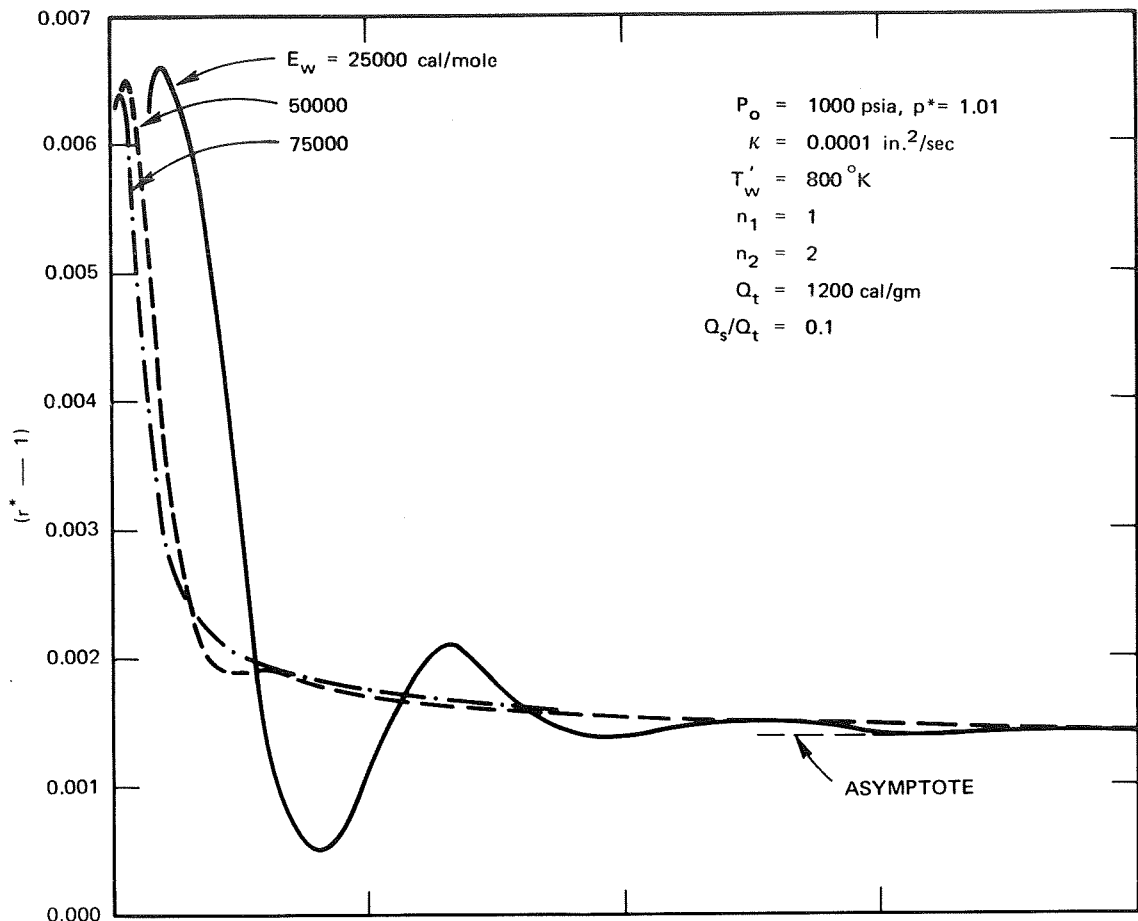


FIGURE 7 EFFECT OF VARIABLE n_1 AT HIGH PRESSURE (PU-269)



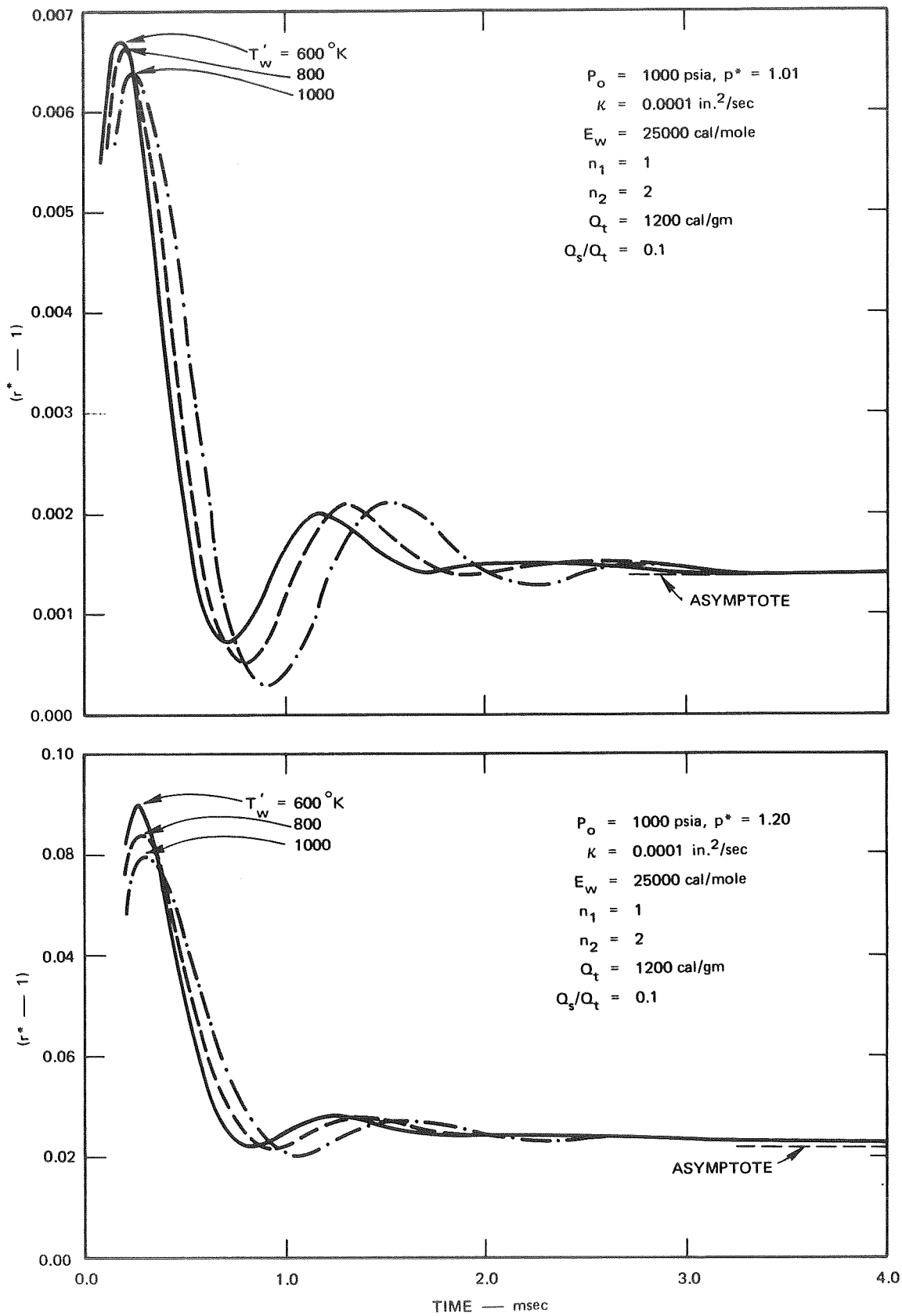
TA-8131-11

FIGURE 8 EFFECT OF VARIABLE n_2 AT HIGH PRESSURE (PU-269)



TA-8131-13

FIGURE 9 EFFECT OF VARIABLE E_w AT HIGH PRESSURE (PU-269)



TA-8131-15

FIGURE 10 EFFECT OF VARIABLE T'_w AT HIGH PRESSURE (PU-269)

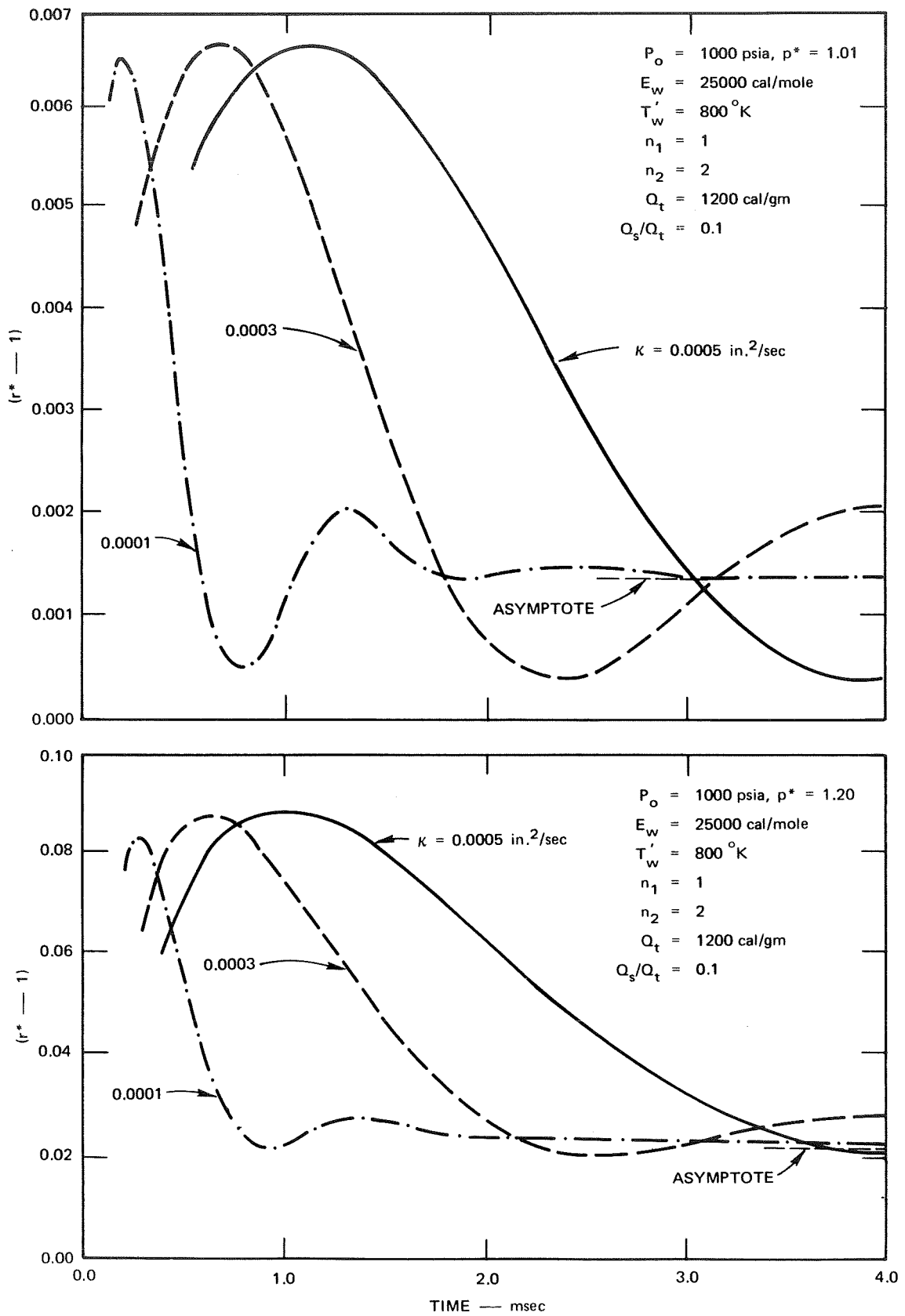


FIGURE 11 EFFECT OF VARIABLE κ AT HIGH PRESSURE (PU-269)

Page intentionally left blank

IV COMPARISONS WITH EXPERIMENTAL DATA

Pressurization Data

Some pressure response data were previously obtained at SRI by rapidly pressurizing a chamber having a very small value of V/A_b ($\sim 0.05-0.1$) with external mass addition.¹¹ The objective was to have a small enough free volume compared to the burning surface area so that the burning rate response would measurably affect the pressure response, and, in fact, an experimentally oscillating pressure response was obtained.¹¹ The previous version of the SRI model appeared to respond as though the burning rate followed the pressure too closely, and no oscillation was obtained.¹¹

Figure 12 shows the previous data and the pressure response of the current model. In this case the calculated pressure is closer to the observed pressure early in the experiment, but clearly no undershoot is obtained. More experiments of this type with other propellants are obviously needed to determine whether the experimental procedure or the mathematical model is responsible for the poor agreement that is observed. The main thrust of this program was to compare the model predictions with the extensive depressurization data collected at UTC,^{5,6} as well as those of SRI.^{8,11} These comparisons follow.

Depressurization Data

Far more data are available in the case of depressurization because of its practical importance in extinguishment. To compare the theoretical model and these results with the least amount of numerical computing, it was decided to proceed by holding as many of the variables as possible constant. The results of the preceding section show that the two most influential variables are κ , which determines the time constant of the propellant response, and Q_t , which must lie between certain bounds in order both to assure the proper variation of α with pressure and to maintain a positive value for the ratio W_1/W_2 .

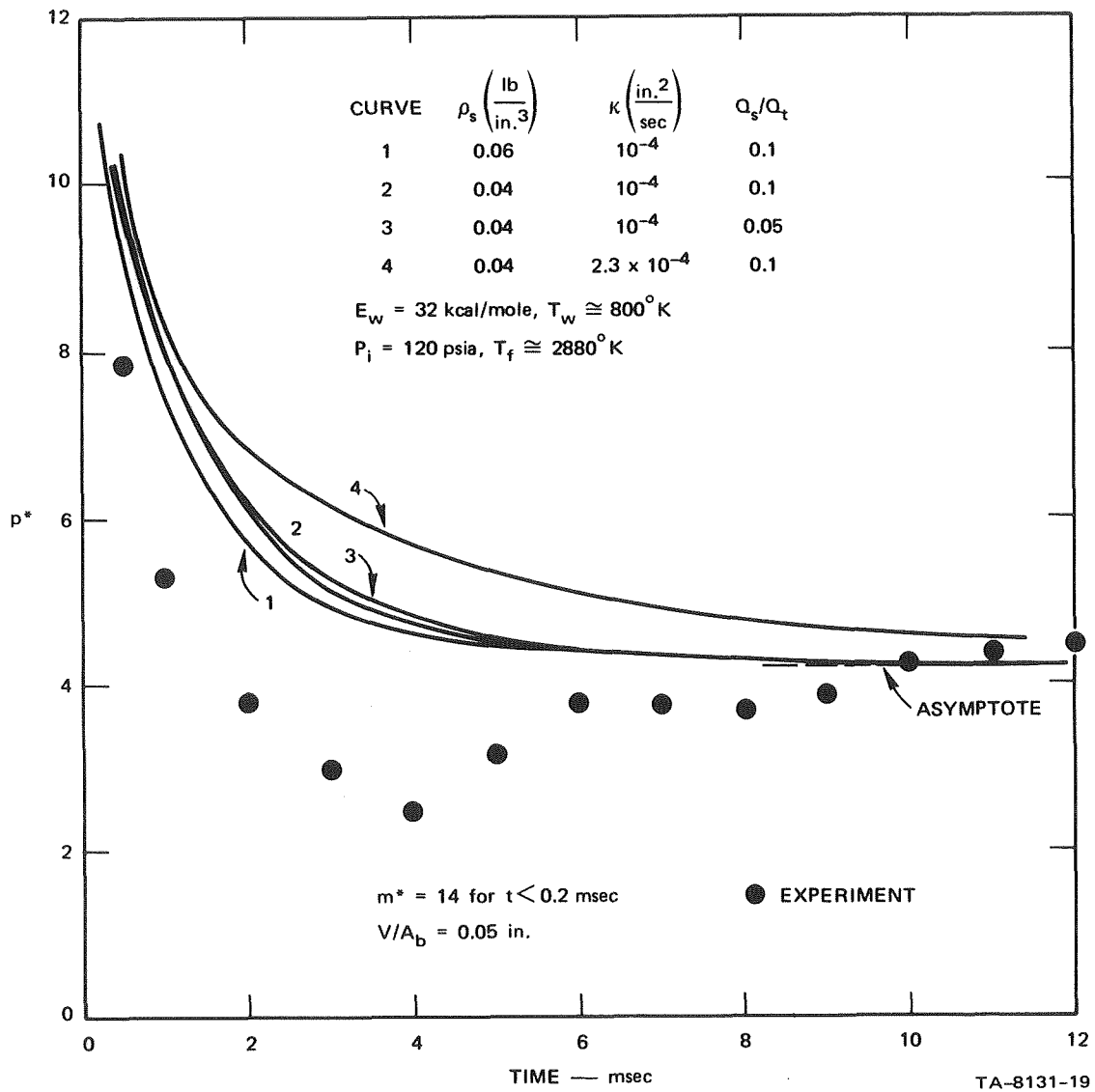


FIGURE 12 COMPARISON OF THEORY WITH OBSERVED PRESSURIZATION RESPONSE (PU-269)

Previous results obtained during depressurization tests on PU-269 can be used to establish values of the constants (excluding those already listed on Page 15); the values are

$$\kappa = 0.0001 \text{ in}^2/\text{sec}$$

$$T'_w = 800^\circ\text{K}$$

$$n_1 = 1$$

$$N_2 = 2$$

$$E_w = 50,000 \text{ cal/mole}$$

$$Q_s/Q_t = 0.1$$

Use of the above values together with $Q_t = 1200 \text{ cal/gm}$ for PU-269 gives good agreement between calculated and observed depressurization rates required for extinction.

Figure 13 shows the calculated behavior of the burning rate and pressure of this propellant at two initial depressurization rates in a small chamber containing an end-burning grain. Extinction data for this propellant in the SRI test apparatus have previously been reported; the critical initial depressurization rate required to reach extinction is somewhat in excess of $100,000 \text{ psi/sec}$.¹¹ Figure 13 is interesting because of the oscillatory behavior exhibited by the burning rate at a depressurization rate of $100,000 \text{ psi/sec}$. Imposition of a higher rate merely leads to extinction sooner and, furthermore, the burning rate oscillations are much less intense.

The procedure followed during the remaining calculations, then, was to vary only the total heat release Q_t in order to satisfy the restrictions mentioned before. Such an approach assumes that the only propellant characteristics in addition to Q_t that affect the transient response are the measured burning rate behavior and the calculated thermochemical flame temperature behavior, since these are the only additional inputs (except for the motor geometry) to the numerical program.

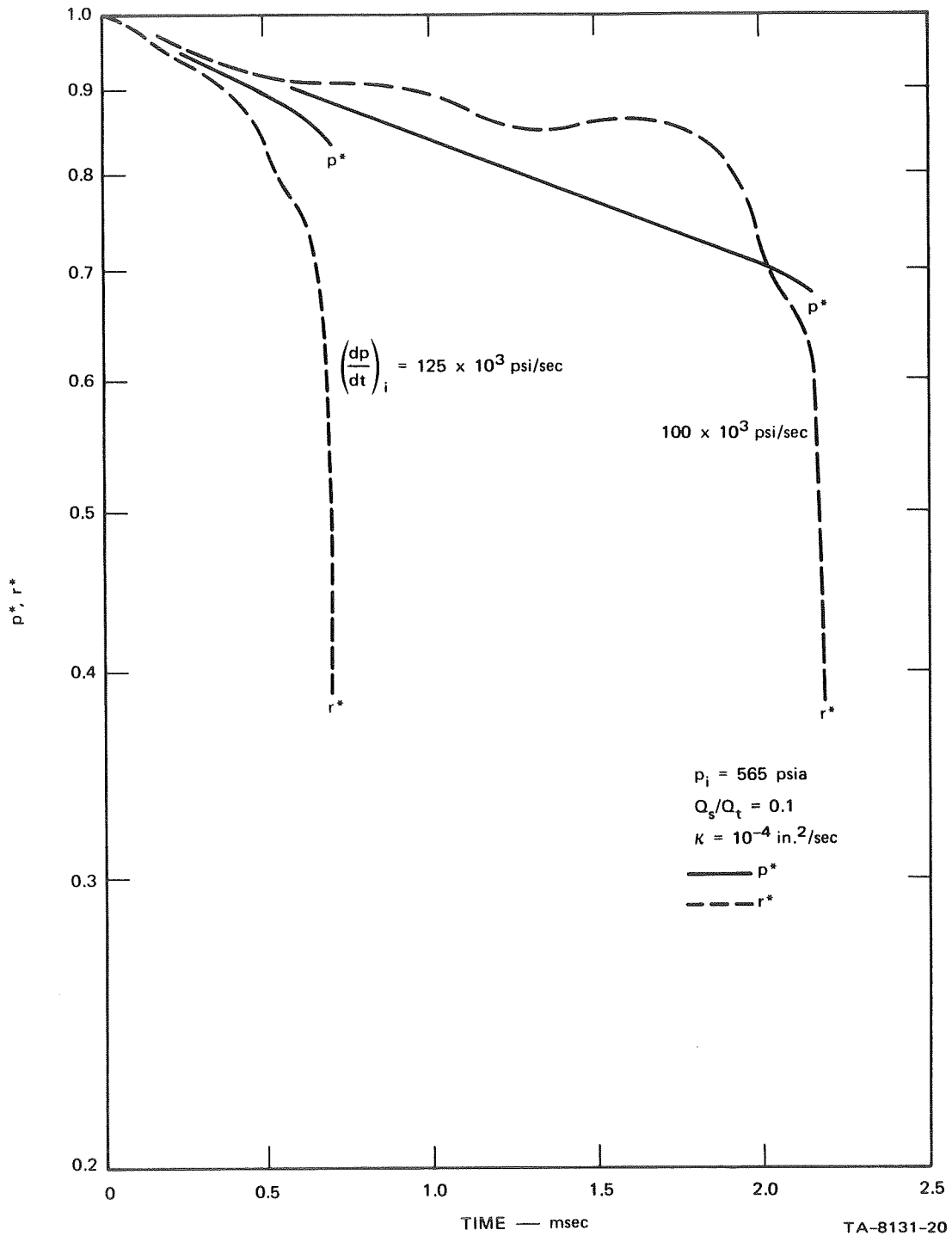


FIGURE 13 CALCULATED EXTINCTION BEHAVIOR (PU-269)

A great deal of extinction data has been obtained for NASA at UTC; a complete description of their studies is given in Refs. 5 and 6. The UTC study was concerned with the effects of systematic variations in propellant binder, oxidizer loading level, burning rate catalyst, metal loading, and exhaust pressure level. From the myriad results presented in Ref. 6, five propellants and three motor geometries were chosen for comparison with and three motor geometries were chosen for comparison with the SRI theory. A description of these propellants is given in Table I (the SRI propellant is included for completeness); they will hereafter be cited by their numerical designation.

Table I

PROPELLANT FORMULATIONS CONSIDERED DURING THIS PROGRAM

| <u>Designation</u> | <u>Binder (%)</u> | <u>Oxidizer (%)</u> | <u>Metal Loading (%)</u> |
|--------------------|-------------------|---------------------|--------------------------|
| UTX-10645 | 16.2 CTPIB | 83.6 AP | — — — |
| UTX-10661 | 16.7 PU | 83.1 AP | — — — |
| UTX-10691 | 16.2 CTPB | 83.1 AP | — — — |
| UTX-11325 | 16.2 CTPB | 67.6 AP | 16% Al |
| UTX-11327 | 20.2 CTPB | 79.6 AP | — — — |
| PU -269 | 20 PU | 80 AP | — — — |

The CTPIB (carboxy-terminated polyisobutylene), PU (polyurethane), and CTPB (carboxy-terminated polybutadiene) propellants were selected for comparison with the model because of their diverse thermal and oxidative degradation characteristics. In addition, one propellant containing aluminum was chosen for comparison. According to Jensen,⁶ the CTPIB and PU formulations are less subject to exothermic oxidative degradation of the binder than are the CTPB formulations, but are more subject to endothermic thermal decomposition. The AP used in each propellant consisted of a 65:35 coarse-to-fine ratio with the mean particle diameter of the coarse AP being 190 μ and that of the fine approximately 6 μ . In the case of the aluminized propellant (UTX-11325), the aluminum replaced part of the coarse AP. Each of the UTC propellants contained 0.2% carbon.

Three motor geometries were used in the UTC work: a slab motor, a window motor, and a swing-nozzle motor. The slab motor was a small motor containing 1-lb slabs and having $V/A_b = 9.8$. The window motor also contained slabs, but had a volume to burning surface area ratio $V/A_b = 4.4$. Finally, the swing-nozzle motor utilized internal-burning cylindrical grains and contained a much higher propellant loading with $V/A_b = 0.30$ for the 5-in. long grain configuration and 0.24 for the 15-in. long configuration. A more detailed description of these motors is given in Ref. 6.

Figure 14 compares calculated and observed results for the standard CTPIB propellant (UTX-10645) burned in the slab motor and the window motor. For this propellant, a value of $Q_t = 1100$ cal/gm was used. Note that, in general, the model suggests that a larger depressurization rate should be required in the window motor because of its smaller value of V/A_b ; however, such a rate is not discernable experimentally.

The calculated transient behavior of the burning rate and pressure in the slab motor at a pressure of 200 psia is shown in Fig. 15; note that in this case no oscillation is visible in the burning rate. As will presently be shown, it occurs only under certain depressurization conditions.

Similar results are shown for the UTC polyurethane formulation (UTX-10661) in the slab and window motors in Figs. 16 and 17. For this propellant a value of $Q_t = 1200$ cal/gm was used, equal to the value used for PU-269. Note once again that better agreement is obtained with the slab motor data and that no oscillation is observed in the calculated burning rate.

Extinguishment characteristics of the UTX-10645 CTPIB propellant considered previously and of the UTX-10691 CTPB propellant (for which 1200 cal/gm was used for Q_t in the calculations) are shown in Fig. 18 for the swingnozzle motor in which V/A_b is an order of magnitude lower. Note that the required depressurization rates are correspondingly an order of magnitude higher than those shown in Fig. 14. In this case the calculated values fall somewhat below the experimental values, perhaps because the numerical calculation is strictly one-dimensional, whereas the apparatus uses cylindrical internal-burning grains.

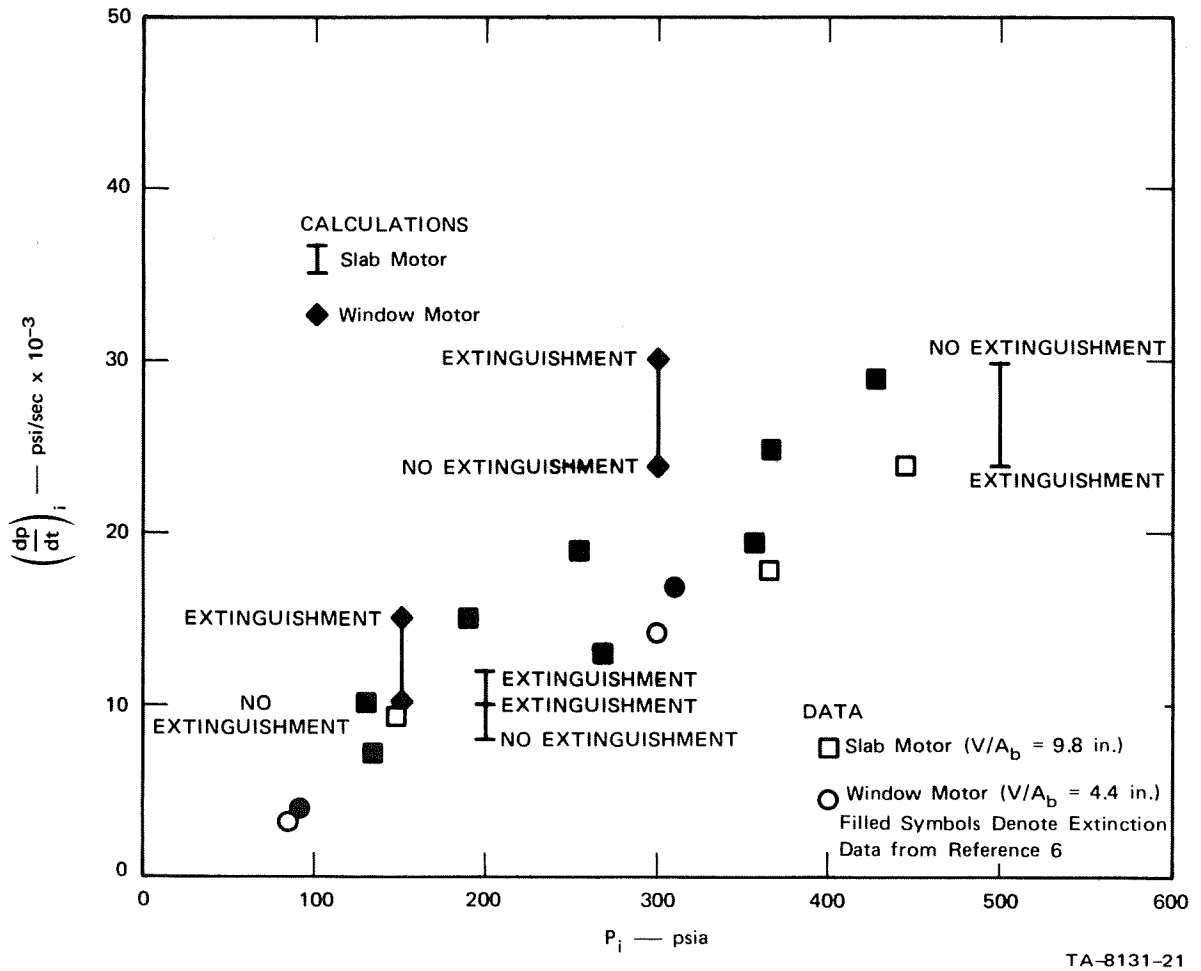


FIGURE 14 COMPARISON OF CALCULATED AND OBSERVED EXTINGUISHMENT BEHAVIOR (UTX-10645)

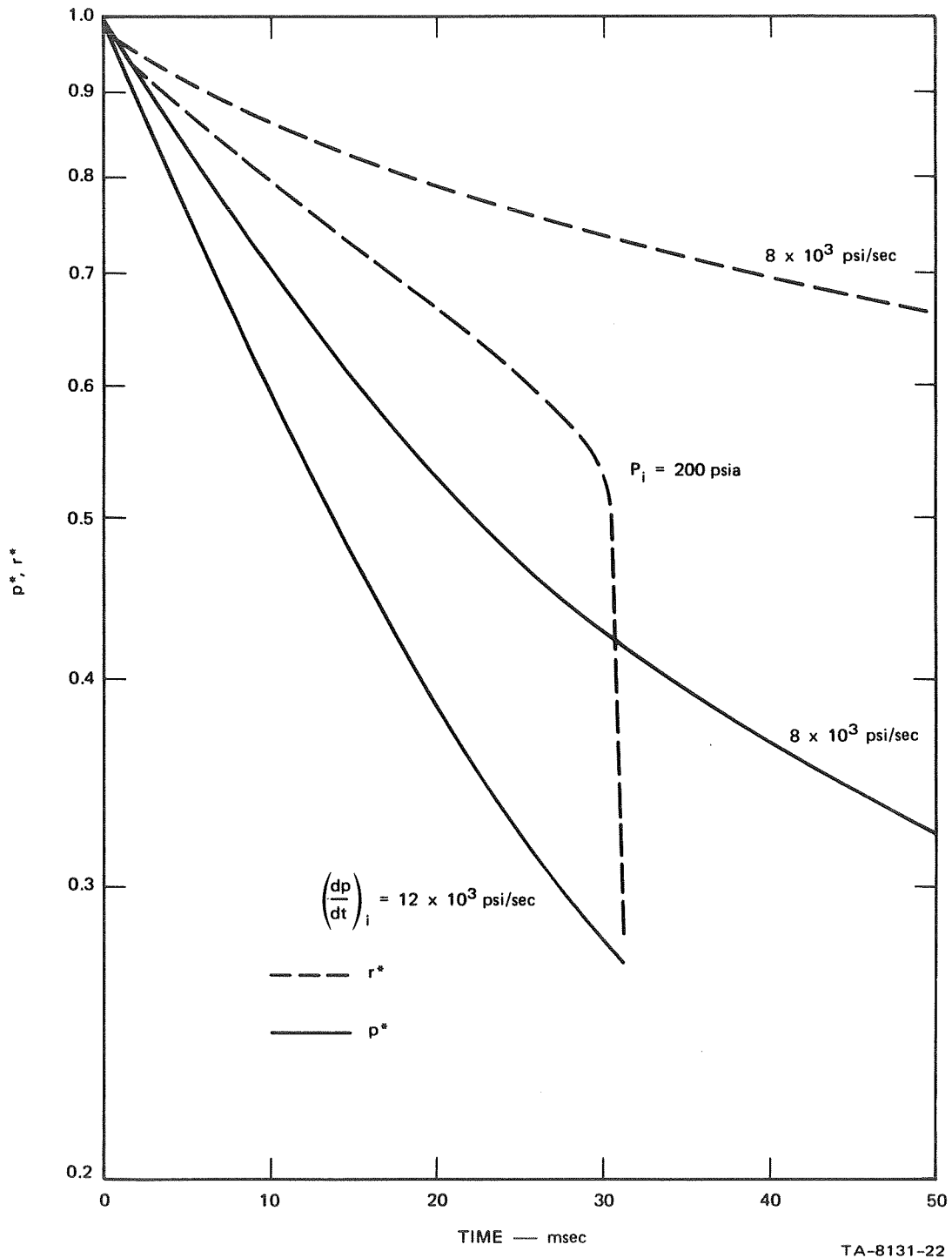


FIGURE 15 CALCULATED EXTINCTION BEHAVIOR IN THE SLAB MOTOR (UTX-10645)

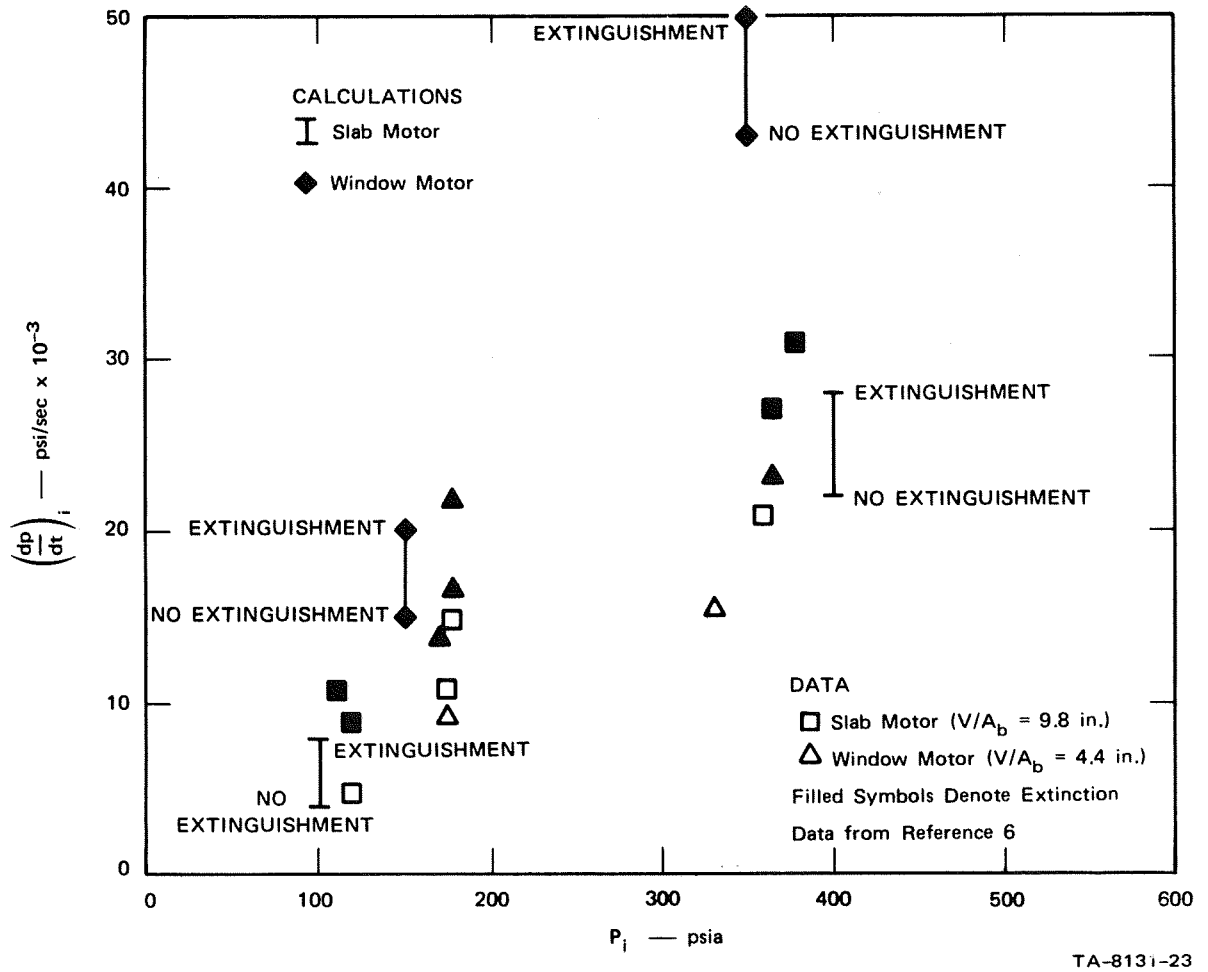


FIGURE 16 COMPARISON OF CALCULATED AND OBSERVED EXTINGUISHMENT BEHAVIOR (UTX-10661)

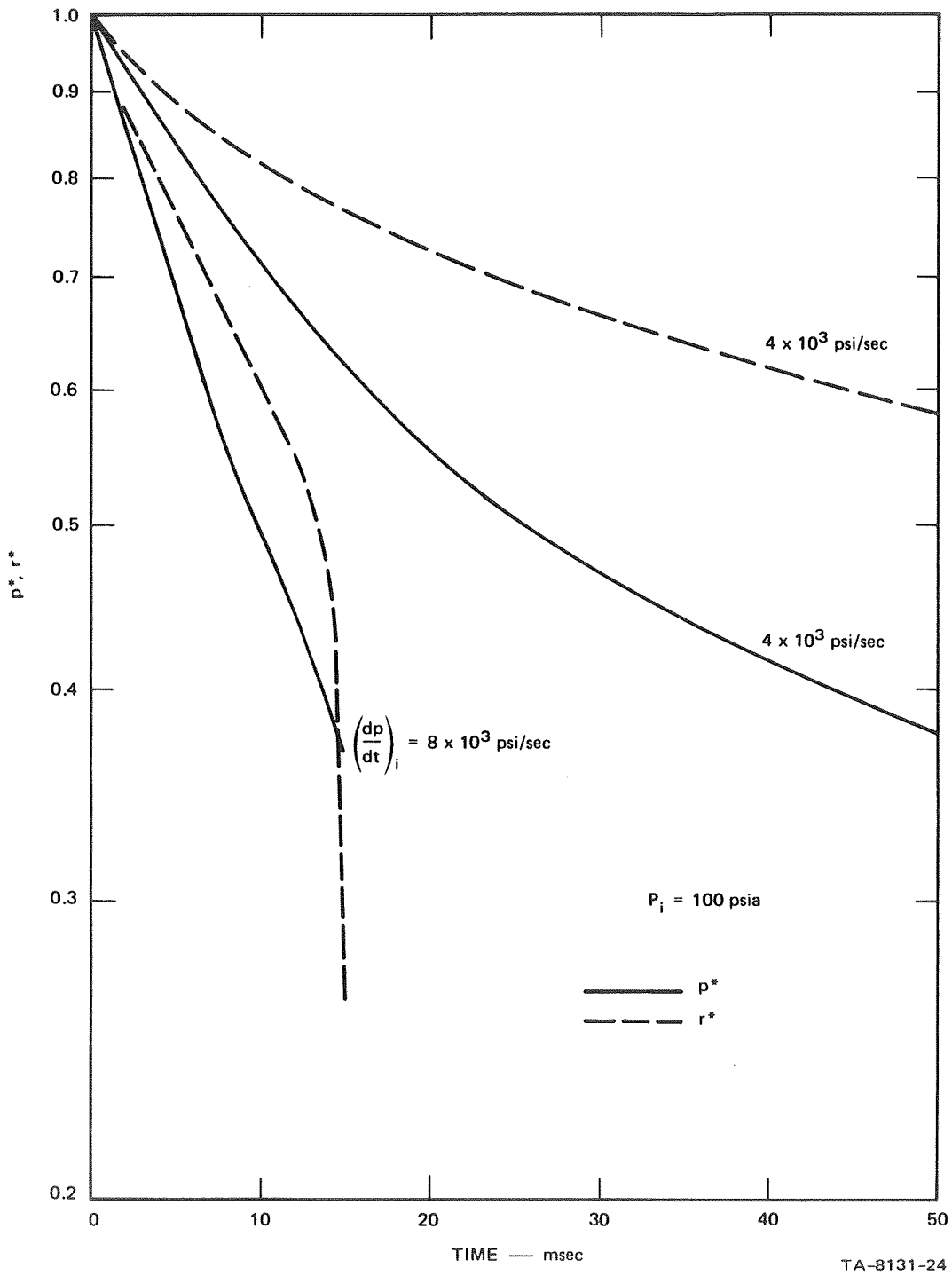


FIGURE 17 CALCULATED EXTINCTION BEHAVIOR IN THE SLAB MOTOR (UTX-10661)

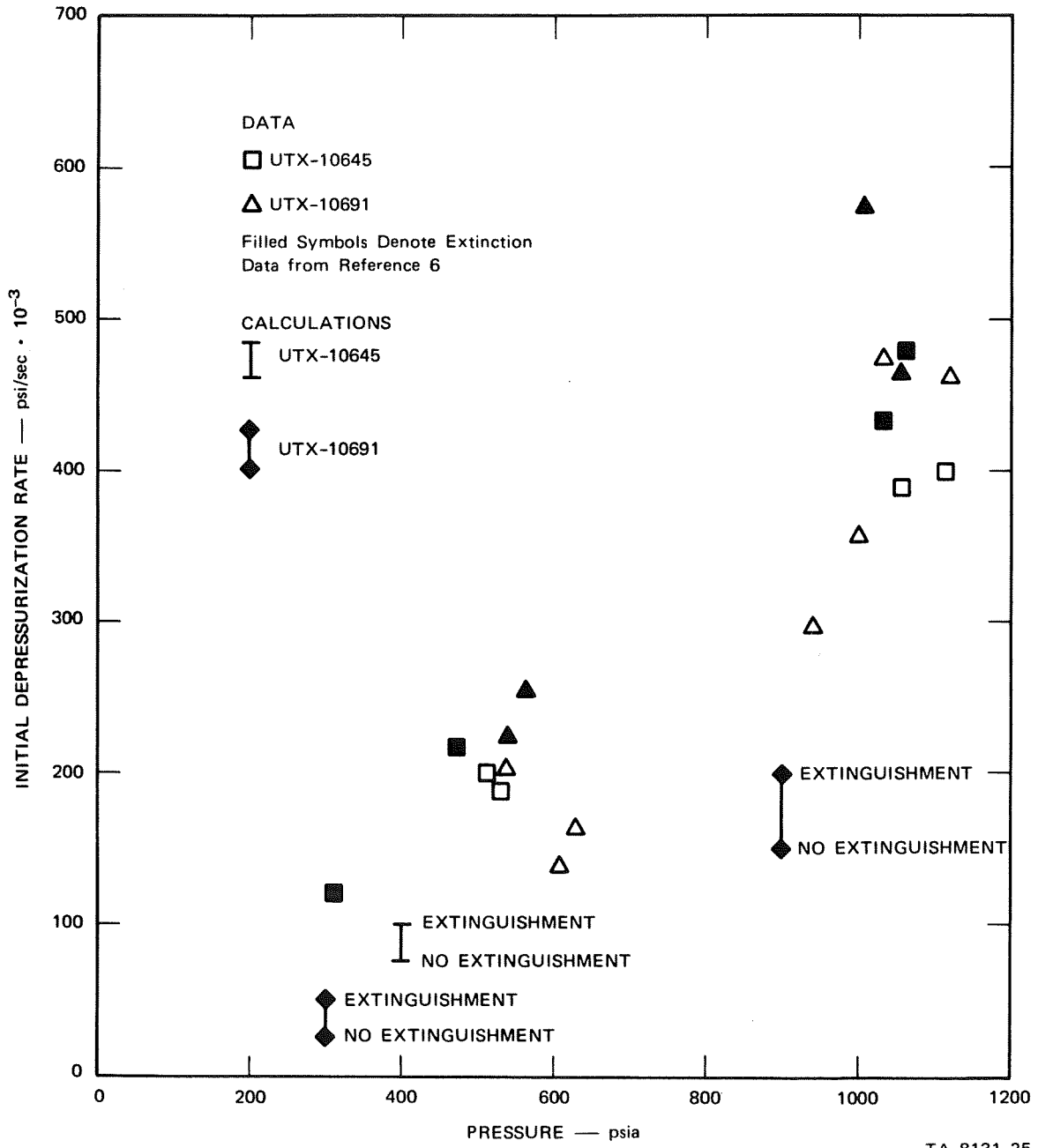
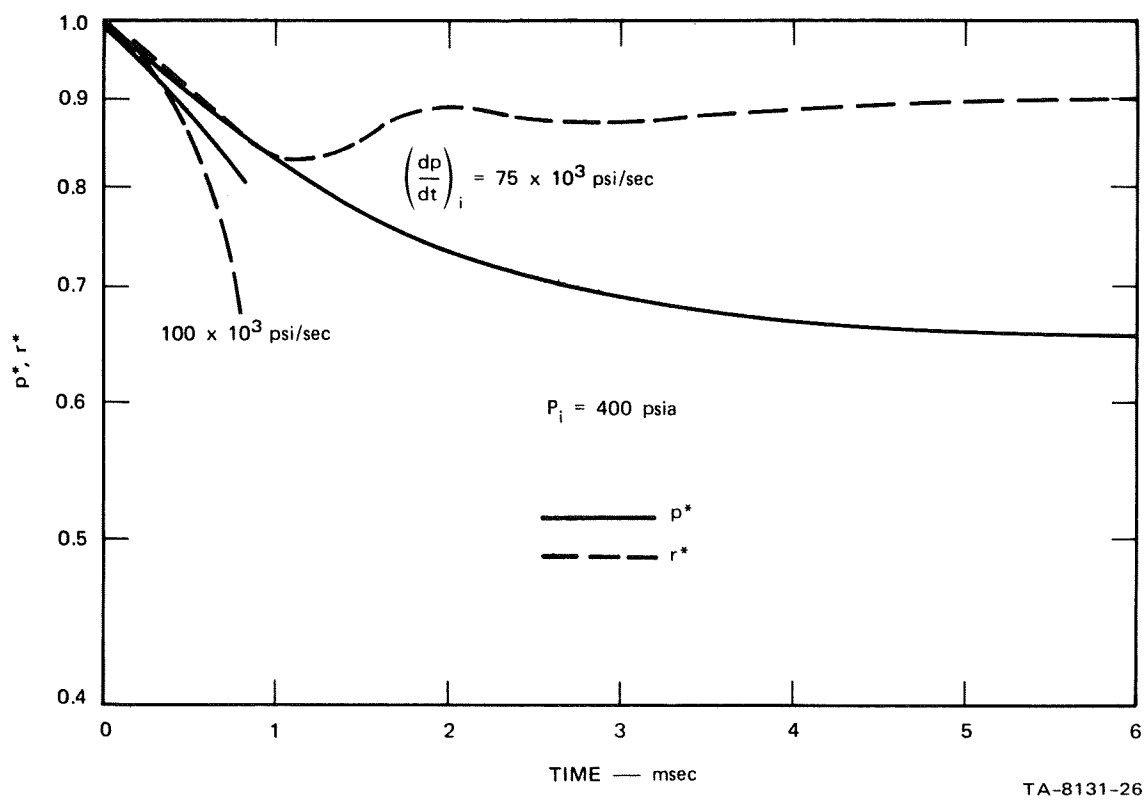


FIGURE 18 EXTINGUISHMENT CHARACTERISTICS OF UTX-10645 AND UTX-10691 IN THE SWING-NOZZLE MOTOR

Also of interest is the calculated pressure and burning rate behavior of the UTX-10645 propellant shown in Fig. 19. In this case an oscillation of the burning rate is evident, whereas it was previously absent at the lower depressurization rate (Fig. 15).

Extinguishment characteristics of the other CTPB propellant (UTX-11327) in the window motor, using $Q_t=1100$ cal/gm, are shown in Fig. 20. In this case the calculated results fall somewhat below the data, perhaps showing the sensitivity to the choice of Q_t . (See the discussion in connection with Fig. 6).

Finally, results are shown in Fig. 21 for the one aluminized propellant (UTX-11325) burned in the window motor. In this case Q_t was chosen as 1400 cal/gm for the numerical calculation and the program was modified to account for the mass of gaseous products that is lost to the formation of aluminum oxide. Considering the simplifications involved in the theory, the agreement is remarkably good.



TA-8131-26

FIGURE 19 CALCULATED EXTINCTION BEHAVIOR IN THE SWING-NOZZLE MOTOR (UTX-10645)

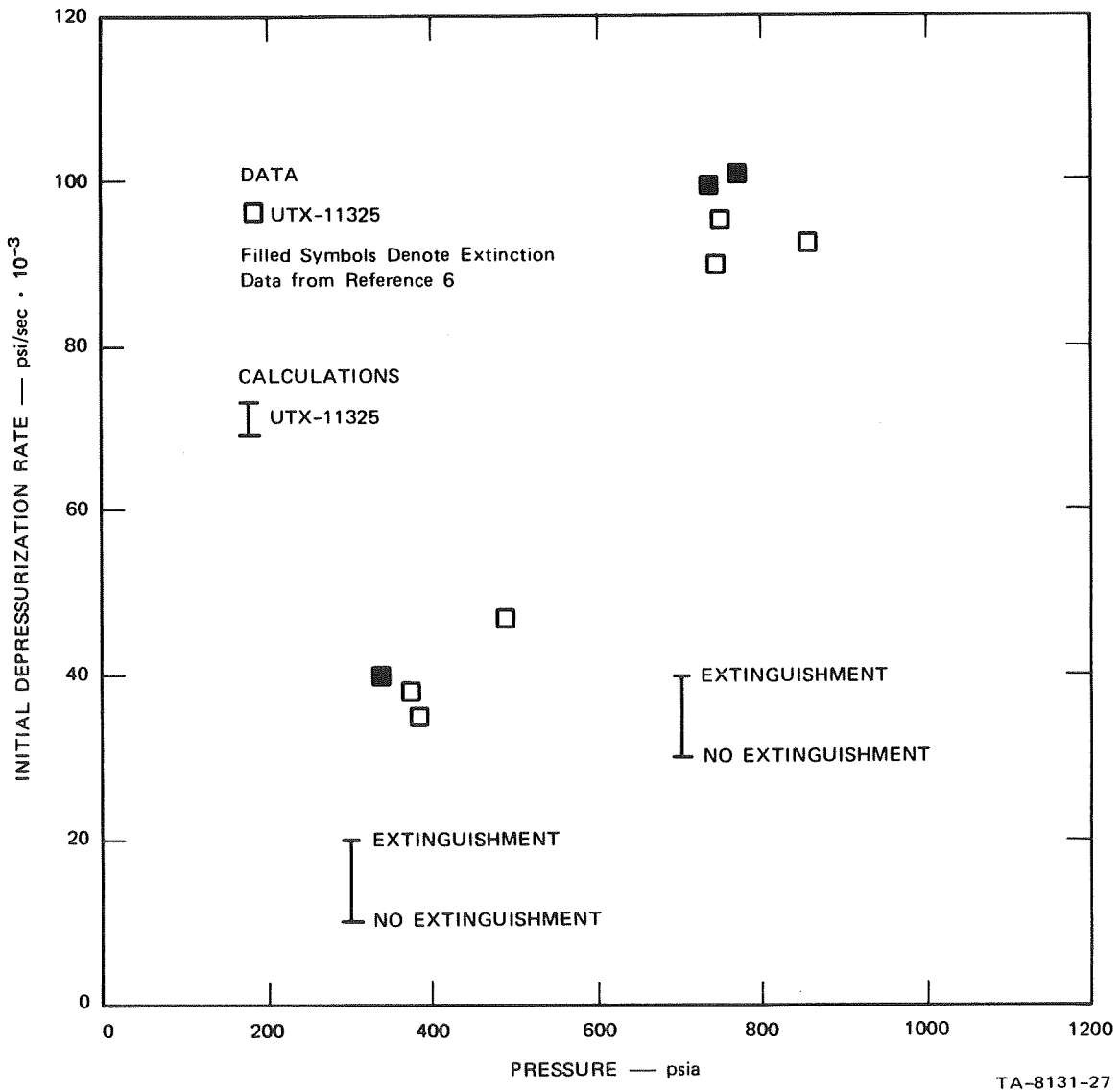


FIGURE 20 EXTINGUISHMENT CHARACTERISTICS OF UTX-11327 IN THE WINDOW MOTOR

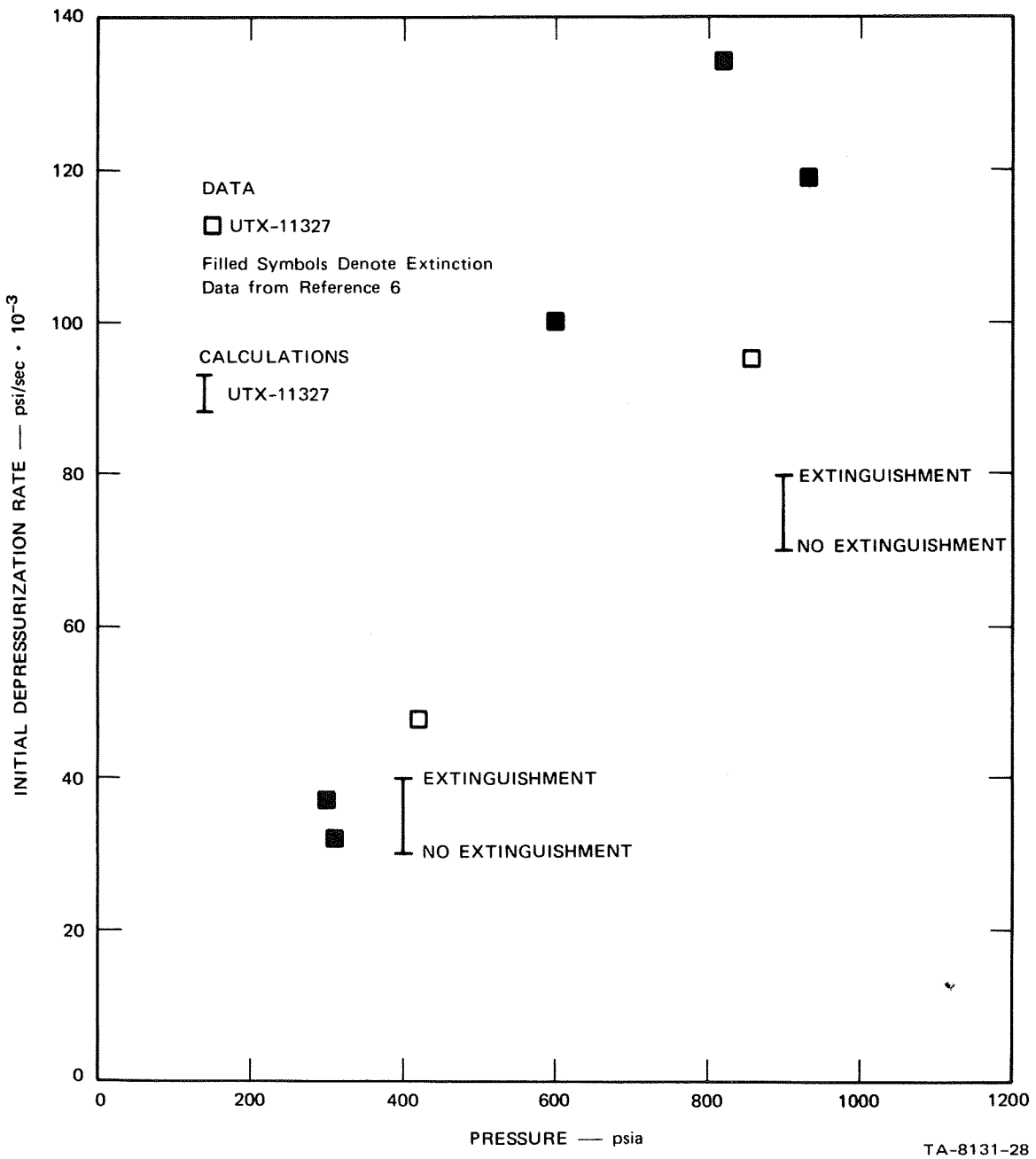


FIGURE 21 EXTINGUISHMENT CHARACTERISTICS OF UTX-11325 IN THE WINDOW MOTOR

Page intentionally left blank

V CONCLUDING REMARKS

During this program an attempt was made to simplify the original SRI combustion model in a way that would still retain the essential features of past observations, the most salient of which is that ammonium perchlorate composite propellants exhibit a "stability limit" in the burning rate/pressure coordinate system. The calculations presented here have shown that the use of this limit line concept alone, together with the burning rate and flame temperature behavior of any given propellant, can predict the extinction behavior of a wide variety of propellants remarkably well without regard for changes in the other parameters of the model, once these parameters have been set by the behavior of one propellant.

Of course, much more could be learned through more extensive computations. One can only say that the limit line concept appears to be as useful as any other that is available today, and the resulting numerical model is a good deal simpler than many others in existence. The ultimate utility of the model cannot be demonstrated until comparisons with large-scale tests are made.

Appendix A

PERTURBATION ANALYSIS OF THE MODEL

The perturbation analysis described here is similar mathematically to that carried out for the previous SRI model.^{7,8} The task is to perturb the solid phase boundary condition and relate the result to the perturbation parameter α , according to the procedure of Denison and Baum.¹³

The solid phase boundary condition is Eq. (8).

$$\left(k_s \frac{\partial T}{\partial x} \right)_w = \rho_s r \left[-c_p (T_f - T_0) - (c_p - c_s) T_0 + c_s (T_w - T_0) + Q_s \frac{W_1}{W_1 + W_2} + Q_g \frac{W_2}{W_1 + W_2} \right] \quad (A1)$$

Expand each of the variables in Eq. (A1) by letting $r = \bar{r} (1 + \tilde{r})$, $T_w = \bar{T}_w (1 + \tilde{T}_w)$, etc. to obtain the perturbation boundary condition:

$$\frac{k_s}{\rho_s \bar{r} c_s} \left(\frac{\partial \tilde{T}}{\partial x} \right)_w = \tilde{r} \left(1 - \frac{T_0}{\bar{T}_w} \right) - \frac{c_p \bar{T}_f}{c_s \bar{T}_w} \tilde{T}_f + \tilde{T}_w + q_s w_1 (\tilde{W}_1 - \tilde{r}) + q_g w_2 (\tilde{W}_2 - \tilde{r}) \quad (A2)$$

Insertion of the perturbation pyrolysis equation

$$\tilde{r} = \frac{E_w}{RT_w} \tilde{T}_w \quad (A3)$$

gives

$$\begin{aligned} \frac{k_s}{\rho_s \bar{r} c_s} \left(\frac{\partial \tilde{T}}{\partial x} \right)_w &= \left[\frac{E_w}{RT_w} \left(1 - \frac{T_0}{\bar{T}_w} - q_s w_1 - q_g w_2 \right) + 1 \right] \tilde{T}_w \\ &\quad - \frac{c_p \bar{T}_f}{c_s \bar{T}_w} \tilde{T}_f + q_s w_1 \tilde{W}_1 + q_g w_2 \tilde{W}_2 \end{aligned} \quad (A4)$$

Perturbations of Eqs. (3), (11), and (12) give

$$\tilde{r} = w_1 \tilde{W}_1 + w_2 \tilde{W}_2 \quad (\text{A5})$$

$$\tilde{W}_1 = n_1 \tilde{p} + N_1 \tilde{T}_w - \frac{\bar{E}_h}{RT_w} \tilde{E}_h \quad (\text{A6})$$

$$\tilde{W}_2 = n_2 \tilde{p} + N_2 \tilde{T}_f - \frac{\bar{E}_f}{RT_f} \tilde{E}_f \quad (\text{A7})$$

Combining Eqs. (A3) and (A5-7) gives an expression for \tilde{T}_f for use in Eq. (A4):

$$\tilde{T}_f = \frac{1}{w_2 N_2} \left\{ \left(\frac{\bar{E}_w}{RT_w} - w_1 N_1 \right) \tilde{T}_w - \left[w_1 \left(n_1 - \frac{\bar{E}_h}{RT_w} \frac{\tilde{E}_h}{\tilde{p}} \right) + w_2 \left(n_2 - \frac{\bar{E}_f}{RT_f} \frac{\tilde{E}_f}{\tilde{p}} \right) \right] \tilde{p} \right\} \quad (\text{A8})$$

It has been explicitly assumed in Eq. (A8) that the activation energies E_h and E_f are functions of pressure only. Expressions for the quantities

$$X = n_1 - \frac{\bar{E}_h}{RT_w} \frac{\tilde{E}_h}{\tilde{p}} \quad (\text{A9})$$

and

$$Y = n_2 - \frac{\bar{E}_f}{RT_f} \frac{\tilde{E}_f}{\tilde{p}} \quad (\text{A10})$$

can be obtained from the simultaneous solution of the steady-state equations that are the equivalents of Eqs. (A4) and (A5):

$$\frac{c \bar{T}_f}{c_s \bar{T}_w} m_1 v = q_s w_1 \left(X + N_1 \frac{RT_w}{E_w} v \right) + q_g w_2 (Y + N_2 m_1 v) - (q_s w_1 + q_g w_2) v \quad (\text{A11})$$

$$v = w_1 \left(X + N_1 \frac{RT_w}{E_w} v \right) + w_2 (Y + N_2 m_1 v) \quad (A12)$$

If Eq. (A4) is now considered to be of the form

$$D = E\tilde{T}_w + F\tilde{p} \quad (A13)$$

it must be true¹³ that

$$E = 1 + A(1-\alpha) \quad (A14)$$

$$F = \alpha v \left(1 - \frac{T_0}{\tilde{T}_w} \right) \quad (A15)$$

The essentials of the task have now been completed; by collecting terms in \tilde{T}_w and \tilde{p} in Eq. (A4) and using the representation of Eqs. (A14) and (A15), two expressions are obtained for α . From the \tilde{T}_w coefficient, the algebraic manipulation gives Eq. (21) of the main body of the report:

$$\begin{aligned} \alpha \left(1 - \frac{T_0}{\tilde{T}_w} \right) &= q_s w_1 + q_g w_2 - \frac{RT_w}{E_w} q_s w_1 N_1 \\ &+ \frac{1}{w_2 N_2} \left(\frac{c \tilde{T}_f}{c_s \tilde{T}_w} - q_g w_2 N_2 \right) \left(1 - \frac{RT_w}{E_w} w_1 N_1 \right) \end{aligned} \quad (A16)$$

From the \tilde{p} coefficient

$$\begin{aligned} \alpha \left(1 - \frac{T_0}{\tilde{T}_w} \right) &= q_s w_1 \left(N_1 \frac{RT_w}{E_w} - 1 \right) + q_g w_2 (N_2 m_1 - 1) \\ &+ \frac{c \tilde{T}_f}{c_s \tilde{T}_w} \left(\frac{1}{w_2 N_2} - \frac{w_1 N_1}{w_2 N_2} \frac{RT_w}{E_w} - 2m_1 \right) \end{aligned} \quad (A17)$$

Since the parameter α is specified at the limiting pressure, Eqs. (A16) and (A17) actually represent two equations for the two unknowns N_1 and N_2 , i.e., E_h and E_f . When they have been solved as indicated in the numerical analysis (Appendix B), the solution is complete in the sense that the desired linear response at the stability limit line has been introduced (through specifying α) and that the proper steady-state behavior will always be achieved after passage through a transient.

Appendix B

COMPUTER CODE AND REPRESENTATIVE OUTPUT FORMAT

This appendix includes a printout of the numerical program and of a representative output format. Comments are included throughout the program to make its use self-explanatory. Four input formats are provided for the calculation of the burning rate response during:

1. depressurization of a chamber
2. pressurization of a chamber
3. depressurization with an exponential pressure decay
4. a sinusoidal pressure variation.

Any other desired pressure-time history could easily be introduced into the program.

Two output formats are provided, one including the temperature profile behavior in the solid and one excluding it. The output Z^* is the non-dimensional heat transfer (i.e., temperature derivative) at the surface with the spatial coordinate considered positive into the grain. The printout excluding the temperature profile is shown here. For an example of the temperature profile printout, see Appendix C.

```

PROGRAM COMB(INPUT,OUTPUT,TAPE5=INPUT,TAPE6=OUTPUT)          0010
C THIS PROGRAM COMPUTES THE TRANSIENT BURNING RATE RESPONSE OF  0020
C COMPOSITE SOLID PROPELLANTS                                  0030
000003 COMMON W,W0,W2,W4, Z,Z1, V,I1,J5,J9,K,K5,L1,L2,N,N2,P5,R5,U2,Y1,  0040
1EPS3,EPS4,EP51,EP52,DI,C9,JERROR,IPLUS, JPRINT,C0,C,P0,R0,QRL,QGP,  0050
2C1,C2,C3,C5,US,POW,N22,W44,E1,C4,U1,W1,M,EHS,EFS,WRR,ZFI,      0060
3CP,CS,QQG,QQS,EFI,EHI,NN2,NN1,WFI,QS,QG,U0,WI,W2I             0070
000003 REAL K,K1,K2,K3,K4,K5,K6,KAPPA,N,M,M1,M2,L1,L2,KIN      0080
000003 REAL L2L1,KL,J3,J7,KK,NN2,NN1,NU,NUM                    0090
000003 DIMENSION AA(100),BB(100),CC(100),DD(100),AVEC(100),BVEC(100),  0100
1 CVEC(100),DVEC(100)                                           0110
000003 DIMENSION W(100), V(100), Z(100),DATE(12),PROP(12),Q(100),GG(100)  0120
000003 DIMENSION AXZ(4,4),BXZ(4),PXZ(4),BBB(5,5),CXZ(4),BXY(4),PXY(4)  0130
000003 JRR=0                                                     0140
000004 JERROR=0                                                 0150
000005 EPS1=0.0001                                             0160
000006 EPS2=0.001
000010 EPS3=1.0E-07                                           0180
000011 EPS4=1.0E-08                                           0190
000013 JPRINT=0                                               0200
C JPRINT=0 EXCLUDES PRINTOUT OF TEMPERATURE PROFILE IN SOLID  0210
C JPRINT=1 INCLUDES PRINTOUT OF TEMPERATURE PROFILE IN SOLID  0220
000014 N2= 0                                                    0230
000015 THETA=0.50                                             0240
000016 Y1= 0.04                                               0250
C Y1 IS NONDIMENSIONAL INCREMENT OF DISTANCE IN SOLID PHASE  0260
000020 N22=5                                                  0270
C VALUE OF N22 ESTABLISHES NUMBER OF POINTS                   0280
C IN TEMPERATURE PROFILE PRINTOUT                             0290
000021 J3=1.0                                                 0300
000022 J5=1                                                    0310
000023 J6=1                                                    0320
000024 J9=1                                                    0330
000025 READ(5,500) (DATE(I),I=1,12)                            0340
000037 500 FORMAT(12A6)                                         0350
000037 READ(5,550) (PROP(I),I=1,12)                            0360
000051 550 FORMAT(12A6)                                         0370
000051 202 READ(5,10)C4,KAPPA,TSTOP,G,U0,CP,P0,E1,NN1,NN2,QQT,QRL,RHS,KK,  0380
1 FR,POW, TSTEP,TCHANGE,TIMFAC,J7,RDL,WRR                    0390
000131 IF(EOF,5)1002,8880                                       0400
000134 8880 WRITE(6,8880)                                       0410
C C4 IS RATIO CP/CS                                           0420
C KAPPA IS THERMAL DIFFUSIVITY OF SOLID (IN**2/SEC)           0430
C TSTOP IS QUIT TIME (SEC)                                     0440
C G IS GAMMA                                                  0450
C U0 IS AMBIENT TEMPERATURE OF SOLID (DEG K)                  0460
C CP IS SPECIFIC HEAT AT CONSTANT PRESSURE (CAL/GM-DEG K)    0470
C P0 IS INITIAL PRESSURE (PSIA)                               0480
C E1 IS ACTIVATION ENERGY OF WALL DECOMPOSITION (CAL/MOLE)  0490
C NN1 IS GAS PHASE ORDER AT WALL                              0500
C NN2 IS GAS PHASE ORDER IN MAIN FLAME                        0510
C QQT IS TOTAL HEAT RELEASE PER UNIT MASS (CAL/GM)           0520
C QRL IS RATIO OF SURFACE TO GAS PHASE HEAT RELEASE          0530
C RHS IS DENSITY OF PROPELLANT (LB/IN**3)                    0540
C KK IS THERMAL CONDUCTIVITY OF THE GAS PHASE (CAL/CM-SEC-DEG K)  0550
C FR IS FLAME TEMPERATURE AT 100 PSIA (DEG K)                0560
C POW IS POWER IN FLAME TEMPERATURE/BURNING RATE EQUATION    0570

```


| | | | |
|--------|------|---|------|
| | | CHANGE ALLOWS CHANGE IN TIME STEP (SEC) | 0580 |
| | | TIMPAC IS FACTOR BY WHICH TIME STEP IS CHANGED | 0590 |
| | | J7 GIVES PRINTOUT AT EACH (J7+1) TIME INCREMENT | 0600 |
| | | RDL IS LOWER DEFLAGRATION LIMIT | 0610 |
| | | WRR IS WALL TEMPERATURE WHEN THE BURNING RATE IS .1 IN/SEC (DEG K) | 0620 |
| 000140 | 8888 | FORMAT(1H1) | 0630 |
| 000140 | | WRITE(6,501) (DATE(I),I=1,12) | 0640 |
| 000152 | 501 | FORMAT(1H,50X,12A6) | 0650 |
| 000152 | | WRITE(6,551) (PROP(I),I=1,12) | 0660 |
| 000164 | 551 | FORMAT(47H SOLID PROPELLANT TRANSIENT COMBUSTION BEHAVIOR/ 11H,12A6) | 0670 |
| 000164 | | READ(5,100) (BXY(I),I=1,4),(PXY(I),I=1,4) | 0680 |
| | | BXY AND PXY ARE FOUR BURNING RATES (IN/SEC) AND FOUR PRESSURES (PSIA) CHOSEN TO FIT MEASURED CURVE | 0690 |
| 000204 | 100 | FORMAT(8F10,4) | 0700 |
| 000204 | | DO 5 I=1,4 | 0710 |
| 000206 | | BXZ(I)=ALOG(BXY(I)) | 0720 |
| 000212 | | PXZ(I)=ALOG(PXY(I)) | 0730 |
| 000216 | | AXZ(I,1)=1.0 | 0740 |
| 000220 | | AXZ(I,2)=PXZ(I) | 0750 |
| 000221 | | AXZ(I,3)=(PXZ(I))**2 | 0760 |
| 000223 | | AXZ(I,4)=(PXZ(I))**3 | 0770 |
| 000225 | 5 | CONTINUE | 0780 |
| 000226 | | CALL SOLVE(AXZ,BXZ,4,4,CXZ,5,888,ISOL) | 0790 |
| 000236 | | C1=CXZ(1) | 0800 |
| 000240 | | C2=CXZ(2) | 0810 |
| 000241 | | C3=CXZ(3) | 0820 |
| 000243 | | C5=CXZ(4) | 0830 |
| 000244 | | PA=500.0 | 0840 |
| 000246 | 560 | F6=C1+C2*ALOG(PA)+C3*(ALOG(PA))**2+C5*(ALOG(PA))**3 | 0850 |
| 000266 | | F6=EXP(F6) | 0860 |
| 000270 | | PB=PA | 0870 |
| 000271 | | PA=(F6/0.00239)**(1.0/0.726) | 0880 |
| 000300 | | IF(PA.LT.(0.999*PB))GO TO 560 | 0890 |
| 000304 | | IF(PA.GT.(1.001*PB))GO TO 560 | 0900 |
| 000307 | | PL=PA | 0910 |
| | | PL IS THRESHOLD PRESSURE FOR TRAVELING WAVE INSTABILITY | 0920 |
| 000307 | | JEXT=1 | 0930 |
| 000310 | | RDL=C1+C2*ALOG(3.0)+C3*(ALOG(3.0))**2+C5*(ALOG(3.0))**3 | 0940 |
| 000330 | | RDL=EXP(RDL) | 0950 |
| 000332 | | R0=C1+C2*ALOG(P0)+C3*(ALOG(P0))**2+C5*(ALOG(P0))**3 | 0960 |
| 000351 | | R0=EXP(R0) | 0970 |
| | | R0 IS THE INITIAL BURNING RATE (IN/SEC) | 0980 |
| 000353 | | UN=C2+2.0*C3*ALOG(PL)+3.0*C5*(ALOG(PL))**2 | 0990 |
| | | UN IS THE SLOPE OF THE BURNING RATE/PRESSURE CURVE AT LIMITING PRESSURE | 1000 |
| 000366 | | NU=C2+2.0*C3*ALOG(P0)+3.0*C5*(ALOG(P0))**2 | 1010 |
| | | NU IS THE SLOPE OF THE BURNING RATE/PRESSURE CURVE AT INITIAL PRESSURE | 1020 |
| 000401 | | RR=C1+C2*ALOG(100.0)+C3*(ALOG(100.0))**2.0+C5*(ALOG(100.0))**3.0 | 1030 |
| 000423 | | RR=EXP(RR) | 1040 |
| | | RR IS THE REFERENCE BURNING RATE AT 100 PSIA (IN/SEC) | 1050 |
| 000426 | | U2=FR*(R0/RR)**POW | 1060 |
| | | U2 IS THE INITIAL FLAME TEMPERATURE (DEG K) | 1070 |
| 000433 | | U1=WRR/(1.0+WRR*ALOG(10.0*R0)/E1) | 1080 |
| | | U1 IS THE INITIAL WALL TEMPERATURE (DEG K) | 1090 |
| 000443 | | W0=U0/U1 | 1100 |
| 000444 | | A=E1*(1.0+W0)/U1 | 1110 |
| | | | 1120 |
| | | | 1130 |

| | | | |
|--------|---|--|------|
| | C | A IS A PYROLYSIS FACTOR ASSOCIATED WITH THE LINEAR BEHAVIOR OF THE | 1140 |
| | C | PROPELLANT | 1150 |
| 000447 | | K5=R0/KAPPA | 1160 |
| 000451 | | K6=R0*K5 | 1170 |
| 000452 | | K=K6*TSTEP/(Y1*Y1) | 1180 |
| 000455 | | KIN=K | 1190 |
| 000456 | | TST=TSTOP | 1200 |
| 000457 | | TSTOP=K6*TSTOP | 1210 |
| 000460 | | RL=C1+C2*ALOG(PL)+C3*(ALOG(PL))**2+C5*(ALOG(PL))**3 | 1220 |
| 000477 | | RL=EXP(RL) | 1230 |
| | C | RL IS THE VALUE OF BURNING RATE (IN/SEC) AT THE THRESHOLD PRESS | 1240 |
| 000501 | | FL=FR*(RL/RR)**POW | 1250 |
| | C | FL IS THE VALUE OF FLAME TEMP. (DEG K) AT THE THRESHOLD PRESSURE | 1260 |
| 000506 | | WL=WRR/(1.0+WRR*ALOG(10.0*RL)/E1) | 1270 |
| | C | WL IS THE VALUE OF WALL TEMP. (DEG K) AT THE THRESHOLD PRESSURE | 1280 |
| 000516 | | AL=E1*(1.0-U0/WL)/WL | 1290 |
| 000522 | | ALPHA=0.226*ALOG(AL)+0.170 | 1300 |
| | C | THIS IS ALPHA AT THE THRESHOLD PRESSURE | 1310 |
| 000526 | | WR=WRR/(1.0+WRR*ALOG(10.0*RR)/E1) | 1320 |
| | C | WR IS THE REFERENCE WALL TEMP. AT 100 PSIA | 1330 |
| 000537 | | CS=CP/C4 | 1340 |
| | C | CS IS SPECIFIC HEAT OF THE SOLID PHASE (CAL/GM-DEG K) | 1350 |
| 000541 | | RHO=RHS*454.0/(2.54)**2 | 1360 |
| 000544 | | QQG=QQT/(1.0+QRL) | 1370 |
| 000547 | | QGP=QQG/CP | 1380 |
| 000550 | | NUM=QGP*FL*U0*(1.0-1.0/C4)*U0 | 1390 |
| 000556 | | DEN=FL*U0*(1.0-1.0/C4)*U0-QRL*QGP | 1400 |
| 000563 | | WRL=NUM/DEN | 1410 |
| 000564 | | ZFL=1.0+1.0/(QGP/((FL-WL)*(1.0+WRL))-1.0) | 1420 |
| 000573 | | XFL=(KK/(RHO*RL*CP))*ALOG(ZFL)*10000.0 | 1430 |
| | C | XFL IS THE DISTANCE FROM THE WALL TO THE GAS PHASE FLAME AT THE | 1440 |
| | C | LIMITING PRESSURE (MICRONS) | 1450 |
| 000602 | | QQS=QRL*QQG | 1460 |
| 000604 | | QG=QQG/(CS*WL) | 1470 |
| 000606 | | QS=QQS/(CS*WL) | 1480 |
| 000610 | | W2L=RHO*RL/(1.0+WRL) | 1490 |
| 000613 | | W1L=WRL*W2L | 1500 |
| 000614 | | B11=W1L/(W1L+W2L) | 1510 |
| 000616 | | B22=W2L/(W1L+W2L) | 1520 |
| 000620 | | BNA=B22*POW*QG*(QG-QS) | 1530 |
| 000625 | | BNB=C4*FL/WL*POW*(3.0*QG-2.0*QS)-QG*B22*(QG-QS)-ALPHA*(1.0-U0/WL) | 1540 |
| | 1 | *(QG-2.0*QS) | 1550 |
| 000650 | | BNC=2.0*C4*FL/WL*(QG-QS+POW/B22*C4*FL/WL) | 1560 |
| 000662 | | BN2=(-BNB*(BNB**2-4.0*BNA*BNC)**0.5)/(2.0*BNA) | 1570 |
| 000674 | | BN1=(-2.0*QS*B11-2.0*QG*B22+QG*B22*BN2*POW+QG-2.0*POW*C4*FL/WL)/ | 1580 |
| | 1 | (QG*B11*WL/E1-2.0*QS*B11*WL/E1) | 1590 |
| 000716 | | EFL=FL*(BN2-NN2-2.0) | 1600 |
| | C | EFL IS GAS PHASE ACTIVATION ENERGY AT THE THRESHOLD PRESSURE | 1610 |
| 000722 | | EHL=WL*(BN1-NN1-2.0) | 1620 |
| | C | EHL IS WALL REACTION ACTIVATION ENERGY AT THE THRESHOLD PRESSURE | 1630 |
| 000725 | | SS1=C4*U2/WL-QS-U0/WL | 1640 |
| 000732 | | SS2=C4*U2/WL-QG-U0/WL | 1650 |
| 000735 | | SS4=R0/RL*(W1L+W2L) | 1660 |
| 000740 | | W2I=-SS1*SS4/(SS2-SS1) | 1670 |
| 000744 | | W1I=SS2*SS4/(SS2-SS1) | 1680 |
| 000746 | | WRI=W1I/W2I | 1690 |
| 000750 | | EHS=(1.0-WL/EHL*(ALOG(W1I/W1L)-NN1*ALOG(P0/PL)-(NN1+2.0)* | 1700 |
| | 1 | ALOG(U1/WL))*U1/WL | 1710 |

| | | |
|--------|--|------|
| 000777 | EFS=(1.0-FL/EFL*(ALOG(W2I/W2L)-NN2*ALOG(P0/PL)-(NN2+2.0)* | 1720 |
| | 1 ALOG(U2/FL)))*U2/PL | 1730 |
| 001026 | QS=QGS/(CS*U1) | 1740 |
| 001031 | QG=QGG/(CS*U1) | 1750 |
| 001033 | EFI=EFS*EFL | 1760 |
| 001035 | EHI=EHS*EHL | 1770 |
| 001037 | ZFI=1.0+1.0/(QGP/((U2-U1)*(1.0*WRI))-1.0) | 1780 |
| 001046 | XFI=(KK/(RHO*RL*CP))*ALOG(ZFI)*10000.0 | 1790 |
| | XFI IS THE DISTANCE FROM THE WALL TO THE GAS PHASE FLAME AT THE | 1800 |
| | C INITIAL PRESSURE (MICRONS) | 1810 |
| 001055 | E11=2.0*E1 | 1820 |
| 001057 | E55=2.0*E5I | 1830 |
| 001060 | E33=2.0*E3I | 1840 |
| 001062 | E44=2.0*E4 | 1850 |
| 001063 | READ(5,11) J | 1860 |
| | C J DETERMINES CASE TO BE CALCULATED | 1870 |
| 001071 | 10 FORMAT(7F10.4) | 1880 |
| 001071 | 11 FORMAT(2I1) | 1890 |
| 001071 | GO TO (12,13,14,15),J | 1900 |
| 001101 | 12 READ(5,16) DECAY,V1,M1,PF | |
| 001115 | K4=1.0+(V1*M1*DECAY)/(1545.0*12.0*1.8*RMS*R0*G*U2*0.7) | |
| | DECAY IS THE INITIAL DECAY RATE IN PSI/SEC | 1920 |
| | C K4 IS THE RATIO AT/ATI=AT* | 1930 |
| | C PF IS THE EXTERNAL PRESSURE | 1940 |
| 001127 | GO TO 17 | 1950 |
| 001127 | 13 READ(5,16) TAU,PF | 1960 |
| | C TAU IS TIME CONSTANT OF DEPRESSURIZATION CURVE | 1970 |
| | C PF IS THE FINAL PRESSURE | 1980 |
| 001137 | GO TO 17 | 1990 |
| 001140 | 14 READ(5,16) P8,F3 | 2000 |
| | C P8 IS THE AMPLITUDE CHOSEN FOR P* | 2010 |
| | C F3 IS THE FREQUENCY IN CPS | 2020 |
| 001150 | GO TO 17 | 2030 |
| 001151 | 15 READ(5,16) TPULSE,V1,M1,M2,K4,PF | 2040 |
| | C TPULSE IS THE DURATION OF EXTERNAL INJECTION | 2050 |
| | C V1 IS RATIO OF CHAMBER VOLUME TO BURNING SURFACE AREA | 2060 |
| | C M1 IS MOLECULAR WEIGHT OF PRODUCT GASES | 2070 |
| | C M2 IS RATIO OF MASS INJECTED TO MASS EVOLVED BY PROPELLANT | 2080 |
| | C K4 IS THE RATIO AT/ATI=AT* | 2090 |
| | C PF IS THE EXTERNAL PRESSURE | 2100 |
| 001171 | 16 FORMAT(7F10.4) | 2110 |
| 001171 | 17 WRITE(6,18)C1,C2,C3,C5,C4,CP,CS,CK,NN1,NN2,U0,FR,WRR,POW,RHS,WRL, | 2120 |
| | 1 QRL,KAPPA,G,TST,TIMFAC,TCHANGE,TSTEP | 2130 |
| 001253 | 18 FORMAT(/16H INPUT CONSTANTS/4H C1=,E15.8/4H C2=,E15.8/4H C3=,E15.8/ | 2140 |
| | 1 /4H C5=,E15.8/4H C4=,E15.8/4H CP=,E15.8/4H CS=,E15.8/4H KG=, | 2150 |
| | 2 E15.8/4H N1=,E15.8/4H N2=,E15.8/4H T0=,E15.8/5H TFR=,E15.8/ | 2160 |
| | 3 5H TWR=,E15.8/5H POW=,E15.8/5H RHO=,E15.8/5H WRL=,E15.8/ | 2170 |
| | 4 5H QRL=,E15.8/7H KAPPA=,E15.8/7H GAMMA=,E15.8/7H TSTOP=, | 2180 |
| | 5 E15.8/8H TIMFAC=,E15.8/9H TCHANGE=,E15.8/11H TIME STEP=, | 2190 |
| | 6 E15.8) | 2200 |
| 001253 | EFI=2.0*EFL | 2210 |
| 001255 | EHI=2.0*EHL | 2220 |
| 001257 | WRITE(6,40)PL,RL, AL,ALPHA, EFL,EHI,FL,WL,XFL,UN | 2230 |
| 001306 | 40 FORMAT(/19H LIMIT POINT VALUES/4H PL=,E15.8/4H RL=,E15.8/ | 2240 |
| | 1 4H AL=,E15.8/8H ALPHA=,E15.8/ | 2250 |
| | 2 5H EFL=,E15.8/5H EHL=,E15.8/5H TFL=,E15.8/5H TWL=,E15.8/ | 2260 |
| | 3 5H XFL=,E15.8/5H NU =,E15.8) | 2270 |
| 001306 | I1=INT(1.0/Y1*0.5) | 2280 |

| | | |
|--------|---|------|
| 001312 | B11=W1/(W1+W2) | 2290 |
| 001314 | B22=W2/(W1+W2) | 2300 |
| 001316 | BN2=NN2*2.0*E1/U2 | 2310 |
| 001322 | BN1=NN1*2.0*E1/U1 | 2320 |
| 001325 | ALPHA=(QS*B11+QG*B22-U1/E1*QS*B11*BN1+(C4*U2/U1-QG*B22*BN2)* | 2330 |
| | 1 ((1.0-U1/E1*B11*BN1)/(B22*BN2))/(1.0-U0/U1) | 2340 |
| 001356 | WRITE(6,41)P0,R0,E11,E55,E33,U2,U1,QQG,QQS,A,ALPHA, NU,XFI | 2350 |
| 001413 | 41 FORMAT(/21H INITIAL POINT VALUES/4H P0=,E15.8/4H R0=,E15.8/4H EW=, | 2360 |
| | 1 E15.8/4H EF=,E15.8/4H EH=,E15.8/4H TF=,E15.8/4H TW=,E15.8/ | 2370 |
| | 2 4H QG=,E15.8/4H QS=,E15.8/4H A =,E15.8/7H ALPHA=,E15.8/ | 2380 |
| | 3 8H NU =,E15.8/8H XFI =,E15.8) | 2390 |
| 001413 | ALPHAL=1.0+(1.0-SQRT(1.0+8.0*A))/(A*A) | 2400 |
| 001425 | WRITE(6,8888) | 2410 |
| 001430 | WRITE(6,501) (DATE(I),I=1,12) | 2420 |
| 001442 | IF(ALPHA-ALPHAL) 720,720,136 | 2430 |
| 001445 | 136 P5=1.0 | 2440 |
| 001447 | R5=1.0 | 2450 |
| 001450 | R3=1.0 | 2460 |
| 001451 | K44=1.0 | 2470 |
| 001452 | W1=1.0 | 2480 |
| 001453 | W2=1.0 | 2490 |
| 001454 | W3=1.0 | 2500 |
| 001455 | W44=1.0 | 2510 |
| 001456 | Z1=(W1-W0) | 2520 |
| 001460 | T00=0.0 | 2530 |
| 001461 | G0=0.0 | 2540 |
| 001462 | G00=1.0 | 2550 |
| | C G00 IS THE INTEGRAL OF THE INITIAL TEMPERATURE PROFILE. | 2560 |
| 001463 | EFS=1.0 | 2570 |
| 001464 | EHS=1.0 | 2580 |
| 001465 | Y=K*Y1*Y1 | 2590 |
| 001467 | IMINUS=I1-1 | 2600 |
| 001471 | IPLUS=I1+1 | 2610 |
| 001472 | GG1=(G-1.0)/2.0*(2.0/(G+1.0))*((G+1.0)/(G-1.0)) | 2620 |
| 001505 | PRF=((G+1.0)/2.0)**(-G/(G-1.0)) | 2630 |
| 001514 | IF(J=1) 52,51,52 | 2640 |
| 001516 | 52 IF(J=2) 171,238,171 | 2650 |
| 001520 | 171 IF(J=3) 172,268,172 | 2660 |
| 001522 | 172 WRITE(6,173) V1, K4, M2, M1, TPULSE,PF | 2670 |
| 001542 | 173 FORMAT(24H EXTERNAL PULSE RESPONSE//8H V/AB =,E15.8/ | 2680 |
| | 1 8H AT/ATI=,E15.8/ 8H M.R. =,E15.8/8H M.W. =,E15.8/ | 2690 |
| | 2 8H TPULSE=,E15.8/8H PF =,E15.8/) | 2700 |
| 001542 | K1=(P0*V1*R0*M1)/(1545.0*12.0*1.8*RHS *KAPPA*U2) | 2710 |
| 001552 | K2=K1/G | 2720 |
| 001554 | IF(JPRINT) 27,26,27 | 2730 |
| 001555 | 26 WRITE(6,28) | 2740 |
| 001561 | 28 FORMAT(9H TIME,11X,2HP*,11X,2HE*,11X,2HZ*,11X,2HR*,11X,3HTW*, | 2750 |
| | 1 10X,3HTF*,10X,3HTC*,10X,3HEF*,10X,3HEH*/ | 2760 |
| 001561 | WRITE(6,29)T00,P5,G00,Z1,R5,W1,W2,W3,EFS,EHS | 2770 |
| 001611 | 29 FORMAT(10E13.4) | 2780 |
| 001611 | 27 CONTINUE | 2790 |
| 001611 | CALL SUB600 | 2800 |
| 001612 | GO TO 210 | 2810 |
| 001613 | 200 IF(T=K6*TPULSE) 210,210,206 | 2820 |
| 001617 | 206 M2=0.0 | 2830 |
| 001620 | 210 PFR=PF/(P5*P0) | 2840 |
| 001623 | IF (PFR=PRF) 211,211,2101 | 2850 |
| 001625 | 2101 K44=(GG1/((1.0-PFR**((G-1.0)/G))*PFR**((2.0/G)))*0.5 | 2860 |

| | | | |
|--------|--------|--|------|
| 001647 | C 2111 | K44 IS PSEUDO THROAT AREA RATIO TO ACCOUNT FOR NOZZLE UNCHOKING | 2870 |
| 001652 | | IF (J9=1) 207,207,208 | 2880 |
| 001666 | 207 | X5=(R5*W2+M2-(K4/K44)*P5*W3**0.5)/K2 | 2890 |
| 001706 | | X6=(K1*X5/W3-R5-M2+(K4/K44)*P5/(W3**0.5))*W3*W3/(K1*P5) | 2900 |
| 001707 | | P50=P5 | 2910 |
| 001710 | | W30=W3 | 2920 |
| 001714 | | P5=P50+X5*K*Y1*Y1 | 2930 |
| 001717 | | W3=W30+X6*K*Y1*Y1 | 2940 |
| 001717 | | GO TO 365 | 2950 |
| 001733 | 208 | X50=(R5*W2+M2-(K4/K44)*P5*W3**0.5)/K2 | 2960 |
| 001753 | | X60=(K1*X50/W3-R5-M2+(K4/K44)*P5/(W3**0.5))*W3*W3/(K1*P5) | 2970 |
| 001762 | | P5=P50+(X5+X50)*K*Y1*Y1/2.0 | 2980 |
| 001770 | | W3=W30+(X6+X60)*K*Y1*Y1/2.0 | 2990 |
| 001770 | | GO TO 365 | 3000 |
| 001773 | 238 | RATE=(P0-PF)/TAU | 3010 |
| 002007 | | WRITE(6,244) TAU,P0,PF,RATE | 3020 |
| | 244 | FORMAT(1H /27H EXPONENTIAL DECAY RESPONSE/ | 3030 |
| | | 1 15H TIME CONSTANT=E15.8/ | 3040 |
| | | 24H P0=E15.8/4H PF=E15.8/20H INITIAL DECAY RATE=E15.8/) | 3050 |
| 002007 | | IF (JPRINT) 900,901,900 | 3060 |
| 002010 | 901 | WRITE(6,28) | 3070 |
| 002014 | | WRITE(6,29) T00,P5,G00,Z1,R5,W1,W2,W3,EFS,EHS | 3080 |
| 002044 | 900 | CONTINUE | 3090 |
| 002044 | | CALL SUB600 | 3100 |
| 002045 | 906 | P5=PF/P0+(1-PF/P0)*EXP(-T/(K6*TAU)) | 3110 |
| 002060 | | GO TO 365 | 3120 |
| 002061 | 51 | WRITE(6,50) DECAY,K4 | 3130 |
| 002071 | 50 | FORMAT(34H CHAMBER DEPRESSURIZATION RESPONSE// | 3140 |
| | | 120H INITIAL DECAY RATE=E15.8/8H AT/ATI=E15.8/) | 3150 |
| 002071 | | IF (JPRINT) 902,903,902 | 3160 |
| 002072 | 903 | WRITE(6,28) | 3170 |
| 002076 | | WRITE(6,29) T00,P5,G00,Z1,R5,W1,W2,W3,EFS,EHS | 3180 |
| 002126 | 902 | CONTINUE | 3190 |
| 002126 | | CALL SUB600 | 3200 |
| 002127 | | K2=-P0*R0*R0*(1-K4)/(KAPPA*DECAY) | 3210 |
| 002137 | | K1=G*K2 | 3220 |
| 002140 | | GO TO 210 | 3230 |
| 002141 | 268 | P81=1.0+P8*TSTEP | 3240 |
| 002144 | | WRITE(6,275) P81,F3 | 3250 |
| 002154 | 275 | FORMAT(20H SINUSOIDAL RESPONSE/4H P*=E15.8/4H F*=E15.8/) | 3260 |
| 002154 | | IF (JPRINT) 904,905,904 | 3270 |
| 002155 | 905 | WRITE(6,28) | 3280 |
| 002161 | | WRITE(6,29) T00,P5,G00,Z1,R5,W1,W2,W3,EFS,EHS | 3290 |
| 002211 | 904 | CONTINUE | 3300 |
| 002211 | | CALL SUB600 | 3310 |
| 002212 | | F3=6.2832*F3/K6 | 3320 |
| 002215 | 280 | IF ((T/K6).GT.(TCHANGE=20.0*TSTEP)) GO TO 365 | 3330 |
| 002224 | | P5=1.0+P8*(T/K6) | 3340 |
| 002226 | 365 | CALL SUB500 | 3350 |
| 002227 | | IF (JERROR=1) 366,745,366 | 3360 |
| 002231 | 366 | W2=W4 | 3370 |
| | C | W2 IS FLAME TEMPERATURE RATIO TF* | 3380 |
| 002233 | | WF2=R5*DI-WF1 | 3390 |
| 002236 | | Z1=R5*(C4*(U2/U1*W2-W0)+(C4-1.0)*W0-(W1-W0)-QS*WF1/(WF1+WF2)-QG* | 3400 |
| | 1 | WF2/(WF1+WF2)) | 3410 |
| 002261 | | W44=W4 | 3420 |
| 002262 | | FNUM=K*(1.0-THETA) | 3430 |
| 002265 | | CONS=FNUM*FNUM | 3440 |

| | | |
|--------|---|------|
| 002266 | THK=K*THETA | 3450 |
| 002267 | DO 20 I=1,I1 | 3460 |
| 002271 | FI=I | 3470 |
| 002272 | CTERM=1.0-(FI-1.0)*Y1 | 3480 |
| 002276 | CTERM=CTERM*CTERM*CONS | 3490 |
| 002300 | AA(I)=1.0+CTERM | 3500 |
| 002303 | 20 BB(I)=1.0-CTERM | 3510 |
| 002306 | CONS=0.5*(R5-1.0)*Y1 | 3520 |
| 002311 | DO 21 I=1,I1 | 3530 |
| 002313 | FI=I | 3540 |
| 002314 | CTERM=1.0-(FI-1.0)*Y1 | 3550 |
| 002320 | CC(I)=CTERM*(CTERM+CONS) | 3560 |
| 002324 | DD(I)=CTERM*(CTERM-CONS) | 3570 |
| 002325 | 21 BVEC(I)=1.0 | 3580 |
| 002331 | CVEC(I)=-FNUM+FNUM)/AA(I) | 3590 |
| 002334 | DO 22 I=2,IMINUS | 3600 |
| 002335 | 22 CVEC(I)=-FNUM*CC(I)/AA(I) | 3610 |
| 002342 | DO 23 I=1,IMINUS | 3620 |
| 002344 | IP=I+1 | 3630 |
| 002346 | 23 AVEC(I)=-FNUM*DD(IP)/AA(IP) | 3640 |
| 002354 | DVEC(I)=(2.0*K*(THETA*V(2)-Y1*Z1*DD(I))+BB(I)*V(I))/AA(I) | 3650 |
| 002365 | DO 24 I=2,IMINUS | 3660 |
| 002366 | 24 DVEC(J)=(THK*(DD(I)*V(I=1)+CC(I)*V(I+1))+BB(I)*V(I))/AA(I) | 3670 |
| 002377 | DVEC(I)=(FNUM*CC(I)*W0+BB(I)*V(I)+THK*(DD(I)*V(I+1)+CC(I)* | 3680 |
| | 1 V(IPLUS)))/AA(I) | 3690 |
| 002414 | CALL TRIDAG(I1,AVEC,BVEC,CVEC,DVEC,W) | 3700 |
| 002420 | W(IPLUS)=W0 | 3710 |
| 002422 | W1=W(1) | 3720 |
| | C W1 IS WALL TEMPERATURE RATIO TW* | 3730 |
| 002424 | R8=R5 | 3740 |
| 002425 | R5=EXP(-E1*(1.0-W1)/(U1*W1)) | 3750 |
| | C R5 IS THE BURNING RATE RATIO R* | 3760 |
| 002436 | RTEST=R8/R5 | 3770 |
| 002437 | IF(RTEST=(1.0-EPS2)) 465,403,403 | 3780 |
| 002443 | 403 IF(RTEST=(1.0+EPS2)) 441,441,465 | 3790 |
| 002447 | 441 J9=1 | 3800 |
| 002450 | GO TO 680 | 3810 |
| 002451 | 446 J3=J3+1.0 | 3820 |
| 002453 | 447 TY=T+K*Y1*Y1 | 3830 |
| 002457 | IF(TY=K6*TCHANGE) 449,448,448 | 3840 |
| 002462 | 448 K=KIN*TIMFAC | 3850 |
| 002464 | 449 T=T+K*Y1*Y1 | 3860 |
| 002467 | IF(T=TSTOP) 455,455,8222 | 3870 |
| 002472 | 8222 CALL SECOND(TME) | 3880 |
| 002474 | WRITE(6,8224) TME | 3890 |
| 002502 | 8224 FORMAT(1H ///14H RUNNING TIME=,E15.8) | 3900 |
| 002502 | GO TO 202 | 3910 |
| 002503 | 455 DO 460 I=1, IPLUS | 3920 |
| 002505 | 460 V(I)=W(I) | 3930 |
| 002511 | R50=R5*R0 | 3940 |
| | C R50 IS THE INSTANTANEOUS BURNING RATE | 3950 |
| 002513 | IF(R50=RD1) 756,756,461 | 3960 |
| 002515 | 461 GO TO (200,906,280,200),J | 3970 |
| 002525 | 465 J9=J9+1 | 3980 |
| 002527 | 496 IF(J9=20) 461,461,716 | 3990 |
| 002532 | 680 IF(J3=J7) 446,446,685 | 4000 |
| 002535 | 685 TK6=T/K6 | 4010 |
| 002537 | N2=0 | 4020 |

| | | |
|--------|---|------|
| 002540 | DO 6000 I=1, IPLUS | 4030 |
| 002541 | Q(I)=(W(I)-W0)/(I,0-W0) | 4040 |
| 002546 | 6000 CONTINUE | 4050 |
| 002550 | DO 6010 I=1, I1 | 4060 |
| 002551 | GG(I)=(Q(I+1)+Q(I))/2.0*Y1 | 4070 |
| 002555 | 6010 CONTINUE | 4080 |
| 002557 | DO 6020 I=1, I1 | 4090 |
| 002561 | GO=GO+GG(I) | 4100 |
| 002563 | 6020 CONTINUE | 4110 |
| 002565 | GO=2.0*GO | 4120 |
| | C GO IS THE INTEGRAL OF THE TEMPERATURE PROFILE | 4130 |
| 002567 | IF(JPRINT) 175,174,175 | 4140 |
| 002570 | 175 WRITE(6,686) TK6 | 4150 |
| 002576 | 686 FORMAT(6H TIME=,E15.8) | 4160 |
| 002576 | DO 696 I=1, IPLUS | 4170 |
| 002600 | L=I-1 | 4180 |
| 002602 | IF(L) 613,613,622 | 4190 |
| 002603 | 613 WRITE(6,614) | 4200 |
| 002607 | 614 FORMAT(8H /9H Y*,13X,7HX (IN.), 6X,14H(T-T0)/(TW-T0)) | 4210 |
| 002607 | 622 IF(L=N2) 696,694,694 | 4220 |
| 002612 | 694 FL=L | 4230 |
| 002614 | PRNT1=FL*Y1 | 4240 |
| 002616 | IF(PRNT1 -1.0) 616,615,616 | 4250 |
| 002620 | 615 ARG=0.001 | 4260 |
| 002622 | PRNT3=0.001 | 4270 |
| 002623 | GO TO 617 | 4280 |
| 002623 | 616 ARG=1.0-PRNT1 | 4290 |
| 002625 | PRNT3=(W(I)-W0)/(W(1)-W0) | 4300 |
| 002633 | 617 PRNT2=-ALOG(ARG)/(K5*R5) | 4310 |
| 002641 | WRITE(6,620) PRNT1,PRNT2,PRNT3 | 4320 |
| 002653 | 620 FORMAT(3E16.8) | 4330 |
| 002653 | N2=N2+N22 | 4340 |
| 002655 | 696 CONTINUE | 4350 |
| 002660 | WRITE(6,629) | 4360 |
| 002663 | 629 FORMAT(1H) | 4370 |
| 002663 | 475 WRITE(6,476) P5,GO, Z1,R5,W1,W2,W3,EFS,EHS | 4380 |
| 002711 | 476 FORMAT(8H P*,13X,2HE*,11X,2HZ*, | 4390 |
| | 112X,2HR*,12X,3HTW*,11X,3HTF*,11X,3HTC*,11X,3HEF*,11X,3HEH*/ | 4400 |
| | 29E14.5) | 4410 |
| 002711 | WRITE(6,610) | 4420 |
| 002715 | 610 FORMAT(1H0) | 4430 |
| 002715 | GO TO 30 | 4440 |
| 002716 | 174 WRITE(6,29)TK6,P5,GO, Z1,R5,W1,W2,W3,EFS,EHS | 4450 |
| 002746 | 30 CONTINUE | 4460 |
| 002746 | J3=1.0 | 4470 |
| 002750 | GO=0.0 | 4480 |
| 002751 | GO TO 447 | 4490 |
| 002751 | 716 WRITE(6,717) | 4500 |
| 002755 | 717 FORMAT(34H FINAL ITERATION DOES NOT CONVERGE) | 4510 |
| 002755 | WRITE(6,7000)R5,R8,TK6 | 4520 |
| 002767 | 7000 FORMAT(4H R5=,E15.8/4H R8=,E15.8/4H T =,E15.8) | 4530 |
| 002767 | GO TO 8222 | 4540 |
| 002770 | 720 WRITE(6,721) | 4550 |
| 002774 | 721 FORMAT(27H LINEAR LIMIT LINE EXCEEDED) | 4560 |
| 002774 | GO TO 8222 | 4570 |
| 002775 | 745 L2L1=L2-L1 | 4580 |
| 002777 | WRITE(6,746) W4,L2L1 | 4590 |
| 003007 | 746 FORMAT(31H IF ITERATION DOES NOT CONVERGE/4H W4=,E15.8,8H F(TF)=, | 4600 |

| | | |
|--------|---|------|
| 003007 | 747 ¹ GO TO 8222 ^{E15.8)} | 4610 |
| 003010 | 756 WRITE(6,758) | 4620 |
| 003014 | 758 FORMAT(44H BURNING RATE BELOW LOWER DEFLAGRATION LIMIT) | 4630 |
| 003014 | 1000 GO TO 8222 | 4640 |
| 003015 | 1001 CONTINUE | 4650 |
| 003015 | 1002 STOP | 4660 |
| 003017 | END | 4670 |
| | | 4680 |

| | | |
|--------|---|------|
| | SUBROUTINE SOLVE(AA, Y, N, NMX, X, NP1, A, ISOL) | 4690 |
| C | SUBROUTINE TO SOLVE AN N BY N SYSTEM OF EQUATIONS OF THE FORM | 4700 |
| C | AA * X = Y --- WRITTEN IN FORTRAN II | 4710 |
| C | | 4720 |
| C | AA CONTAINS THE GIVEN N BY N COEFFICIENT MATRIX | 4730 |
| C | Y CONTAINS THE GIVEN N BY 1 RIGHT HAND SIDE | 4740 |
| C | N IS A POSITIVE INTEGER | 4750 |
| C | NMX IS THE GIVEN DIMENSION OF AA, X, AND Y IN THE CALLING PROGRAM | 4760 |
| C | X IS THE N BY 1 SOLUTION VECTOR | 4770 |
| C | NP1 IS A POSITIVE INTEGER GREATER THAN OR EQUAL TO N+1 | 4780 |
| C | A IS AN NP1 BY NP1 SCRATCH ARRAY | 4790 |
| C | ISOL IS RETURNED AS 1 IF A SOLUTION EXISTS, 0 IF NO SOLUTION EXISTS | 4800 |
| 000013 | DIMENSION AA(NMX, 1), Y(NMX), X(NMX), A(NP1, 1) | 4810 |
| 000013 | NM = N + 1 | 4820 |
| 000015 | DO 1 I = 1, N | 4830 |
| 000016 | A(I, NM) = Y(I) | 4840 |
| 000024 | DO 1 J = 1, N | 4850 |
| 000025 | 1 A(I, J) = AA(I, J) | 4860 |
| 000044 | DO 6 I = 1, N | 4870 |
| 000046 | IE = 0 | 4880 |
| 000047 | 2 IF (A(I, I)) 3, 400, 3 | 4890 |
| 000054 | 3 DIAGST = A(I, I) | 4900 |
| 000061 | DO 4 J = I, NM | 4910 |
| 000062 | 4 A(I, J) = A(I, J) / DIAGST | 4920 |
| 000072 | IX = I + 1 | 4930 |
| 000074 | DO 6 K = IX, N | 4940 |
| 000075 | ROWMUL = A(K, I) | 4950 |
| 000102 | DO 6 L = I, NM | 4960 |
| 000103 | 6 A(K, L) = A(I, L) * ROWMUL * (-1.) + A(K, L) | 4970 |
| 000126 | M = N | 4980 |
| 000127 | X(M) = A(M, NM) | 4990 |
| 000135 | 7 M = M - 1 | 5000 |
| 000137 | DO 8 IA = 1, M | 5010 |
| 000140 | 8 A(IA, NM) = A(IA, NM) - A(IA, M + 1) * A(M + 1, NM) | 5020 |
| 000162 | X(M) = A(M, NM) | 5030 |
| 000166 | IF (M = 1) 502, 502, 7 | 5040 |
| 000171 | 400 IE = IE + 1 | 5050 |
| 000173 | IZ = I + IE | 5060 |
| 000174 | IF (I + IE = N + 1) 401, 481, 481 | 5070 |
| 000177 | 401 DO 404 ID = I, NM | 5080 |
| 000201 | SWITCH = A(I, ID) | 5090 |
| 000206 | A(I, ID) = A(IZ, ID) | 5100 |
| 000215 | 404 A(IZ, ID) = SWITCH | 5110 |
| 000223 | GO TO 2 | 5120 |
| 000223 | 481 ISOL = 0 | 5130 |
| 000224 | RETURN | 5140 |
| 000225 | 502 ISOL = 1 | 5150 |
| 000227 | RETURN | 5160 |
| 000227 | END | 5170 |

```

SUBROUTINE SUB500
SUBROUTINE TO SOLVE FLAME SPEED EQUATION FOR TF*
COMMON W,W0,W2,W4, Z,Z1, V,I1,J5,J9,K,K5,L1,L2,N,N2,P5,R5,U2,Y1,
1EPS3,EPS4,EPS1,EPS2,DI,C9,JERROR,IPLUS, JPRINT,C0,C,P0,R0,QL,QGP,
2C1,C2,C3,C5,US,POW,N22,W44,E1,C4,U1,W1,M,EHS,EFS,WRR,ZFI,
3CP,CS,QQG,QQS,EFI,EHI,NN2,NN1,WFI,GS,QG,U0,W1I,W2I
DIMENSION W(100), V(100), Z(100)
REAL K,K5,L1,L2,N,M,NN2,NN1
REAL LTEST
W4=W2
P6=P5*P0
RS=C1+C2*ALOG(P6)+C3*(ALOG(P6))**2+C5*(ALOG(P6))**3
RS=EXP(RS)
US=U2*(RS/R0)**POW
WS=WRR/(1.0-WRR*ALOG(10.0*RS)/E1)
SX1=C4*U2/U1*US/U2-GS-U0/U1
SX2=C4*U2/U1*US/U2-QG-U0/U1
SX4=RS/R0*(W1I+W2I)
WW2=-SX1*SX4/(SX2-SX1)
WW1=SX2*SX4/(SX2-SX1)
WRW=WW1/WW2
EHS=(1.0-U1/EHI*(ALOG(WW1/W1I)-NN1*ALOG(P6/P0)-(NN1+2.0)*
1 ALOG(WS/U1)))*WS/U1
EFS=(1.0-U2/EFI*(ALOG(WW2/W2I)-NN2*ALOG(P6/P0)-(NN2+2.0)*
1 ALOG(US/U2)))*US/U2
EF* IS ASSUMED TO BE A FUNCTION OF PRESSURE ONLY
AND IS CALCULATED FROM STEADY STATE CONDITIONS
DI=W1I+W2I
WF1=W1I*P5**NN1*W1**((NN1+2.0)*EXP(EHI/U1*(W1-EHS)/W1)
L1=ALOG(R5*DI-WF1)-NN2*ALOG(P5)-ALOG(W2I)
510 L2=(NN2+2.0)*ALOG(W4)+(EFI/U2)*(1.0-EFS/W4)
LTEST=L2/L1
IF(LTEST=(1.0-EPS3)) 530,404,404
404 IF(LTEST=(1.0-EPS3)) 522,522,530
522 J5=1
GO TO 525
530 WSQ=W4*W4
F1=(NN2+2.0)/W4+(EFI/U2)*(EFS/WSQ)
F1 IS FIRST DERIVATIVE OF L2
F2=-((NN2+2.0)/WSQ-2.0*(EFI/U2)*(EFS/(WSQ*W4)))
F2 IS SECONDD DERIVATIVE OF L2
W4=W4-(L2-L1)/(F1-F2*(L2-L1)/(F1+F1))
W4 IS FLAME TEMPERATURE RATIO TF*
513 J5=J5+1
IF(J5=50) 510,510,524
524 JERROR=1
525 CONTINUE
RETURN
END

```

| | | | |
|--------|-----|---|------|
| | | SUBROUTINE SUB600 | 5670 |
| | C | SUBROUTINE TO SOLVE FOR INITIAL TEMPERATURE PROFILE IN SOLID | 5680 |
| 000002 | | COMMON W,W0,W2,W4, Z,Z1, V,I1,J5,J9,K,K5,L1,L2,N,N2,P5,R5,U2,Y1, | 5690 |
| | | 1EPS3,EPS4,EPS1,EPS2,DI,C9,JERROR,IPLUS, JPRINT,C0,C,P0,R0,QRL,QGP, | 5700 |
| | | 2C1,C2,C3,C5,US,POW,N22,W44,E1,C4,U1,W1,M,EMS,EFS,WRR,ZFI, | 5710 |
| | | 3CP,CS,QQG,QQS,EFI,EMI,NN2,NN1,WFI,QS,QQ,U0,W1I,W2I | 5720 |
| 000002 | | DIMENSION W(100), V(100), Z(100) | 5730 |
| 000002 | | REAL K,K5,L1,L2,N,M | 5740 |
| 000002 | | DO 625 I=1,IPLUS | 5750 |
| 000004 | | L=I-1 | 5760 |
| 000005 | | FL=L | 5770 |
| 000007 | | V(I)=(1.0-FL*Y1)*(1.0-W0)+W0 | 5780 |
| 000017 | | IF(JPRINT) 618,625,618 | 5790 |
| 000020 | 618 | IF(J9=1) 612,612,625 | 5800 |
| 000023 | 612 | IF(L) 613,613,622 | 5810 |
| 000025 | 613 | WRITE(6,614) | 5820 |
| 000031 | 614 | FORMAT(8H TIME=0/9H Y*,13X,7HX (IN.), 6X,14H(T-T0)/(TW-T0)) | 5830 |
| 000031 | 622 | IF(L=N2) 625,623,623 | 5840 |
| 000034 | 623 | FL=L | 5850 |
| 000035 | | PRNT1=FL*Y1 | 5860 |
| 000037 | | IF(PRNT1=1.0) 616,615,616 | 5870 |
| 000042 | 615 | ARG=0.001 | 5880 |
| 000043 | | PRNT3=0.001 | 5890 |
| 000045 | | GO TO 617 | 5900 |
| 000045 | 616 | ARG=1.0-PRNT1 | 5910 |
| 000047 | | PRNT3=(V(I)-W0)/(1.0-W0) | 5920 |
| 000055 | 617 | PRNT2=-ALOG(ARG)/(K5*R5) | 5930 |
| 000063 | | WRITE(6,620) PRNT1,PRNT2,PRNT3 | 5940 |
| 000075 | 620 | FORMAT(3E16.8) | 5950 |
| 000075 | | N2=N2+N22 | 5960 |
| 000077 | 625 | CONTINUE | 5970 |
| 000102 | 630 | DO 634 I=1, IPLUS | 5980 |
| 000104 | 634 | W(I)=V(I) | 5990 |
| 000111 | | RETURN | 6000 |
| 000112 | | END | 6010 |

| | | | |
|--------|---|--|------|
| | | SUBROUTINE TRIDAG(N,AVEC,BVEC,CVEC,DVEC,SVEC) | 6020 |
| | C | SUBROUTINE TO SOLVE FOR INSTANTANEOUS TEMPERATURE PROFILE IN SOLID | 6030 |
| | C | SOLVES TRIDIAGONAL MATRIX | 6040 |
| 000011 | | DIMENSION AVEC(1),BVEC(1),CVEC(1),DVEC(1),SVEC(1) | 6050 |
| 000011 | | DVEC(1)=DVEC(1)/BVEC(1) | 6060 |
| 000012 | | W=BVEC(1) | 6070 |
| 000013 | | DO 2 J=2,N | 6080 |
| 000015 | | JJ=J-1 | 6090 |
| 000016 | | BVEC(JJ)=CVEC(JJ)/W | 6100 |
| 000022 | | W=BVEC(J)-AVEC(JJ)*BVEC(JJ) | 6110 |
| 000026 | 2 | DVEC(J)=(DVEC(J)-AVEC(JJ)*DVEC(JJ))/W | 6120 |
| 000036 | | IM=N-1 | 6130 |
| 000040 | | DO 3 J=1,IM | 6140 |
| 000041 | | JJ=N-J | 6150 |
| 000042 | 3 | DVEC(JJ)=DVEC(JJ)-BVEC(JJ)*DVEC(JJ+1) | 6160 |
| 000051 | | DO 4 J=1,N | 6170 |
| 000052 | 4 | SVEC(J)=DVEC(J) | 6180 |
| 000056 | | RETURN | 6190 |
| 000056 | | END | 6200 |

JULY 20 1970

SOLID PROPELLANT TRANSIENT COMBUSTION BEHAVIOR
UTX 11327

INPUT CONSTANTS

C1=-3.08174274E+00
C2=-2.70948178E-01
C3= 1.44544251E-01
C5=-9.98599071E-03
C4= 1.00000000E+00
CP= 4.00000000E-01
CS= 4.00000000E-01
KG= 4.00000000E-04
N1= 1.00000000E+00
N2= 2.00000000E+00
T0= 3.00000000E+02
TFR= 2.41900000E+03
TWR= 8.00000000E+02
POW= 1.05000000E-02
RHO= 8.00000000E-02
WRL= 1.94071918E-01
GRL= 1.00000000E-01
KAPPA= 1.00000000E-04
GAMMA= 1.20000000E+00
TSTOP= 7.00000000E-02
TIMFAC= 1.00000000E+00
TCHANGE= 1.00000000E-03
TIME STEP= 1.00000000E-05

LIMIT POINT VALUES

PL= 4.27591898E+02
RL= 1.94264798E-01
AL= 1.93599454E+01
ALPHAL= 8.39684615E-01
EFL= 5.37787134E+05
EHL= 1.02230756E+05
TFL= 2.43430861E+03
TWL= 8.17368812E+02
XFL= 1.35302233E+01
NU = 3.80898941E-01

INITIAL POINT VALUES

P0= 7.00000000E+02
R0= 2.32014316E-01
EW= 5.00000000E+04
EF= 5.42757819E+05
EH= 1.03395534E+05
TF= 2.43885176E+03
TW= 8.22142032E+02
QG= 1.00000000E+03
QS= 1.00000000E+02
A = 1.93123427E+01
ALPHA= 8.38358051E-01
NU = 3.37197914E-01
XFI = 1.34515667E+01

JULY 20 1970

CHAMBER DEPRESSURIZATION RESPONSE

INITIAL DECAY RATE= 6.0000000E+04
AT/ATI= 4.49511536E+00

| TIME | P* | F* | Z* | R* | TW* | TF* | TC* | EF* | EM* |
|------------|------------|------------|-------------|------------|------------|------------|------------|------------|------------|
| 0. | 1.0000E+00 | 1.0000E+00 | -6.3510E-01 | 1.0000E+00 | 1.0000E+00 | 1.0000E+00 | 1.0000E+00 | 1.0000E+00 | 1.0000E+00 |
| 4.0000E-04 | 9.6628E-01 | 1.0019E+00 | -6.2238E-01 | 9.5506E-01 | 9.9849E-01 | 9.9965E-01 | 9.9432E-01 | 9.9936E-01 | 9.9923E-01 |
| 8.0000E-04 | 9.3382E-01 | 1.0060E+00 | -6.1334E-01 | 9.3621E-01 | 9.9784E-01 | 9.9947E-01 | 9.8874E-01 | 9.9873E-01 | 9.9845E-01 |
| 1.2000E-03 | 9.0270E-01 | 1.0102E+00 | -6.0483E-01 | 9.1980E-01 | 9.9726E-01 | 9.9930E-01 | 9.8328E-01 | 9.9810E-01 | 9.9769E-01 |
| 1.6000E-03 | 8.7286E-01 | 1.0148E+00 | -5.9656E-01 | 9.0459E-01 | 9.9671E-01 | 9.9915E-01 | 9.7794E-01 | 9.9747E-01 | 9.9692E-01 |
| 2.0000E-03 | 8.4426E-01 | 1.0195E+00 | -5.8856E-01 | 8.9046E-01 | 9.9620E-01 | 9.9900E-01 | 9.7273E-01 | 9.9686E-01 | 9.9616E-01 |
| 2.4000E-03 | 8.1683E-01 | 1.0242E+00 | -5.8071E-01 | 8.7686E-01 | 9.9570E-01 | 9.9885E-01 | 9.6763E-01 | 9.9624E-01 | 9.9541E-01 |
| 2.8000E-03 | 7.9053E-01 | 1.0290E+00 | -5.7303E-01 | 8.6383E-01 | 9.9521E-01 | 9.9870E-01 | 9.6265E-01 | 9.9563E-01 | 9.9466E-01 |
| 3.2000E-03 | 7.6531E-01 | 1.0339E+00 | -5.6549E-01 | 8.5116E-01 | 9.9473E-01 | 9.9856E-01 | 9.5780E-01 | 9.9503E-01 | 9.9392E-01 |
| 3.6000E-03 | 7.4111E-01 | 1.0388E+00 | -5.5809E-01 | 8.3886E-01 | 9.9425E-01 | 9.9841E-01 | 9.5306E-01 | 9.9443E-01 | 9.9319E-01 |
| 4.0000E-03 | 7.1789E-01 | 1.0436E+00 | -5.5081E-01 | 8.2686E-01 | 9.9379E-01 | 9.9827E-01 | 9.4844E-01 | 9.9384E-01 | 9.9246E-01 |
| 4.4000E-03 | 6.9561E-01 | 1.0485E+00 | -5.4365E-01 | 8.1513E-01 | 9.9332E-01 | 9.9813E-01 | 9.4394E-01 | 9.9326E-01 | 9.9173E-01 |
| 4.8000E-03 | 6.7422E-01 | 1.0534E+00 | -5.3662E-01 | 8.0354E-01 | 9.9286E-01 | 9.9799E-01 | 9.3955E-01 | 9.9268E-01 | 9.9101E-01 |
| 5.2000E-03 | 6.5368E-01 | 1.0583E+00 | -5.2964E-01 | 7.9238E-01 | 9.9240E-01 | 9.9785E-01 | 9.3527E-01 | 9.9210E-01 | 9.9030E-01 |
| 5.6000E-03 | 6.3395E-01 | 1.0632E+00 | -5.2288E-01 | 7.8132E-01 | 9.9195E-01 | 9.9771E-01 | 9.3111E-01 | 9.9153E-01 | 9.8959E-01 |
| 6.0000E-03 | 6.1499E-01 | 1.0681E+00 | -5.1617E-01 | 7.7046E-01 | 9.9150E-01 | 9.9758E-01 | 9.2706E-01 | 9.9097E-01 | 9.8889E-01 |
| 6.4000E-03 | 5.9678E-01 | 1.0729E+00 | -5.0957E-01 | 7.5978E-01 | 9.9105E-01 | 9.9744E-01 | 9.2311E-01 | 9.9041E-01 | 9.8820E-01 |
| 6.8000E-03 | 5.7926E-01 | 1.0777E+00 | -5.0307E-01 | 7.4928E-01 | 9.9060E-01 | 9.9730E-01 | 9.1928E-01 | 9.8986E-01 | 9.8751E-01 |
| 7.2000E-03 | 5.6243E-01 | 1.0825E+00 | -4.9667E-01 | 7.3894E-01 | 9.9015E-01 | 9.9716E-01 | 9.1555E-01 | 9.8931E-01 | 9.8682E-01 |
| 7.6000E-03 | 5.4624E-01 | 1.0873E+00 | -4.9038E-01 | 7.2876E-01 | 9.8970E-01 | 9.9703E-01 | 9.1193E-01 | 9.8876E-01 | 9.8615E-01 |
| 8.0000E-03 | 5.3066E-01 | 1.0920E+00 | -4.8417E-01 | 7.1873E-01 | 9.8926E-01 | 9.9689E-01 | 9.0841E-01 | 9.8823E-01 | 9.8547E-01 |
| 8.4000E-03 | 5.1566E-01 | 1.0967E+00 | -4.7807E-01 | 7.0884E-01 | 9.8881E-01 | 9.9675E-01 | 9.0499E-01 | 9.8769E-01 | 9.8481E-01 |
| 8.8000E-03 | 5.0123E-01 | 1.1014E+00 | -4.7205E-01 | 6.9909E-01 | 9.8836E-01 | 9.9662E-01 | 9.0167E-01 | 9.8717E-01 | 9.8415E-01 |
| 9.2000E-03 | 4.8734E-01 | 1.1060E+00 | -4.6613E-01 | 6.8947E-01 | 9.8792E-01 | 9.9648E-01 | 8.9845E-01 | 9.8664E-01 | 9.8350E-01 |
| 9.6000E-03 | 4.7395E-01 | 1.1107E+00 | -4.6029E-01 | 6.7998E-01 | 9.8747E-01 | 9.9635E-01 | 8.9533E-01 | 9.8613E-01 | 9.8285E-01 |
| 1.0000E-02 | 4.6106E-01 | 1.1152E+00 | -4.5455E-01 | 6.7061E-01 | 9.8703E-01 | 9.9621E-01 | 8.9230E-01 | 9.8561E-01 | 9.8221E-01 |
| 1.0400E-02 | 4.4863E-01 | 1.1198E+00 | -4.4888E-01 | 6.6135E-01 | 9.8659E-01 | 9.9607E-01 | 8.8937E-01 | 9.8511E-01 | 9.8157E-01 |
| 1.0800E-02 | 4.3665E-01 | 1.1243E+00 | -4.4329E-01 | 6.5219E-01 | 9.8614E-01 | 9.9594E-01 | 8.8653E-01 | 9.8460E-01 | 9.8094E-01 |
| 1.1200E-02 | 4.2510E-01 | 1.1287E+00 | -4.3778E-01 | 6.4314E-01 | 9.8569E-01 | 9.9580E-01 | 8.8378E-01 | 9.8411E-01 | 9.8031E-01 |
| 1.1600E-02 | 4.1396E-01 | 1.1332E+00 | -4.3235E-01 | 6.3420E-01 | 9.8525E-01 | 9.9567E-01 | 8.8112E-01 | 9.8361E-01 | 9.7969E-01 |
| 1.2000E-02 | 4.0321E-01 | 1.1376E+00 | -4.2700E-01 | 6.2535E-01 | 9.8480E-01 | 9.9553E-01 | 8.7854E-01 | 9.8312E-01 | 9.7908E-01 |
| 1.2400E-02 | 3.9283E-01 | 1.1419E+00 | -4.2170E-01 | 6.1654E-01 | 9.8434E-01 | 9.9539E-01 | 8.7605E-01 | 9.8264E-01 | 9.7847E-01 |
| 1.2800E-02 | 3.8281E-01 | 1.1463E+00 | -4.1645E-01 | 6.0772E-01 | 9.8389E-01 | 9.9526E-01 | 8.7364E-01 | 9.8216E-01 | 9.7787E-01 |
| 1.3200E-02 | 3.7312E-01 | 1.1506E+00 | -4.1125E-01 | 5.9895E-01 | 9.8342E-01 | 9.9512E-01 | 8.7132E-01 | 9.8168E-01 | 9.7727E-01 |
| 1.3600E-02 | 3.6377E-01 | 1.1548E+00 | -4.0615E-01 | 5.9043E-01 | 9.8297E-01 | 9.9498E-01 | 8.6907E-01 | 9.8121E-01 | 9.7668E-01 |
| 1.4000E-02 | 3.5473E-01 | 1.1591E+00 | -4.0125E-01 | 5.8244E-01 | 9.8254E-01 | 9.9485E-01 | 8.6690E-01 | 9.8075E-01 | 9.7609E-01 |
| 1.4400E-02 | 3.4600E-01 | 1.1632E+00 | -3.9653E-01 | 5.7498E-01 | 9.8213E-01 | 9.9472E-01 | 8.6481E-01 | 9.8028E-01 | 9.7551E-01 |
| 1.4800E-02 | 3.3756E-01 | 1.1673E+00 | -3.9175E-01 | 5.6708E-01 | 9.8169E-01 | 9.9459E-01 | 8.6280E-01 | 9.7983E-01 | 9.7493E-01 |
| 1.5200E-02 | 3.2939E-01 | 1.1714E+00 | -3.8612E-01 | 5.5922E-01 | 9.8106E-01 | 9.9441E-01 | 8.6086E-01 | 9.7937E-01 | 9.7436E-01 |
| 1.5600E-02 | 3.2141E-01 | 1.1756E+00 | -3.8059E-01 | 5.5292E-01 | 9.7950E-01 | 9.9403E-01 | 8.5893E-01 | 9.7892E-01 | 9.7378E-01 |

BURNING RATE BELOW LOWER DEFLAGRATION LIMIT

RUNNING TIME= 3.35110000E+01

Appendix C

TRANSIENT COMBUSTION BEHAVIOR WITH A DECREASE IN BURNING RATE

In this appendix, a test calculation is shown that was run early in the program to ensure that correct behavior of the temperature profile was being attained as the combustion process moves from one steady state to another in which $r^* < 1$. This calculation must be carefully examined because of the nonanalyticity of the temperature profile at the cold end in the transformed coordinate system.

In the case considered here, the pressure was reduced from 200 to 150 psia over a period of 10 msec and then then the computer was allowed to run for an additional 20 msec. At that time the burning rate has very nearly achieved its asymptotic value and one can compare the numerical temperature profile with the equation obtained from the transformation (Eq. (26) of the main body):

$$\frac{T-T_0}{T_w-T_0} = (1-y^*)^{r^*} \quad (C1)$$

Note that $y^* = 1$ corresponds to $x = \infty$ and $T = T_0$; what has been printed out instead opposite $y^* = 1$ is the value of x for which $\frac{T-T_0}{T_w-T_0} = 0.001$ in order to give some measure of the temperature profile thickness.

The calculated asymptotic profile from Eq. (C1) is shown opposite the last printout; it can be seen that there is no difficulty of the type encountered by Merkle, et al.⁴

JUNE 26 1970

SOLID PROPELLANT TRANSIENT COMBUSTION BEHAVIOR
PU 269

INPUT CONSTANTS

C1=-5.07776492E+00
C2= 6.36824580E-01
C3= 3.57458855E-02
C5=-6.93449490E-03
C4= 1.00000000E+00
CP= 4.00000000E-01
CS= 4.00000000E-01
KG= 4.00000000E-04
N1= 1.00000000E+00
N2= 2.00000000E+00
T0= 3.00000000E+02
IFR= 2.82800000E+03
TWR= 8.00000000E+02
POW= 2.50000000E-02
RHO= 6.00000000E-02
WRL= 6.39611342E-02
URL= 1.00000000E-01
KAPPA= 1.00000000E-04
GAMMA= 1.20000000E+00
TSTOP= 3.00000000E+02
TIMFAC= 1.00000000E+00
TCHANGE= 1.02000000E-02
TIME STEP= 1.00000000E-05

LIMIT POINT VALUES

PL= 6.45228635E+02
RL= 2.62007004E-01
AL= 1.92793167E+01
ALPHA1= 8.38741423E-01
EFL= 2.51478200E+05
EHL= 1.77375374E+05
TFL= 2.81971517E+03
TWL= 8.25442135E+02
ZFL= 5.03552841E+00
NU= 2.28601891E-01

INITIAL POINT VALUES

P0= 2.00000000E+02
R0= 1.77000000E-01
EW= 5.00000000E+04
EF= 2.37747253E+05
EH= 1.73490978E+05
TF= 2.85161600E+03
TW= 8.14889121E+02
QG= 1.09090909E+03
GS= 1.09090909E+02
A = 1.93845929E+01
ALPHA= 9.73163177E-01
NU = 4.31611778E-01
ZFI = 5.11151233E+00

JUNE 26 1970

SINUSOIDAL RESPONSE

P* = 9.99750000E-01

F* = 0.

TIME=0

| Y* | X (IN.) | (T-T0)/(TW-T0) |
|----------------|----------------|----------------|
| 0. | -0. | 1.00000000E+00 |
| 2.00000000E-01 | 1.26069803E-04 | 8.00000000E-01 |
| 4.00000000E-01 | 2.88602047E-04 | 6.00000000E-01 |
| 6.00000000E-01 | 5.17678380E-04 | 4.00000000E-01 |
| 8.00000000E-01 | 9.09286956E-04 | 2.00000000E-01 |
| 1.00000000E+00 | 3.90268660E-03 | 1.00000000E-01 |

TIME = 2.00000000E-04

| Y* | X (IN.) | (T-T0)/(TW-T0) |
|----------------|----------------|----------------|
| 0. | -0. | 1.00000000E+00 |
| 2.00000000E-01 | 1.26839058E-04 | 8.00264957E-01 |
| 4.00000000E-01 | 2.90363044E-04 | 6.00271804E-01 |
| 6.00000000E-01 | 5.20837158E-04 | 4.00189648E-01 |
| 8.00000000E-01 | 9.14835258E-04 | 2.00094979E-01 |
| 1.00000000E+00 | 3.92650008E-03 | 1.00000000E-01 |

| P* | F* | Z* | R* | TW* | TF* | TC* | EF* | EH* |
|-------------|-------------|--------------|-------------|-------------|-------------|-------------|-------------|-------------|
| 9.95000E-01 | 1.00003E+00 | -6.30228E-01 | 9.93935E-01 | 9.99802E-01 | 9.99883E-01 | 1.00000E+00 | 9.99754E-01 | 9.99897E-01 |

TIME = 4.00000000E-04

| Y* | X (IN.) | (T-T0)/(TW-T0) |
|----------------|----------------|----------------|
| 0. | -0. | 1.00000000E+00 |
| 2.00000000E-01 | 1.27683922E-04 | 8.00616398E-01 |
| 4.00000000E-01 | 2.92797127E-04 | 6.00725858E-01 |
| 6.00000000E-01 | 5.24306409E-04 | 4.00549867E-01 |
| 8.00000000E-01 | 9.20928895E-04 | 2.00279796E-01 |
| 1.00000000E+00 | 3.95265415E-03 | 1.00000000E-01 |

| P* | F* | Z* | R* | TW* | TF* | TC* | EF* | EH* |
|-------------|-------------|--------------|-------------|-------------|-------------|-------------|-------------|-------------|
| 9.90000E-01 | 1.00025E+00 | -6.28519E-01 | 9.87358E-01 | 9.99585E-01 | 9.99749E-01 | 1.00000E+00 | 9.99506E-01 | 9.99784E-01 |

TIME = 6.00000000E-04

| Y* | X (IN.) | (T-T0)/(TW-T0) |
|----------------|----------------|----------------|
| 0. | -0. | 1.00000000E+00 |
| 2.00000000E-01 | 1.28399548E-04 | 8.00989416E-01 |
| 4.00000000E-01 | 2.93935355E-04 | 6.01252728E-01 |
| 6.00000000E-01 | 5.27244972E-04 | 4.01011598E-01 |
| 8.00000000E-01 | 9.26090396E-04 | 2.00529304E-01 |
| 1.00000000E+00 | 3.97480746E-03 | 1.00000000E-01 |

| P* | F* | Z* | R* | TW* | TF* | TC* | EF* | EH* |
|-------------|-------------|--------------|-------------|-------------|-------------|-------------|-------------|-------------|
| 9.85000E-01 | 1.00063E+00 | -6.26847E-01 | 9.81856E-01 | 9.99403E-01 | 9.99634E-01 | 1.00000E+00 | 9.99258E-01 | 9.99675E-01 |

TIME = 8.00000000E-04

| Y* | X (IN.) | (T-T0)/(TW-T0) |
|----------------|----------------|----------------|
| 0. | -0. | 1.00000000E+00 |
| 2.00000000E-01 | 1.29012739E-04 | 8.01370931E-01 |
| 4.00000000E-01 | 2.95339088E-04 | 6.01817694E-01 |
| 6.00000000E-01 | 5.29762910E-04 | 4.01539777E-01 |

8.00000000E-01 9.30513080E-04 2.00831452E-01
1.00000000E+00 3.99378975E-03 1.00000000E-03

P* E* Z* R* TW* TF* TC* EF* EH*
9.80000E-01 1.00112E+00 -6.25214E-01 9.77189E-01 9.99248E-01 9.99533E-01 1.00000E+00 9.99008E-01 9.99566E-01

TIME= 1.00000000E-03

Y* X (IN.) (T-T0)/(TW-T0)
0. -0. 1.00000000E+00
2.00000000E-01 1.29560372E-04 8.01754964E-01
4.00000000E-01 2.96592743E-04 6.02406231E-01
6.00000000E-01 5.32011648E-04 4.02114737E-01
8.00000000E-01 9.34462923E-04 2.01177760E-01
1.00000000E+00 4.01074260E-03 1.00000000E-03

P* F* Z* R* TW* TF* TC* EF* EH*
9.75000E-01 1.00168E+00 -6.23608E-01 9.73058E-01 9.99111E-01 9.99441E-01 1.00000E+00 9.98756E-01 9.99456E-01

TIME= 1.20000000E-03

Y* X (IN.) (T-T0)/(TW-T0)
0. -0. 1.00000000E+00
2.00000000E-01 1.30067604E-04 8.02146325E-01
4.00000000E-01 2.97753911E-04 6.03011580E-01
6.00000000E-01 5.34094485E-04 4.02724988E-01
8.00000000E-01 9.38121366E-04 2.01561804E-01
1.00000000E+00 4.02644474E-03 1.00000000E-03

P* F* Z* R* TW* TF* TC* EF* EH*
9.70000E-01 1.00230E+00 -6.22019E-01 9.69264E-01 9.98983E-01 9.99355E-01 1.00000E+00 9.98504E-01 9.99345E-01

TIME= 1.40000000E-03

Y* X (IN.) (T-T0)/(TW-T0)
0. -0. 1.00000000E+00
2.00000000E-01 1.30549433E-04 8.02538634E-01
4.00000000E-01 2.98856926E-04 6.03630198E-01
6.00000000E-01 5.36073013E-04 4.03363395E-01
8.00000000E-01 9.41596592E-04 2.01978580E-01
1.00000000E+00 4.04136051E-03 1.00000000E-03

P* F* Z* R* TW* TF* TC* EF* EH*
9.65000E-01 1.00297E+00 -6.20438E-01 9.65686E-01 9.98863E-01 9.99273E-01 1.00000E+00 9.98250E-01 9.99234E-01

TIME= 1.60000000E-03

Y* X (IN.) (T-T0)/(TW-T0)
0. -0. 1.00000000E+00
2.00000000E-01 1.31014601E-04 8.02933722E-01
4.00000000E-01 2.99921800E-04 6.04259963E-01
6.00000000E-01 5.37983125E-04 4.04025222E-01
8.00000000E-01 9.44951649E-04 2.02424122E-01
1.00000000E+00 4.05576052E-03 1.00000000E-03

P* F* Z* R* TW* TF* TC* EF* EH*
9.60000E-01 1.00366E+00 -6.18863E-01 9.62258E-01 9.98748E-01 9.99194E-01 1.00000E+00 9.97995E-01 9.99122E-01

TIME= 1.80000000E-03

Y* X (IN.) (T-T0)/(TW-T0)

| | | |
|----------------|----------------|----------------|
| 0. | -0. | 1.00000000E+00 |
| 2.00000000E-01 | 1.31468373E-04 | 8.03331476E-01 |
| 4.00000000E-01 | 3.00960584E-04 | 6.04899457E-01 |
| 6.00000000E-01 | 5.39846439E-04 | 4.04707137E-01 |
| 8.00000000E-01 | 9.48224505E-04 | 2.02895247E-01 |
| 1.00000000E+00 | 4.06988771E-03 | 1.00000000E-03 |

| | | | | | | | | |
|--------------|-------------|--------------|-------------|-------------|-------------|-------------|-------------|-------------|
| P* | E* | Z* | R* | TW* | TF* | TC* | EF* | EH* |
| 9.555000E-01 | 1.00439E+00 | -6.17289E-01 | 9.58936E-01 | 9.98635E-01 | 9.99116E-01 | 1.00000E+00 | 9.97739E-01 | 9.99009E-01 |

TIME= 2.0000000E-03

| | | |
|----------------|----------------|----------------|
| Y* | X (IN.) | (T-T0)/(TW-T0) |
| 0. | -0. | 1.00000000E+00 |
| 2.00000000E-01 | 1.31914123E-04 | 8.03731805E-01 |
| 4.00000000E-01 | 3.01981005E-04 | 6.05547665E-01 |
| 6.00000000E-01 | 5.41676814E-04 | 4.05406685E-01 |
| 8.00000000E-01 | 9.51439505E-04 | 2.03389369E-01 |
| 1.00000000E+00 | 4.08360659E-03 | 1.00000000E-03 |

| | | | | | | | | |
|-------------|-------------|--------------|-------------|-------------|-------------|-------------|-------------|-------------|
| P* | E* | Z* | R* | TW* | TF* | TC* | EF* | EH* |
| 9.50000E-01 | 1.00515E+00 | -6.15715E-01 | 9.55696E-01 | 9.98525E-01 | 9.99039E-01 | 1.00000E+00 | 9.97481E-01 | 9.98896E-01 |

TIME= 2.80000000E-02

| | | |
|----------------|----------------|----------------|
| Y* | X (IN.) | (T-T0)/(TW-T0) |
| 0. | -0. | 1.00000000E+00 |
| 2.00000000E-01 | 1.44196698E-04 | 8.22016328E-01 |
| 4.00000000E-01 | 3.30098574E-04 | 6.38287900E-01 |
| 6.00000000E-01 | 5.92112553E-04 | 4.46540115E-01 |
| 8.00000000E-01 | 1.04002841E-03 | 2.41753537E-01 |
| 1.00000000E+00 | 4.46383279E-03 | 1.00000000E-03 |

| | | | | | | | | |
|-------------|-------------|--------------|-------------|-------------|-------------|-------------|-------------|-------------|
| P* | F* | Z* | R* | TW* | TF* | TC* | EF* | EH* |
| 7.50000E-01 | 1.05582E+00 | -5.50932E-01 | 8.74290E-01 | 9.95640E-01 | 9.96678E-01 | 1.00000E+00 | 9.85892E-01 | 9.93702E-01 |

TIME= 2.82000000E-02

| | | |
|----|---------|----------------|
| Y* | X (IN.) | (T-T0)/(TW-T0) |
|----|---------|----------------|

| | | |
|----------------|----------------|----------------|
| 0. | -0. | 1.00000000E+00 |
| 2.00000000E-01 | 1.44195474E-04 | 8.22016468E-01 |
| 4.00000000E-01 | 3.30095772E-04 | 6.38288500E-01 |
| 6.00000000E-01 | 5.92107527E-04 | 4.46541579E-01 |
| 8.00000000E-01 | 1.04001958E-03 | 2.41756251E-01 |
| 1.00000000E+00 | 4.46379490E-03 | 1.00000000E-03 |

| | | | | | | | | |
|-------------|-------------|--------------|-------------|-------------|-------------|-------------|-------------|-------------|
| P* | E* | Z* | R* | TW* | TF* | TC* | EF* | EH* |
| 7.50000E-01 | 1.05582E+00 | -5.50932E-01 | 8.74298E-01 | 9.95640E-01 | 9.96678E-01 | 1.00000E+00 | 9.85892E-01 | 9.93702E-01 |

TIME= 2.84000000E-02

| | | |
|----------------|----------------|----------------|
| Y* | X (IN.) | (T-T0)/(TW-T0) |
| 0. | -0. | 1.00000000E+00 |
| 2.00000000E-01 | 1.44194314E-04 | 8.22016601E-01 |
| 4.00000000E-01 | 3.30093117E-04 | 6.38289068E-01 |
| 6.00000000E-01 | 5.92102765E-04 | 4.46542966E-01 |
| 8.00000000E-01 | 1.04001122E-03 | 2.41758822E-01 |
| 1.00000000E+00 | 4.46375900E-03 | 1.00000000E-03 |

| | | | | | | | | |
|-------------|-------------|--------------|-------------|-------------|-------------|-------------|-------------|-------------|
| P* | E* | Z* | R* | TW* | TF* | TC* | EF* | EH* |
| 7.50000E-01 | 1.05582E+00 | -5.50932E-01 | 8.74305E-01 | 9.95641E-01 | 9.96678E-01 | 1.00000E+00 | 9.85892E-01 | 9.93702E-01 |

TIME= 2.86000000E-02

| | | |
|----------------|----------------|----------------|
| Y* | X (IN.) | (T-T0)/(TW-T0) |
| 0. | -0. | 1.00000000E+00 |
| 2.00000000E-01 | 1.44193215E-04 | 8.22016727E-01 |
| 4.00000000E-01 | 3.30090601E-04 | 6.38289607E-01 |
| 6.00000000E-01 | 5.92098252E-04 | 4.46544280E-01 |
| 8.00000000E-01 | 1.04000329E-03 | 2.41761259E-01 |
| 1.00000000E+00 | 4.46372497E-03 | 1.00000000E-03 |

| | | | | | | | | |
|-------------|-------------|--------------|-------------|-------------|-------------|-------------|-------------|-------------|
| P* | E* | Z* | R* | TW* | TF* | TC* | EF* | EH* |
| 7.50000E-01 | 1.05583E+00 | -5.50932E-01 | 8.74312E-01 | 9.95641E-01 | 9.96679E-01 | 1.00000E+00 | 9.85892E-01 | 9.93702E-01 |

TIME= 2.88000000E-02

| | | |
|----------------|----------------|----------------|
| Y* | X (IN.) | (T-T0)/(TW-T0) |
| 0. | -0. | 1.00000000E+00 |
| 2.00000000E-01 | 1.44192174E-04 | 8.22016846E-01 |
| 4.00000000E-01 | 3.30088217E-04 | 6.38290117E-01 |
| 6.00000000E-01 | 5.92093975E-04 | 4.46545526E-01 |
| 8.00000000E-01 | 1.03999578E-03 | 2.41763568E-01 |
| 1.00000000E+00 | 4.46369274E-03 | 1.00000000E-03 |

| | | | | | | | | |
|-------------|-------------|--------------|-------------|-------------|-------------|-------------|-------------|-------------|
| P* | E* | Z* | R* | TW* | TF* | TC* | EF* | EH* |
| 7.50000E-01 | 1.05583E+00 | -5.50933E-01 | 8.74318E-01 | 9.95641E-01 | 9.96679E-01 | 1.00000E+00 | 9.85892E-01 | 9.93702E-01 |

TIME= 2.90000000E-02

| | | |
|----------------|----------------|----------------|
| Y* | X (IN.) | (T-T0)/(TW-T0) |
| 0. | -0. | 1.00000000E+00 |
| 2.00000000E-01 | 1.44191187E-04 | 8.22016960E-01 |
| 4.00000000E-01 | 3.30085958E-04 | 6.38290601E-01 |
| 6.00000000E-01 | 5.92089923E-04 | 4.46546707E-01 |
| 8.00000000E-01 | 1.03998866E-03 | 2.41765756E-01 |
| 1.00000000E+00 | 4.46366219E-03 | 1.00000000E-03 |

| | | | | | | | | |
|-------------|-------------|--------------|-------------|-------------|-------------|-------------|-------------|-------------|
| P* | E* | Z* | R* | TW* | TF* | TC* | EF* | EH* |
| 7.50000E-01 | 1.05583E+00 | -5.50933E-01 | 8.74324E-01 | 9.95641E-01 | 9.96679E-01 | 1.00000E+00 | 9.85892E-01 | 9.93702E-01 |

TIME= 2.9200000E-02

| Y* | X (IN.) | (T-T0)/(TW-T0) | P* | E* | Z* | R* | TW* | TF* | TC* | EF* | EM* |
|---------------|----------------|----------------|-------------|-------------|--------------|-------------|-------------|-------------|-------------|-------------|-------------|
| 0. | -0. | 1.0000000E+00 | 7.50000E-01 | 1.05583E+00 | -5.50933E-01 | 8.74330E-01 | 9.95642E-01 | 9.96679E-01 | 1.00000E+00 | 9.85892E-01 | 9.93702E-01 |
| 2.0000000E-01 | 1.44190252E-04 | 8.22017067E-01 | | | | | | | | | |
| 4.0000000E-01 | 3.30083818E-04 | 6.38291059E-01 | | | | | | | | | |
| 6.0000000E-01 | 5.92086084E-04 | 4.46547825E-01 | | | | | | | | | |
| 8.0000000E-01 | 1.03998192E-03 | 2.41767829E-01 | | | | | | | | | |
| 1.0000000E+00 | 4.46363324E-03 | 1.0000000E-03 | | | | | | | | | |

TIME= 2.9400000E-02

| Y* | X (IN.) | (T-T0)/(TW-T0) | P* | F* | Z* | R* | TW* | TF* | TC* | EF* | EM* |
|---------------|----------------|----------------|-------------|-------------|--------------|-------------|-------------|-------------|-------------|-------------|-------------|
| 0. | -0. | 1.0000000E+00 | 7.50000E-01 | 1.05583E+00 | -5.50933E-01 | 8.74335E-01 | 9.95642E-01 | 9.96679E-01 | 1.00000E+00 | 9.85892E-01 | 9.93702E-01 |
| 2.0000000E-01 | 1.44189366E-04 | 8.22017168E-01 | | | | | | | | | |
| 4.0000000E-01 | 3.30081790E-04 | 6.38291494E-01 | | | | | | | | | |
| 6.0000000E-01 | 5.92082446E-04 | 4.46548886E-01 | | | | | | | | | |
| 8.0000000E-01 | 1.03997553E-03 | 2.41769793E-01 | | | | | | | | | |
| 1.0000000E+00 | 4.46360582E-03 | 1.0000000E-03 | | | | | | | | | |

TIME= 2.9600000E-02

| Y* | X (IN.) | (T-T0)/(TW-T0) | P* | E* | Z* | R* | TW* | TF* | TC* | EF* | EM* |
|---------------|----------------|----------------|-------------|-------------|--------------|-------------|-------------|-------------|-------------|-------------|-------------|
| 0. | -0. | 1.0000000E+00 | 7.50000E-01 | 1.05584E+00 | -5.50933E-01 | 8.74340E-01 | 9.95642E-01 | 9.96679E-01 | 1.00000E+00 | 9.85892E-01 | 9.93702E-01 |
| 2.0000000E-01 | 1.44168526E-04 | 8.22017265E-01 | | | | | | | | | |
| 4.0000000E-01 | 3.30079868E-04 | 6.38291905E-01 | | | | | | | | | |
| 6.0000000E-01 | 5.92078998E-04 | 4.46549890E-01 | | | | | | | | | |
| 8.0000000E-01 | 1.03996947E-03 | 2.41771655E-01 | | | | | | | | | |
| 1.0000000E+00 | 4.46357983E-03 | 1.0000000E-03 | | | | | | | | | |

TIME= 2.9800000E-02

| Y* | X (IN.) | (T-T0)/(TW-T0) | P* | F* | Z* | R* | TW* | TF* | TC* | EF* | EM* |
|---------------|----------------|----------------|-------------|-------------|--------------|-------------|-------------|-------------|-------------|-------------|-------------|
| 0. | -0. | 1.0000000E+00 | 7.50000E-01 | 1.05584E+00 | -5.50933E-01 | 8.74345E-01 | 9.95642E-01 | 9.96679E-01 | 1.00000E+00 | 9.85892E-01 | 9.93702E-01 |
| 2.0000000E-01 | 1.44187731E-04 | 8.22017356E-01 | | | | | | | | | |
| 4.0000000E-01 | 3.30078046E-04 | 6.38292296E-01 | | | | | | | | | |
| 6.0000000E-01 | 5.92075731E-04 | 4.46550842E-01 | | | | | | | | | |
| 8.0000000E-01 | 1.03996373E-03 | 2.41773419E-01 | | | | | | | | | |
| 1.0000000E+00 | 4.46355520E-03 | 1.0000000E-03 | | | | | | | | | |

TIME= 3.0000000E-02

| Y* | X (IN.) | (T-T0)/(TW-T0) | (1-y*) ^{T*} |
|---------------|----------------|----------------|----------------------|
| 0. | -0. | 1.0000000E+00 | 1.0 |
| 2.0000000E-01 | 1.44186977E-04 | 8.22017443E-01 | 0.823 |
| 4.0000000E-01 | 3.30076321E-04 | 6.38292665E-01 | 0.640 |
| 6.0000000E-01 | 5.92072636E-04 | 4.46551744E-01 | 0.449 |
| 8.0000000E-01 | 1.03995829E-03 | 2.41775091E-01 | 0.245 |
| 1.0000000E+00 | 4.46353186E-03 | 1.0000000E-03 | 0 |

C-7

| P* | E* | Z* | R* | TW* | TF* | TC* | EF* | EH* |
|-------------|-------------|--------------|-------------|-------------|-------------|-------------|-------------|-------------|
| 7.50000E-01 | 1.05584E+00 | -5.50934E-01 | 8.74349E-01 | 9.95642E-01 | 9.96679E-01 | 1.00000E+00 | 9.85892E-01 | 9.93702E-01 |

C-8

RUNNING TIME= 5.13460000E+01

REFERENCES

1. Culick, F. E. C., "An Elementary Calculation of the Combustion of Solid Propellants," Astronautica Acta 14, 171-181 (1969).
2. Culick, F. E. C., and G. L. Dehority, "An Elementary Calculation for the Burning Rate of Composite Solid Propellants," WSS/CI Paper 69-7, presented at 1969 Spring Meeting, Western States Section, The Combustion Institute, China Lake, California, April 1969.
3. Krier, H., T'ien, J. S., Sirignano, W. A., and Summerfield, M., "Non-steady Burning Phenomena of Solid Propellants: Theory and Experiments," AIAA J. 6, 278-285 (1968).
4. Merkle, C. L., Turk, S. L., and Summerfield, M., "Extinguishment of Solid Propellants by Rapid Depressurization," Aerospace and Mechanical Sciences Report No. 880, ONR Contract Nonr 1858(32), Princeton University, Princeton, New Jersey.
5. Jensen, G. E., "A Stop-Start Study of Solid Propellants," Final Report, Contract No. NAS 1-6601, NASA CR-66488, United Technology Center, Sunnyvale, California, November 1967.
6. Jensen, G. E., "An Experimental Study of Solid Propellant Extinguishment by Rapid Depressurization," Final Report, Contract No. NAS 1-7815, NASA CR-66747, United Technology Center, Sunnyvale, California, March 1969.
7. Marxman, G. A., and Wooldridge, C. E.: "Effect of Surface Reactions on the Solid Propellant Response Function," AIAA J. 6, 471-478 (1968).
8. Wooldridge, C. E., Marxman, G. A., and Capener, E. L., "Propellant Combustion Phenomena During Rapid Depressurization," Final Report, Stanford Research Institute, Contract No. NAS 7-389, NASA CR-66500, October 1967.
9. Capener, E. L., Dickinson, L. A., and Kier, R. J., "Driving Processes of Finite-Amplitude Axial-Mode Instability in Solid Propellant Rockets," AIAA J. 5, 938-945 (1967).
10. Marxman, G. A., and Wooldridge, C. E., "Finite-Amplitude Axial Stability in Solid Rocket Combustion," Proceedings of the 12th Symposium (International) on Combustion, 115-127, The Combustion Institute, Pittsburgh (1969).

11. Wooldridge, C. E., Marxman, G. A., and Kier, R. J., "A Theoretical and Experimental Study of Propellant Combustion Phenomena During Rapid Depressurization," Final Report, Stanford Research Institute, Contract No. NAS 1-7349, NASA CR-66733, February 1969.
12. Capener, E. L., Dickinson, L. A., Kier, R., R. J., Marxman, G. A., and Wooldridge, C. E., "Response of a Burning Propellant Surface to Erosive Transients," Final Report (AFOSR No. 68-0771), Stanford Research Institute, Contract No. AF 49(638)-1965, April 1968.
13. Denison, M. R., and Baum, E., "A Simplified Model of Unstable Burning in Solid Propellants," ARS J. 31, 1112-1122 (1961).